INVESTIGATION ON MECHANICAL PROPERTIES OF
FILAMENT WOUND COMPOSITES FOR PRESSURE VESSEL

Thesis

Submitted in partial fulfillment of the requirements for the degree of

DOCTOR OF PHILOSOPHY

by

SRIKUMAR BIRADAR

(158018ME15F24)

DEPARTMENT OF MECHANICAL ENGINEERING

NATIONAL INSTITUTE OF TECHNOLOGY KARNATAKA

SURATHKAL, MANGALURU-575025

SEPTEMBER, 2021

INVESTIGATION ON MECHANICAL PROPERTIES OF
FILAMENT WOUND COMPOSITES FOR
PRESSURE VESSEL

Thesis

Submitted in partial fulfillment of the requirements for the degree of

DOCTOR OF PHILOSOPHY

by

SRIKUMAR BIRADAR
(158018ME15F24)

Under the Guidance of

Dr. SHARNAPPA JOLADARASHI.

Associate Professor

and

Dr. S.M. KULKARNI

Professor

DEPARTMENT OF MECHANICAL ENGINEERING

NATIONAL INSTITUTE OF TECHNOLOGY KARNATAKA

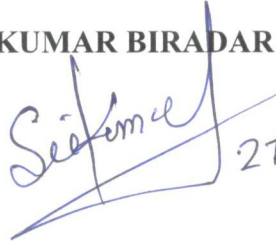## SURATHKAL, MANGALURU-575025

SEPTEMBER, 2021

DECLARATION

I hereby declare that the Research Thesis titled **"INVESTIGATION ON MECHANICAL PROPERTIES OF FILAMENT WOUND COMPOSITES FOR PRESSURE VESSEL"**, which is being submitted to the **National Institute of Technology Karnataka, Surathkal,** in partial fulfilment of the requirements for the award of the Degree of **Doctor of Philosophy** in **Mechanical Engineering** is a *bonafide report of the research work carried out by me*. The material contained in this Research Thesis has not been submitted to any other University or Institution for the award of any degree.

Register Number: 158018ME15F24

Name of the Research Scholar: **SRIKUMAR BIRADAR**

Signature of the Research Scholar:　　　27/09/2021
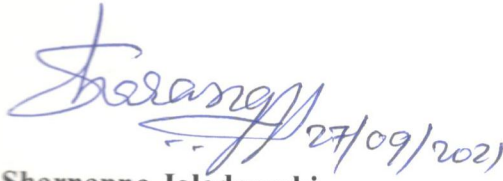
Department of Mechanical Engineering

Place: NITK, Surathkal

Date: 25-09-2021

CERTIFICATE

This is to certify that the Research Thesis titled **"INVESTIGATION ON MECHANICAL PROPERTIES OF FILAMENT WOUND COMPOSITES FOR PRESSURE VESSEL"**, submitted by **Mr. SRIKUMAR BIRADAR** (Register Number: **158018ME15F24)** as the record of the research work carried out by him, *is accepted as the Research Thesis submission* in partial fulfilment of the requirements for the award of Degree of **Doctor of Philosophy.**

Research Guide(s)

27/09/2021

Dr. Sharnappa Joladarashi

Associate Professor

Department of Mechanical Engineering

Dr. S. M. Kulkarni

Professor

Department of Mechanical Engineering

Chairman-DRPC

Date: 2 7 SEP 2021

ACKNOWLEDGEMENT

ABSTRACT

Metallic pressure vessels or cylinders used over many decades for processing food and beverages products, transportation of chemicals, storage of hazardous and nonhazardous chemicals for prolonged durations have been carrying limitations throughout their service period. Few limitations such as, the weight of the cylinders, corrosion and erosion effect, risk of sudden failure. The current study is connected to development of an alternative material for existing metallic cylinders to overcome few limitations. In the present study, filament wound GFRP (Glass fiber Reinforced Polymer) is proposed, which is having high strength to weight ratio compared to the existing metallic material. The FE (Finite Element) analysis of cylindrical pressure vessels used for LPG storage is carried out by alternative materials such as LCS (Low Carbon Steel), Aluminium 6061 T6, and GFRP. Based on maximum specific strength, the best alternative material obtained among others is GFRP, and this material is chosen for further studies. The GFRP pressure vessel cylinder is further studied by varying filament winding process parameters such as fiber volume fraction (0.55,0.65,0.75), winding angle ($\pm45°, \pm50°, \pm55°, \pm60°, \pm65°, \pm70°,\pm75°$) and stacking sequence (SS1, SS2, SS3, SS4, SS5, SS6) using FE analysis tool. A total of 336 FE simulations were carried out, i.e., with PVC (Poly-Vinyl Chloride) liner (168) and without PVC liner (168). The optimization tool MCDM (Multi criteria Decision Making) VIKOR method is used for the selection of best alternative among existing 168 FE simulation compositions (with PVC liner). The liner act as leak-proof material in filament wound composite vessels and hence can be used for storage or processing of different viscous and non-viscous fluids. The optimization of the FE simulation result leads to best attribute, which is selected and fabricated as per its respective fabrication

process parameters for experimental studies. Similarly, next to five attributes are selected as per available testing laboratory facilities (physical, mechanical and tribological, hygrothermal ageing). The filament wound GFRP cylinders are cut into test coupons for physical, mechanical, and tribological characterization studies.

Further hygrothermal ageing of all 6 compositions are studied. In hygrothermal ageing effect is studied using three different fluids such as tap water, sea water, and tap water with oil. The hygrothermal ageing is carried out for a period of 45 days at a constant temperature of 80°C. The aged and unaged samples are subjected to mechanical tests such as hoop tensile strength, tensile, compression, and bending tests. The mechanical test results are compared for a possible reduction in strength of aged filament wound GFRP samples. The obtained results are further examined with fractography study using Scanning Electron Microscope (SEM). The different mechanical testing results (ultimate tensile strength, ultimate compressive strength, ultimate flexural strength, hoop tensile strength) highlights that the filament wound GFRP samples are moderately affected by ageing.

In overall, in the case of FE simulations studies, the product with composition of fiber volume fraction, $V_f = 0.55$, winding angle $= \pm55°$ and stacking sequence of $(\pm55°_2/90°_2/\pm55°_2)$ is suggested as the best alternative or attribute-based on average Von Mises of 45.64 MPa and hoop stress of 44.82 MPa compared to other compositions. As far as the experimental study of filament wound GFRP test coupons is concerned, retention of important mechanical properties such as tensile, compression, flexural, and hoop tensile strength is the main factor. Hence it is observed from different hygrothermal ageing effect studies that filament wound GFRP material with 1200TEX is least or moderately

affected by hygrothermal ageing. The product which has the least ageing effect and having the highest strength (hoop tensile, tensile, compression, and flexural strength) retention rate (nearly 90%) is product-P1(055WA55SS1) with compositions of fiber volume fraction, V_f = 0.55, winding angle of ±55º, stacking sequence of SS1 = $(\pm\varphi°_2/90°_2/\pm\varphi°_2)$. Hence this product P1 can be suggested as an alternative material to existing metallic material for elevated temperature applications (up to 80ºC).

Keywords: FE simulation, Filament winding, GFRP, Hoop tensile strength, Hygrothermal ageing, Pressure vessel, mechanical properties, stacking sequence, winding angle, fiber volume fraction.

TABLE OF CONTENTS

vi

LIST OF FIGURES

LIST OF TABLES

LIST OF EQUATIONS

ACRONYMS

FW	Filament Winding
HA	Hygrothermal Ageing
TW	Tap Water
SW	Sea Water
TWWO	Tap Water With Oil
GFRP	Glass Fiber Reinforced Polymer
CFRP	Carbon Fiber Reinforced Polymer
AFRP	Aramid Fiber Reinforced Polymer
LCS	Low Carbon Steel
Al 6061 T6	Aluminium 6061 T6
FEM	Finite Element Method
LPG	Liquefied Petroleum Gas
HTS	Hoop Tensile Strength
UTM	Universal Testing Machine
MCDM	Multi Criteria Decision Method
UTS	Ultimate Tensile Strength
FRCs	Fiber Reinforced Composites
SEM	Scanning Electron Microscope
ASTM	American Standard Testing Methods

CHAPTER 1

INTRODUCTION

Over many decades' pressure vessels have been used in many commercial and domestic industries as the main container for processing, storage, and transportation purposes. These pressure vessels were made basically from iron-based materials (low carbon steel (LCS), stainless steel, etc.) as per the individual application demands. Since, iron-based metals have many limitations which act as roadblocks for a longer, brighter, and safer future of iron-based products. The corrosion, erosion, sudden failure due to sub-surface cracks, difficulty in handling heavy containers, especially during transportation of goods, are few important limitations of iron-based pressure vessel cylinders. In order to address these difficulties, many researchers have worked on alternative materials which can provide equal strength or even higher strength compared to iron-based materials. In the early '90s, people have started using aluminium alloy-based materials such as Al 6061 T6 for domestic LPG cylinders as an alternative to iron-based alloys to make pressure vessel containers.

In later years, based on experimental studies by researchers who have proposed the polymer composites as an alternative material to metallic pressure vessel cylinder.
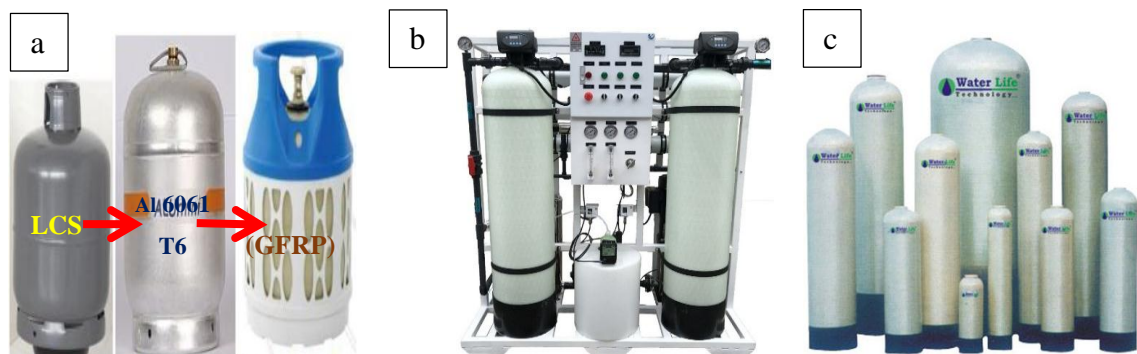
Figure. 1.1A Polymer composites application: (a) LPG (LCS, Al 6061, GFRP composite (Moketla and Shukla 2012) (b) Water storage tanks, (c) Water treatment RO plant

1

Figure. 1.1B Polymer composites application: (a) Transportation, (b) Fire extinguisher

The primary objective of any material is to provide better strength to weight ratio when compared to previous material used. Industrial products where composite material can be a game-changer are household applications such as LPG cylinder, textile, chemical, and food processing industries, aerospace, automobile, fire extinguisher cylinders. Figure 1.1A and Figure 1.1B highlighting the application areas where polymer composites will be a better alternative material.

1.1 Materials used for pressure vessel

As mentioned in the above paragraph, iron-based material such as low carbon steel (LCS) is being used as a base material for many pressure vessel applications such as processing of fluids; containers are used for transporting chemicals from one place to another large storage towers. In later years' alternative metallic materials such stainless-steel, aluminium based alloys (Al 6061 T6) have been tried as a base material for pressure vessel applications. Even though there exist some limitations in using metallic-based vessels still in many industries are extensively using LCS and Aluminium alloy-based vessels for their primary applications, as mentioned early in the paragraph. Currently, researchers have proposed composite material as an alternative material for metal-based pressure vessels to overcome the limitations of metallic materials (handling, risk of sudden failure, etc.).

1.1.1 Composite materials for pressure vessel

In any polymer matrix composite materials, variation in strength and stiffness can be obtained by changing the fiber orientations and hence molecular structure. Since fibers are of smaller cross-sectional area, they are not usable in engineering applications directly. Fibers are embedded in a suitable matrix material in order to form fibrous composites. This matrix helps in binding all fibers together, also helps in transferring applied load from one fiber to another, prevents environmental effects, and protects the damage of fibers during handling. Any composite cylindrical vessel is made from a shell-like structure having multi-layered fibrous composite. Hence each layer of the shell is called the lamina, and each lamina has different orientations, thickness, fiber volume fraction, and these parameters are varied according to design requirements. Some of the cylindrical composite vessel applications are cryogenics fluid storage tanks basically made from CFRP composites, CNG (Compressed Natural Gas) composite cylinders made from GFRP for automobiles, LPG (Liquefied Petroleum Gas) composite cylinders made from GFRP composites, etc. (Raju and Rao 2015).

Applications of Composite Materials

Previously composite materials applications were limited to aircraft industries. This is because composites are light in weight, corrosion resistance property, required directional properties. For example, Boeing 757, at present 80%-85% of Aircraft body is made of composites. In the 21st-century application of composites has extended to other fields such as LPG cylinders for household applications, Hydrogen storage vessels, underwater fuel storage tanks, race cars, tennis rackets, golf clubs, and other leisure products.

1.1.2 Composite material

The composite material consists of two or more constituents combined at a macroscopic level, and they are soluble in each other. Here one constituent is reinforcement, for example, fiber, which is being embedded into a constituent called the matrix, for example,

resin. The schematic of the mixing of fiber and resin leading to the formation of composite is shown in Figure 1.2. The matrix is a continuous phase, whereas fiber or reinforcement has a continuous and discontinuous phase. Reinforcements are basically fibers, particles, and flakes. Examples of composite systems include concrete reinforced with steel and epoxy reinforced with graphite fibers, etc. (Kaw and Group 2006).
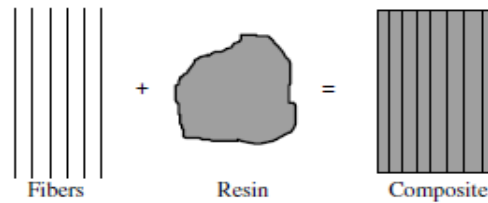
Figure 1.2 Formation of a composite material using fibers and resin.

The major functions of fibers in any composite are:
- ➢ In any structural composites, the maximum load is carried by fibers.
- ➢ The major mechanical properties, such stiffness, strength, thermal stability, etc., of any composite depend purely on fibers.

The major functions of matrix material in any composite are:
- ➢ The matrix helps in binding fibers together properly.
- ➢ The load applied on a composite is distributed on all fibers. Transfer of load from one fiber to another is done with the help of the matrix.
- ➢ Each fiber in a composite is isolated from other fibers; this helps in reducing the speed of crack propagation.
- ➢ The damage of fibers due to impact load or any other load is reduced because of protection from the matrix.
- ➢ Proper selection of matrix helps to avoid chemical attacks on fibers.

1.1.2 (a) Reinforcements

A Fiber-reinforced composite is having a major or most important constituent called reinforcement, also known as fiber. Most of the load applied on any composite is carried by fibers, and hence its composition is higher in almost all composite materials. Some of

the following features are affected by fiber category, fiber dimension, fibers weight or volume fraction, fiber orientation.

- ➤ Density of fibers
- ➤ UTS and Young's modulus
- ➤ Electrical and thermal conductivity
- ➤ Failure strength and its mechanism of failure
- ➤ UCS and Modulus of elasticity due to compressive load
- ➤ Cost of fiber (Mallick 1998)

Various fibers used in Polymer Matrix Composites (PMCs): (Kaw and Group 2006)

There are many types of fibers used in PMCs; a few commonly used fibers are Glass, Graphite/carbon, Kevlar/aramid. Some of the mechanical properties of these fibers are compared with steel and aluminium are highlighted in Table 1.1.

Table 1.1 Typical mechanical properties of fibers used in polymer matrix composites

Property	Units	Graphite	Aramid	Glass	Steel	Aluminium
Specific gravity	-	1.8	1.4	2.5	7.8	2.6
Young's modulus	GPa	230	124	85	206.8	68.95
Ultimate tensile strength	MPa	2067	1379	1550	648.1	275.8
Axial coefficient of thermal expansion	μm/m/°C	−1.3	−5	5	11.7	23
Density	(g/cm^3)	1.9	1.45	2.54	7.8	2.7
Diameter	(μm)	7.5	12	15	-	-
% Elongation at Break	-	1.5	3.5	5.7	-	-

Description of glass fiber

The most commonly used fiber in PMCs is glass fiber. Some of its advantages are high

strength to weight ratio, high chemical resistance, low cost, good insulating properties. (Kaw and Group 2006)

Types of Glass Fibers: The most popularly used glass fibers are **E**-Glass (Fiber glass), **S**-Glass. The E-Glass is mainly suited for Electrical applications. S-Glass fiber is suited for structural applications where strength is a basic criterion.

Generally, Glass fibers are divided into subcategories as follows:

> ➢ **E**-Glass: For resistivity and high strength-to-weight ratio.
> ➢ **S**-glass: Is Suitable for high strength, under extreme corrosive environment and extreme temperature.
> ➢ **R**-Glass: Have improved mechanical properties.
> ➢ **C**-Glass: High acidic environments corrosion resistance.
> ➢ **D**-Glass: Have better dielectric properties.

Note: As per our requirement, we are using **E-Glass** Fiber. The reason for the selection of E-Glass fiber is its high strength to weight ratio.

1.1.2 (b) Matrix Materials

As we know, composite is a mixture of fiber and matrix in an appropriate ratio to obtain the required property. The prime function of any matrix material is to safeguard the fibers from chemicals and direct the applied load. For the full functioning of fibers, the matrix or resin should have a lesser modulus (Sanjay K. Mazumdar 2001).

Epoxy

It's a flexible resin structure, open for a wide range of features and capability in handling different processes. Epoxy material is having the best adhesiveness and low contraction towards different substrate materials. The epoxies are having a wide variety of applications starting from space to sports equipment. The epoxies are available in different grades as per the application demands. The composition of epoxies can be altered as per the performance requirement of products or applications. By altering the composition(formulation), the characteristics or properties of epoxies such as cure time

alteration, temperature for processing, and tack and drape can be altered, alteration in toughness is possible, the improvement in resistance against temperature is observed, etc. The chemical reaction with alcohols, phenols, amines, carboxylic acids, anhydrides helps in curing the epoxies. The Diglycidylether of Bisphenol A (DGEBA) is one of the epoxide groups out of several epoxide groups of liquid epoxy resin. There exists one oxygen and 2 carbon atoms in a 3-membered ring in any epoxide group. The toughness is increased by the addition of liquids such as diluents and flexibilities to epoxide groups. The curing agent (e.g., diethylenetriamine [DETA]) is a hardener that is added to have a curing reaction (cross-linking). Figure 1.3 clearly highlighting the cross-linking phenomenon as the curing process commences, DGEBA molecules start forming cross-linkages. A solid epoxy resin is formed after the completion of a 3-dimensional cross-linkages network. Proper usage of catalyst and or hardener helps in controlling the curing process time. The controlling of cure time and hardener help in obtaining varied properties and characteristics of the resin. The high volume of production of resin is possible with higher cure time and reduced process cycle duration. The epoxies are having better performances at elevated and room temperature. The epoxy resin is having a temperature range of 93°C-121°C. The higher temperature epoxies have also existed, but prices are higher with increased performances in corrosion resistance and chemical resistance. The liquid, semi-solid, and solid-state/phases are three forms of epoxies.
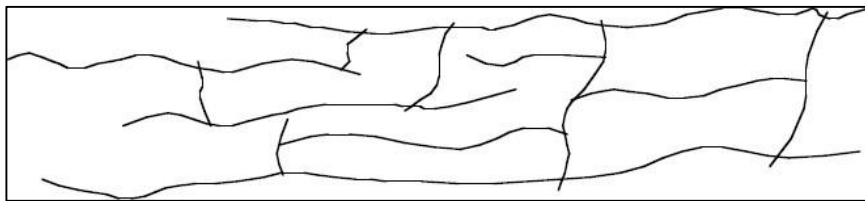
Figure 1.3 Cross-linking of thermoset molecules during curing(Sangamesh et al. 2017)

The reinforcing fibers such as boron, aramid, carbon, and glass are most commonly use liquid epoxy resins. The RTM (Resin Transfer Molding), hand layup, filament winding, pultrusion are few composite fabrication methods in which liquid resin is frequently used. In the case of autoclave and vacuum bagging processes, the semi-solid epoxies are used in

prepregs form. In the case of bonding, solid epoxies are used.

In comparison to vinyl and polyester resins, the epoxies are costly. Hence epoxies are not used in price-affected industries (marine and automobile industries), only in unavoidable circumstances used in price-oriented industries. The toughened epoxies have been developed by combining the thermal property of thermoset and the toughness of thermoplastic using patented processes. The Table 1.2 highlights about few thermoset resins.

Table 1.2 Typical thermosetting resin properties

RESIN	DENSITY(g/cm^3)	TENSILE MODULUS(GPa)	TENSILE STRENGTH(MPa)
EPOXY	1.25-1.35	2.55-4.95	55-105
PHENOLIC	1.25-1.35	2.75-4.05	40-55
POLYESTER	1.25-1.35	1.65-4.05	40-90

Specific information about epoxy:(Krishan K 2013)

Epoxies are the most frequently used matrices. These are low molecular weight organic liquids that contain epoxide groups. This epoxide group has three members as one oxygen and the other two are carbon atoms. The epoxies are mostly formed by the reaction of epichlorohydrin with phenols or aromatic amines. The wide range of properties such as impact strength, viscosity, degradation, etc., are obtained by adding some additives to epoxies such as hardeners, plasticizers, fillers. The Properties of epoxy at room temperature are given in Table 1.3.

Table 1.3 Room Temperature Properties of a Typical Epoxy(Krishan K 2013)

Property	Units	Value
System of units: SI		
Specific gravity	—	1.28
Young's modulus	GPa	3.792
Ultimate tensile strength	MPa	82.74

Note: For the present study, the **Epoxy** resin is selected because of the following reasons:

- ➢ High strength to weight ratio.
- ➢ Good wettability of fiber leads to proper alignment of fibers because of lower viscosity and flow rate.
- ➢ Reduction in the absorption of large shear stresses by the bond between the resin and reinforcement due to lower shrinkage effect.
- ➢ The epoxy is available in more than 20 grades and hence obtaining specific property is not difficult.

Different resins in PMCs: (Kaw and Group 2006)

These polymers include epoxy, phenolics, acrylic, urethane, and polyamide. Each polymer has its advantages and drawbacks in its use. Some of the important properties include smoke emission, maximum strength, service temperature, cost, etc. The comparative study of these resins with respect to epoxy properties helps in finding the most desirable material for an application.
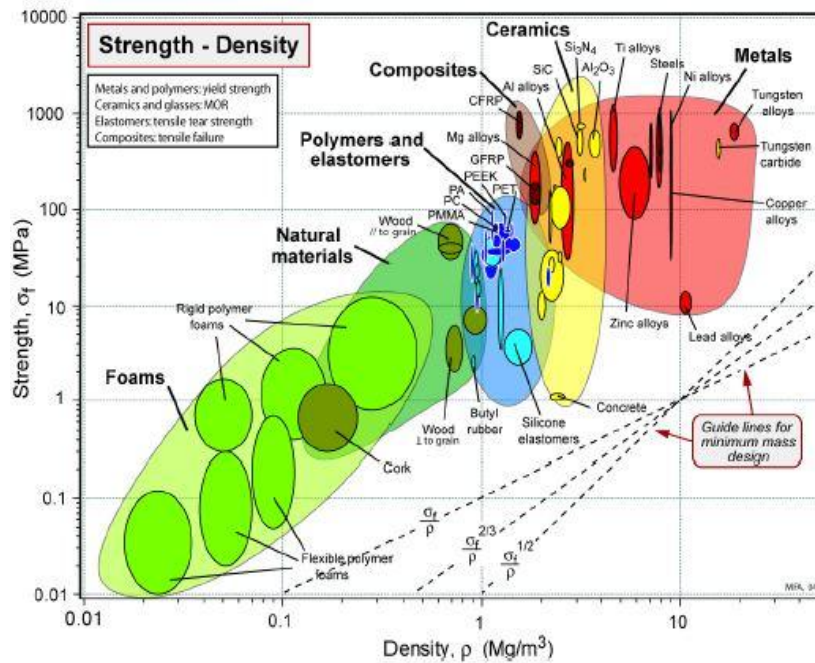
Figure 1.4 Ashby chart for material selection (Ashby and Ashby 2011)

Figure 1.4 is used for designing light, strong structures. The "strength" for metals is the 0.2% offset yield strength. For polymers, it is the stress at which the stress-strain curve

becomes markedly non-linear -typically, a strain of about 1%. For ceramics and glasses, it is the compressive crushing strength; remember that this is roughly 15 times larger than the tensile (fracture) strength. For composites, it is the tensile strength.

Polymer Matrix Composites(PMCs):(Kaw and Group 2006)

The most common advanced composites are polymer matrix composites consisting of a polymer (e.g., epoxy, polyester, urethane) reinforced by thin diameter fibers (e.g., graphite, aramids, boron). For example, graphite/epoxy composites are approximately five times stronger than steel. Table 1.4 highlights the list of reinforcements and matrix materials used for making polymer matrix composites.

Table 1.4 Types of Fibers and resins list (Sanjay K. Mazumdar 2001)

	Synthetic fibers:
Fiber/reinforcement	Aluminium, Aluminium oxide, Aluminium silica, Asbestos, Beryllium, Beryllium carbide, Beryllium oxide, Carbon (Graphite) Glass (E-glass, S-glass, D-glass), Molybdenum, Polyamide (Aromatic polyamide, Aramid), e.g., Kevlar 29 and Kevlar 49, Polyester, Quartz (Fused silica), Steel, Tantalum
	Natural Fibers:
	Jute, Flax, Hemp, Sisal, Coconut fiber (coir), Banana fiber (abaca), Particulate, Wood powder, Carbon black, Graphite, Fly ash, Alumina
Resin/matrix	**Thermosets:**
	Epoxy, Phenolic, Polyester, Vinylester, Cynate ester, Polyurethane
	Thermoplastic resins:
	Nylon, Polypropelene(PP), Polyethyletherketone(PEEK), Polyphenylene Sulfide(PPS)

1.2 Composite Product Fabrication (Sanjay K. Mazumdar 2001)

Composite products are fabricated by transforming the raw material into the final shape using one of the manufacturing processes. Figure 1.5 classifies the frequently used composites processing techniques in the composites industry.

There are various methods used for manufacturing of PMCs; some of them are filament winding process (used basically for making cylindrical components to store, transport, and processing of fluids), Resin Transfer Molding (automotive industries), Autoclave forming (to obtain low void, high quality, complex shape structures). One of the PMCs

Composites Processing

Thermoset Composites Processing — Thermoplastic Composites Processing

Composites
-SMC Molding
-SRIM
-BMC Molding
-Spray up
-Injection Molding

Continuous fiber Composites
-FILAMENT WINDING
-Pultrusion
- RTM
-Hand Layup
-Autoclave Process
-Roll wrapping
-SCRIMP
-Bladder Molding

Short fiber composites
-Injection Molding
-Blow Molding

Continuous fiber Composites
-Thermoforming
-Tape Winding
-Compression Molding
-Autoclave
-Diaphragm Forming

manufacturing methods is explained in detail in this chapter.

Figure 1.5 Classification of composites processing techniques. (Sanjay K. Mazumdar 2001)

1.3 Filament Winding

In this process, basically, two winding methods are used, such as wet winding and dry winding. In wet winding, the continuous fiber called filament is impregnated with resin in a resin bath before winding onto the mandrel as per the property required. Hence this process is a cheaper and more controlled one. The dry winding process is similar to the wet winding process but with slight modifications. In the dry winding process, prepregs are used; hence there is no need for a resin bath. Therefore, this process is a clean but little expensive and uncommon process. The winding patterns such as helical, hoop, and polar are used as per properties required in the final product. The application of heat or pressure is used for curing the filament wounded product. The mandrel is made from different materials, such as steel, salts, wood, aluminium etc. Based on application such as if the vessel is closed one, then low meting

11
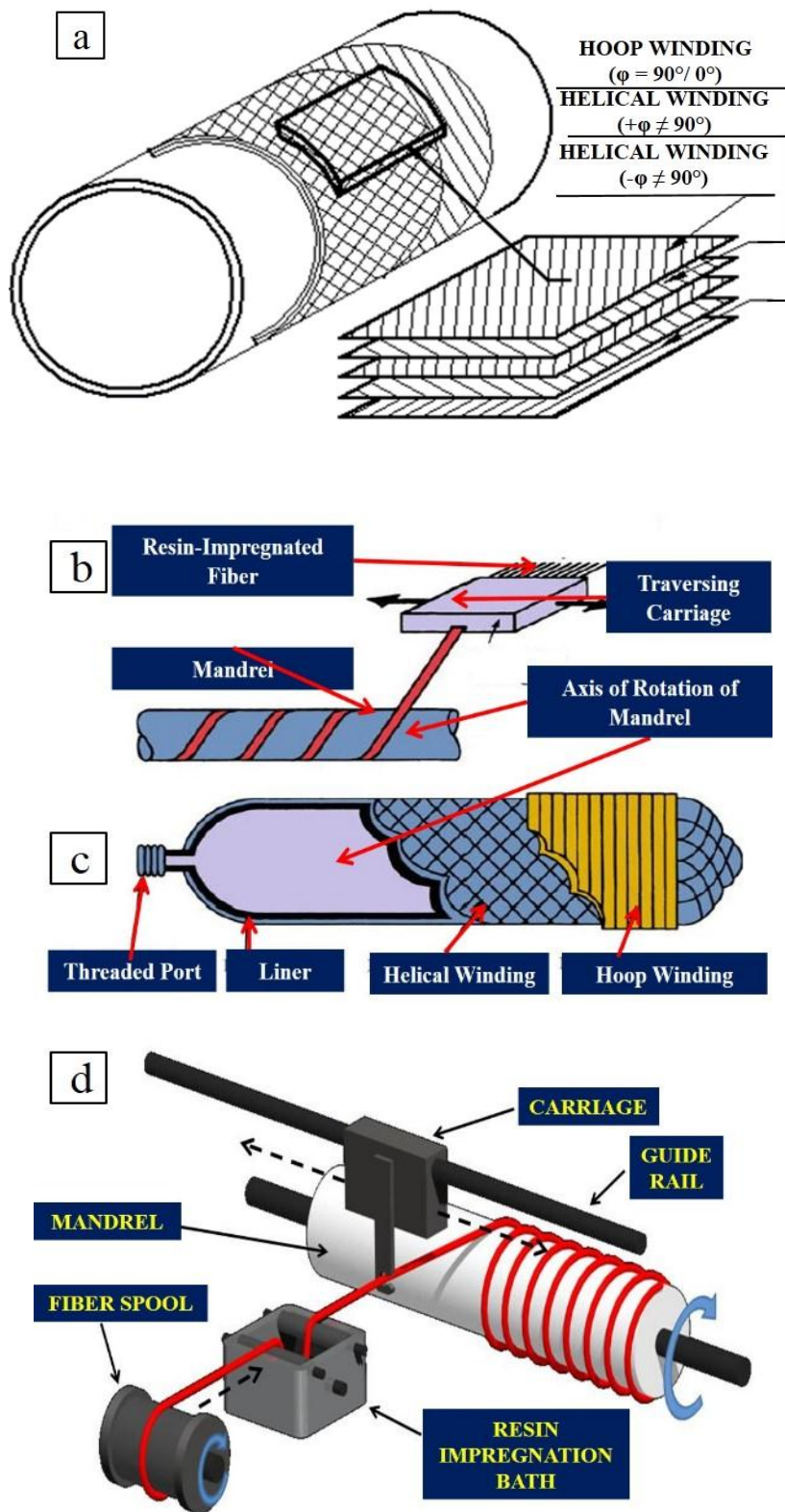
Figure 1.6 (a) Schematic representation of filament wound GFRP cylinder, (b) Different parts highlighting the filament winding process, (c) Filament wound pressure vessel with liner.(Krishan K 2013), (d) 3-Dimensional view of filament winding set up

alloy or water-soluble salt is used as a mandrel; if the vessel is open-ended, then steel can be used as a mandrel. The schematic view and 3-D view of filament winding setup are shown in Figure 1.6.

1.4 Summary

In the present chapter, we have studied about limitations and drawbacks of using metallic material in pressure vessel cylinders, and hence alternative materials are proposed by various researchers to overcome these limitations are discussed. The application of composite materials in different commercial and domestic industries is also discussed. The polymer composites are made from a proper combination of reinforcement and matrix material which is explained along with a list of commonly used reinforcements and matrix materials along with their material properties. The fabrication techniques used for composite material products are shown, along with a special focus on the filament winding process. The mere focus on the use of polymer composites for various applications and knowledge of polymer composites fabrication is not enough for beginning of any new research work. Hence a detailed literature study on fiber-reinforced polymer composites for pressure vessel cylinders is a must. In the next chapter, we will be discussing on literature survey on pressure vessel cylinders by various researchers in a categorical manner (FE analysis, material used, experimental studies). The objectives of the present research work are framed based on outcomes of the literature survey.

CHAPTER 2

LITERATURE REVIEW

2.1 Overview

This chapter gives more details about the research works conducted by researchers across the globe. The research work is categorized into different sections based on different research topics which are further related to our research work area. The finite element analysis of composite pressure vessel, material characterization, and hygrothermal ageing are few important areas of the present literature survey. The detailed literature survey is followed by a summary of the literature review and motivation. The objective and scope of the present research work are also discussed in the later part of this chapter.

2.2 Literature survey based on different criteria

2.2.1 Literature survey based on constituent materials for composite pressure vessels

Table 2.1 List of research articles based on the material used for composite pressure vessel

S.No.	Paper Title, Author	Constituent material used
1	Analytical and finite element modelling of pressure vessels for seawater reverse osmosis desalination plants-A.M. Kamal, T.A. El-Sayed, A.M.A. El-Butch, S.H. Farghaly(Kamal et al. 2016)	Carbon Epoxy (AS4/3501-6), GFRP, stainless steel(316L).
2	Continuum damage modelling and progressive failure analysis of carbon fiber/epoxy composite pressure vessel-Liang Wang, Chuanxiang Zheng, Hongying Luo, Shuang Wei, Zongxin Wei(Wang et al. 2015)	6061-T6 aluminium liner, T700 Carbon fiber -Epoxy
3	Application of variable slippage coefficients to the design of filament wound toroidal pressure vessels-Lei Zu, Weidong Zhu, Huiyue Dong, Yinglin Ke(Zu et al. 2017)	T300/5208 graphite-Epoxy
4	Numerical simulation and optimal	6061-T6 aluminium liner, T700

	design for composite high-pressure hydrogen storage vessel: A review-P.F. Liu, J.K. Chu, S.J. Hou, P. Xu, J.Y. Zheng(Liu et al. 2012)	Carbon fiber -Epoxy
5	Trans-scale analysis of composite overwrapped pressure vessel at cryogenic temperature-MingFa Rena, Xin Chang, H.Y. Xu, Tong Li(Ren et al. 2017)	IM7 graphite fiber, 977-3 epoxy, aluminum liner
6	Structural design and experimental investigation on filament-wound toroidal pressure vessels-Haixiao Hu, Shuxin Li, Jihui Wang, Lei Zu(Hu et al. 2015)	Ti alloy liner, aramid Fibers (Kevlar-49, Dupont)/ Epoxy Resin (E-44, Sinopec)
7	Experimental and analytical investigation of the cylindrical part of a metallic vessel reinforced by filament winding while submitted to internal pressure-A. Hocine, D. Chapelle, M.L. Boubakar, A. Benamar, A. Bezazi(Hocine et al. 2009)	Aluminum 6061 tube as a liner, T700 carbon fiber, M10 epoxy resin
8	Design and Finite Element Analysis of FRP LPG Cylinder-Moyahabo Bradley Moketla & Mukul Shukla(Moketla and Shukla 2012)	E-glass fiber, vinylester resin and HDPE liner
9	Development of an automated design system of a CNG composite vessel using a steel liner manufactured using the DDI process-J.C. Choi · Chul Kim · S.Y. Jung(Choi et al. 2004)	GFRP, steel liner Cr-Mo4
10	Optimization of Composite Material System and Lay-up to Achieve Minimum Weight Pressure Vessel-Haris Hameed Mian&Gang Wang&Uzair Ahmed Dar& Weihong Zhang(Mian et al. 2013)	S-glass/Epoxy, Kevlar/Epoxy Carbon/Epoxy, Aluminium.
11	Numerical/experimental impact events on filament wound composite pressure vessel-Giovanni Perillo, Frode Grytten, Steinar Sørbø, Virgile Delhaye(Perillo et al. 2015)	Polyethylene liner, E-Glass fiber and vinyl ester resin.
12	Composite Pressure Vessels-Rao Yarrapragada K.S.S, R.Krishna	GFRP, carbon-Epoxy, Armid-Epoxy.

	Mohan, B.Vijay Kiran(K.S.S. et al. 2012)	
13	Composite LPG Cylinders as an Alternative to Steel Cylinders: Finite Element Approach-Naser S. Al-Huniti and Osama M. Al-Habahbeh (Naser S. A-Huniti 2014)	GFRP plain weave woven ply, steel

With increasing industrial demands for high-quality products at reliable properties such as high strength, stiffness, there is a need for alternative materials to overcome one of the major problems, such as the weight of the product. If we focus mainly on pressure vessels, the composite material can play a huge role. For decades the various combination of polymer composite materials has been tried for different applications of pressure vessels. The carbon-epoxy combination along with aluminium 6061 T6 liner has been suggested by many researchers (Hocine et al. 2009; Liu et al. 2014a; Ren et al. 2017) and are widely used because of its high strength to low weight ratio, also due to high corrosion resistance. Various researchers(Hocine et al. 2009; Liu et al. 2014b; Mehar et al. 2015; Reddy et al. 2015; Ren et al. 2017; Wang et al. 2016) used the carbon fiber(CFRP-carbon fiber reinforced polymer) material combination with different liner and resins in order to enhance the mechanical properties of the composite pressure vessel. The other polymer composites, such as glass fiber reinforced polymer (GFRP) also used as an alternative to existing metal to reduce the weight of the vessel and hence to improve mechanical properties such as strength, stiffness, reduce cost (compared to CFRP). The numerous researchers used GFRP as a prime reinforcement along with distinct liners such as GFRP-Stainless steel liner(Kamal et al. 2016), GFRP-High Density Polyethylene(HDPE)(Moketla and Shukla 2012; Naser S. A-Huniti 2014; Perillo et al. 2014), Glass fiber with vinyl ester as resin along with polyethylene liner(Perillo et al. 2014). Some limited research was also done with a combination of kevlar-epoxy along with Titanium liner in order to study toroid pressure vessels (Hu et al. 2015).

16

2.2.2 Literature survey based on composite pressure vessels in different fields

Table 2.2 List of research articles based on the application of composite pressure vessel in different fields

S.No.	Paper Title, Author	Application areas
1	Analytical and finite element modelling of pressure vessels for seawater reverse osmosis desalination plants-A.M. Kamal, T.A. El-Sayed, A.M.A. El-Butch, S.H. Farghaly(Kamal et al. 2016)	Seawater reverse osmosis (SWRO) for desalination plants
2	Continuum damage modelling and progressive failure analysis of carbon fiber/epoxy composite pressure vessel-Liang Wang, Chuanxiang Zheng, Hongying Luo, Shuang Wei, Zongxin Wei(Wang et al. 2015)	Hydrogen storage/ hydrogen fuel cell with 74L capacity
3	Application of variable slippage coefficients to the design of filament wound toroidal pressure vessels-Lei Zu, Weidong Zhu, Huiyue Dong, Yinglin Ke(Zu et al. 2017)	Nuclear underwater, transportation, storage, etc.
4	Numerical simulation and optimal design for composite high-pressure hydrogen storage vessel: A review-P.F. Liu, J.K. Chu, S.J. Hou, P. Xu, J.Y. Zheng(Liu et al. 2012)	Hydrogen storage vessel
5	Trans-scale analysis of composite overwrapped pressure vessel at cryogenic temperature-MingFa Rena, Xin Chang, H.Y. Xu, Tong Li(Ren et al. 2017)	Liquid hydrogen (LH2) fuel tank
6	Structural design and experimental investigation on filament wound toroidal pressure vessels-Haixiao Hu, Shuxin Li, Jihui Wang, Lei Zu(Hu et al. 2015)	1.For the space-limited storage. 2.Endless cylinder that saves the materials on end caps.
7	Experimental and analytical investigation of the cylindrical part of a metallic vessel reinforced by filament winding while submitted to internal pressure-A. Hocine, D. Chapelle, M.L. Boubakar, A. Benamar, A. Bezazi(Hocine et al. 2009)	Hydrogen storage vessel in the field of energy carrier, storage of CNG, LNG
8	Design and Finite Element Analysis of FRP LPG Cylinder-Moyahabo Bradley Moketla & Mukul Shukla(Moketla and Shukla 2012)	LPG cylinder

9	Development of an automated design system of a CNG composite vessel using a steel liner manufactured using the DDI process-J.C. Choi · Chul Kim · S.Y. Jung(Choi et al. 2004)	CNG composite vessel
10	Optimization of Composite Material System and Lay-up to Achieve Minimum Weight Pressure Vessel-Haris Hameed Mian&Gang Wang&Uzair Ahmed Dar& Weihong Zhang(Mian et al. 2013)	Aerospace industry
11	Composite Pressure Vessels-Rao Yarrapragada K.S.S, R.Krishna Mohan, B.Vijay Kiran(K.S.S. et al. 2012)	Deep submarine exploration housings and autonomous underwater vehicles
12	Composite LPG Cylinders as an Alternative to Steel Cylinders: Finite Element Approach-Naser S. Al-Huniti and Osama M. Al-Habahbeh	Store and transport liquefied petroleum gas (LPG).
13	Stress analysis of LPG cylinder with composites-M Dhanunjayaraju, TL Rakesh Babu(Dhanunjayaraju and Babu 2015)	Liquid petroleum gas (LPG) cylinder
14	Experimental Study on Composite Containment Vessels-Qi Dong, Yan Gu(Dong and Gu 2014)	Composite explosion containment vessels (CECVs)
15	Design and analysis of full composite pressure-vessels-M .Kuhn ,N .Himmel ,M .Maier(M. Kuhn, N. Himmel 2000)	CNG- pressure vessels
16	Comparison of bursting pressure results of LPG tank using experimental and finite element method-M. Egemen Aksoley, Babur Ozcelik, Ismail Bican(Aksoley et al. 2008)	LPG tank
17	Experimental and numerical analysis of a LLDPE/HDPE liner for a composite pressure vessel-E.S. Barboza Neto, M. Chludzinski, P.B. Roese, J.S.O. Fonseca, S.C. Amico, C.A. Ferreira(Barboza Neto et al. 2011)	All composite carbon/ epoxy Compressed Natural Gas (CNG) shell
18	Stress analysis in specimens made of multi-layer polymer/composite used for hydrogen storage application: Comparison with experimental results-Benoit Gentilleau, Maxime Bertin, Fabienne Touchard, Jean-	Hydrogen type IV high-pressure storage vessel

	Claude Grandidier(Gentilleau et al. 2011)	
19	Effect of the loading rate on ultimate strength of composites. Application: Pressure vessel slow burst test- H.Y. Chou, A.R. Bunsell, G. Mair, A. Thionnet(Chou et al. 2013)	Pressure vessels for the storage of hydrogen or other gases
20	Cold hydrogen delivery in glass fiber composite pressure vessels: Analysis, manufacture and testing- Andrew Weisberg, Salvador M. Aceves(Weisberg et al. 2013)	Hydrogen storage
21	Evolution of manufacturing processes for fiber reinforced thermoset tanks, vessels, and silos: a review-Marc Gascons, Norbert Blanco & Koen Matthys(Gascons et al. 2012)	Tanks, vessels, and silos come in all shapes and sizes
22	New generation of filament-wound composite pressure vessels for commercial applications-V.V. Vasiliev, A.A. Krikanov, A.F. Razin(Vasiliev et al. 2003)	Nuclear, underwater, transportation, storage, etc
23	Buckling of filament-wound composite cylinders subjected to hydrostatic pressure for underwater vehicle applications- Chul-Jin Moon, In-Hoon Kim, Bae-Hyeon Choi, Jin-Hwe Kweon , Jin-Ho Choi(Moon et al. 2010)	Underwater vehicles
24	Burst Pressure Prediction of Composite Pressure Chambers Using Acoustic Emission Technique: A Review-R. Joselin, T. Chelladurai(Joselin and Chelladurai 2011)	Aerospace
25	Finite Element Modeling of a Lightweight Composite Blast Containment Vessel-Mohamed B. Trabia, Brendan J. O'Toole, Jagadeep Thota(Trabia et al. 2008)	Blast containment vessels for the temporary storage of explosive materials.
26	Experimental Study on Composite Containment Vessels-Qi Dong, Yan Gu(Dong and Gu 2014)	Composite explosion containment vessels (CECVs)
27	Response of fiber-reinforced composites to underwater explosive loads-R.C. Batra, N.M. Hassan(Batra and Hassan 2007)	Marine vessels
28	Experimental, numerical and analytical investigation of free vibrational behavior of GFRP-stiffened composite cylindrical	Used in civil, aviation, and aerospace industries (e.g., pressure vessels, launch vehicles,

	shells-M. Hemmatnezhad, G.H. Rahimi, M. Tajik, F. Pellicano(Hemmatnezhad et al. 2015)	Re-entry vehicles, aircraft fuselages, spacecraft, etc.).
29	Numerical Modelling of stress- strain behaviour of Composite Overwrapped Pressure Vessel(COPV)-Egor Moskvichev(Moskvichev 2016)	To store pressurized xenon gas for an electric propulsion system on a satellite
30	Design, Analysis, Fabrication and Testing of CFRP with CNF Composite Cylinder for Space Applications-S. Sankar Reddy, C. Yuvraj, K. Prahlada Rao(Reddy et al. 2015)	1. RVS (re-entry vehicle system) structural protection to the weapon system during re-entry. 2. Filament Wound Rocket Motor Case.

The presently used pressure vessels in several applications need up-gradation to overcome various aspects. Some of these aspects are weight, corrosion resistance. Hence the researchers are working in different fields to enhance the properties like strength, stiffness and reduce the losses due to the corrosion effect. The storage and transportation of highly flammable fuels like hydrogen is still a tedious job as there is a risk of explosion, damage of vessels due to handling, and many more reasons. In order to overcome such issues, the composite material has been introduced in place of metals. Many researchers(Chou et al. 2013; Gentilleau et al. 2011; Hocine et al. 2009; Ren et al. 2018; Weisberg et al. 2013; Xu et al. 2009) have worked on various aspects of using composite material for hydrogen fuel storage to enhance the best utilization of material properties some of them are Liang Wang et al., P.F. Liu et al., Benoit Gentilleau et al., H.Y. Chou et al., A. Hocine et al., Andrew Weisberg et al. The Compressed Natural Gas(CNG) cylinders used in automobiles, and other fields are most often subjected to failure due to sudden leakage of fuel leading to major explosions. To overcome this problem, many researchers (Bae and Kim 2013; Barboza Neto et al. 2011; Choi et al. 2004; M. Kuhn, N. Himmel 2000) such as J.C. Choi et al., Jun-Ho Bae et al., E.S. Barboza Neto et al., M. Kuhn et al., have worked on different issues of compressed Natural Gas cylinder. They came up with the fiber-reinforced composite cylinder as an alternative, which converts sudden failure mode to progressive failure mode, also called safe failure mode. Here similar to CNG cylinders, currently used steel LPG (Liquified Petroleum Gas) cylinders need to be replaced by fiber-reinforced

polymer material in order to overcome problems like rustiness of cylinder due to corrosive environment, the weight of the vessel, ease handling, fuel level indicator. The study on composite LPG cylinder as an alternative to steel is carried by various researchers(Aksoley et al. 2008; Dhanunjayaraju and Babu 2015; Moketla and Shukla 2012; Naser S. A-Huniti 2014) such as Moyahabo Bradley Moketla et al., M. Egemen Aksoley et al., Naser S. Al-Huniti et al., M Dhanunjayaraju et al.

Space vehicles such as aircraft, aerospace launch vehicle, and satellite launch vehicle where even a small gram of weight-saving leads to large amount fuel savings, Fiber-reinforced polymer material can be used as an alternative to aluminium and titanium at certain places where we can reduce the weight of the vehicle according to various literature works carried by many researchers(Hemmatnezhad and Ansari 2010; Joselin and Chelladurai 2011; Mian et al. 2013). To store xenon gas for an electric propulsion system on a satellite, we needed to have a very light weight material such as CFRP material with thin titanium liner as suggested by Egor Moskvichev *et al.* (Moskvichev 2016), The rocket motor cases are needed to be made of light weight (Filament wound) in order to reach the target as early as possible with the lesser fuel consumption according to literature study by S. Sankar Reddy *et al.*(Reddy et al. 2015). In the marine field, major challenges faced by any vessel or container are corrosion due to sea water, unstable buckling. According to literature, CFRP material is suggested for underwater vehicles, also for sea water reverse osmosis for desalination by various researchers (Batra and Hassan 2007; K.S.S. et al. 2012; Kamal et al. 2016; Moon et al. 2010). We have been using explosives materials in many applications, mainly military, nuclear power plants. To transport these explosive materials always been a challenging job. There is always a chance for accidents, to overcome these accidents, the vessel or containers which are made by steel are replaced by hybrid composites according to literature study as per suggestions from researchers(Dong and Gu 2014; Trabia et al. 2008) so that we can reduce or avoid the damage due to accidents.

2.2.3 Literature survey based on different processes used for composite pressure vessel manufacturing

Table 2.3 List of research articles based on the fabrication of composite pressure vessel

S.No.	Paper Title, Author	Manufacturing method
1	Application of variable slippage coefficients to the design of filament wound toroidal pressure vessels-Lei Zu, Weidong Zhu, Huiyue Dong, Yinglin Ke(Zu et al. 2017)	Filament winding
2	Numerical simulation and optimal design for composite high-pressure hydrogen storage vessel: A review-P.F. Liu, J.K. Chu, S.J. Hou, P. Xu, J.Y. Zheng(Liu et al. 2012)	Filament winding
3	New generation of filament-wound composite pressure vessels for commercial applications-V.V. Vasiliev, A.A. Krikanov, A.F. Razin(Vasiliev et al. 2003)	Continuous filament winding and tape winding
4	Buckling of filament-wound composite cylinders subjected to hydrostatic pressure for underwater vehicle applications- Chul-Jin Moon, In-Hoon Kim, Bae-Hyeon Choi, Jin-Hwe(Moon et al. 2010)	Filament winding
5	Stress analysis in specimens made of multi-layer polymer/composite used for hydrogen storage application: Comparison with experimental results-Benoit Gentilleau, Maxime Bertin, Fabienne Touchard, Jean-Claude Grandidier(Gentilleau et al. 2011)	Filament winding
6	Experimental, numerical and analytical investigation of free vibrational behavior of GFRP-stiffened composite cylindrical shells-M. Hemmatnezhad, G.H. Rahimi, M. Tajik, F. Pellicano(Hemmatnezhad et al. 2015)	Filament winding
7	Structural design and experimental investigation on filament wound toroidal pressure vessels-Haixiao Hu,	Filament winding

	Shuxin Li, Jihui Wang, Lei Zu(Hu et al. 2015)	
8	The influence of manufacturing variances on the progressive failure of filament wound cylindrical pressure vessels-Brian Ellul, Duncan Camilleri(Ellul and Camilleri 2015)	Filament winding
9	High pressure strength of carbon fiber reinforced vinylester and epoxy vessels- Yongzheng Shao, Andrea Betti, Valter Carvelli, Toru Fujii, Kazuya Okubo, Ou Shibata,Yukiko Fujita(Shao et al. 2016)	Filament winding
10	Experimental and analytical investigation of the cylindrical part of a metallic vessel reinforced by filament winding while submitted to internal pressure-A. Hocine, D. Chapelle, M.L. Boubakar, A. Benamar, A. Bezazi(Hocine et al. 2009)	Filament winding
11	Cold hydrogen delivery in glass fiber composite pressure vessels: Analysis, manufacture and testing- Andrew H. Weisberg, Salvador M. Aceves, Francisco Espinosa-Loza, Elias Ledesma-Orozco(Weisberg et al. 2013)	Filament winding
12	Micromechanics-based progressive failure analysis of carbon fiber/ epoxy composite vessel under combined internal pressure and thermomechanical loading-Liang Wang, Chuanxiang Zheng, Shuang Wei, Zongxin Wei(Wang et al. 2016)	Filament winding
13	Experimental Investigation and FE Analysis of CFRP Composites-Afroz Mehar, G.M.Sayeed Ahmed, G.Prassana Kumar, Md. Aaqib Rahman, M.A.Qayum(Mehar et al. 2015)	Filament winding
14	Numerical Modelling of stress- strain behaviour of Composite Overwrapped Pressure Vessel(COPV)-Egor Moskvichev(Moskvichev 2016)	Filament winding

15	Development of an automated design system of a CNG composite vessel using a steel liner manufactured using the DDI process-J.C. Choi · Chul Kim · S.Y. Jung(Choi et al. 2004)	Filament winding
16	Evolution of manufacturing processes for fiber reinforced thermoset tanks, vessels, and silos: a review-Marc Gascons, Norbert Blanco & Koen Matthys(Gascons et al. 2012)	Hand lay-up-Storage tanks, RTM-Immersion bottle, food industry, Compression molding- Industrial supply air storage, Filament winding-hydrogen storage, Spray-up-grain silo, septic tank, Roll wrapping-motor sport, underwater tank
17	Design and Finite Element Analysis of FRP LPG Cylinder-Moyahabo Bradley Moketla & Mukul Shukla(Moketla and Shukla 2012)	Filament winding, blow moulding
18	Experimental and numerical analysis of a LLDPE/HDPE liner for a composite pressure vessel-E.S. Barboza Neto, M. Chludzinski, P.B. Roese, J.S.O. Fonseca, S.C. Amico, C.A. Ferreira(Barboza Neto et al. 2011)	Filament winding
19	Numerical/experimental impact events on filament wound composite pressure vessel-Giovanni Perillo, Frode Grytten, Steinar Sørbø, Virgile Delhaye(Perillo et al. 2015)	Filament winding
20	Influence of filament winding parameters on composite vessel quality and strength-D. Cohen(Cohen 1997)	Filament Winding
21	Composite Pressure Vessels-Rao Yarrapragada K.S.S, R.Krishna Mohan, B.Vijay Kiran(K.S.S. et al. 2012)	Filament Winding
22	Design, Analysis, Fabrication and Testing of CFRP with CNF Composite Cylinder for Space Applications-S. Sankar Reddy, C. Yuvraj, K. Prahlada Rao(Reddy et al. 2015)	Filament Winding
23	Composite LPG Cylinders as an Alternative to Steel Cylinders: Finite Element Approach-Naser S. Al-Hunit(Naser S. A-Huniti 2014)	Filament Winding
24	Design and Analysis of Filament	Filament Winding

| | Wound Composite Pressure Vessel with Integrated-end Domes-M. Madhavi, K.V.J.Rao and K.Narayana Rao(Madhavi et al. 2009a) | |

Most of the composite pressure vessels manufactured in today's industry are by filament winding technique(Barboza Neto et al. 2011; Quanjin et al. 2018; Reddy et al. 2015; Vasiliev et al. 2003). The main reason for selecting the filament winding process is its simple steps of the fabrication process; by this method, we obtain the desired properties in the final product with ease. One more important aspect of this process is an accumulation of very few stress concentration zones in the final finished product. Many research works have been done on this process, such as the orientation of filament, winding angle, fiber volume fraction, etc. Some of the authors have focussed basically on this method for manufacturing of composites pressure vessels are Lei Zu *et al.* (Zu et al. 2017), V.V. Vasiliev *et al.* (Vasiliev et al. 2003), Chul-Jin Moon *et al.* (Moon et al. 2010), Giovanni Perillo *et al.* (Perillo et al. 2014), D. Cohen *et al.* (Cohen 1997; Cohen et al. 2001). The rapid winding process is one of the types of filament winding process; it is also called a dry winding process where Pre-impregnated resin is wound on a mandrel at a faster rate than the normal case. Hence the production time reduces, which intern reduces the labour cost, also helps in manufacturing uniformly thinner, lesser weight composite pressure vessels as per literature studies by Andrew Weisberg *et al.* (Weisberg et al. 2013). According to the literature review of Marc Gascons *et al.* (Gascons et al. 2012), winding on any pressure vessels can be done by many methods, but each composite fabrication method suits for a particular application. Some of them are hand lay-up for water storage tanks, resin transfer molding for impression bottles, Compression molding for air storage for industrial supply, filament winding for hydrogen storage, roll wrapping for under water tank.

2.2.4 Literature survey based on modelling and FE analysis of composite pressure vessels

Table 2.4 List of research articles based on FE analysis of composite pressure vessel

S.No.	Paper Title, Author	FE analysis details
1	Analytical and finite element modelling of pressure vessels for seawater reverse osmosis desalination plants-A.M. Kamal, T.A. El-Sayed, A.M.A. El-Butch, S.H. Farghaly(Kamal et al. 2016)	1.FE solutions: The same vessel wall thickness is obtained as in the analytical solution. 2.The finite element modelling results are close to that obtained from the analytical solution within an acceptable range
2	Finite element modelling of low-velocity impact on laminated composite plates and cylindrical shells-S.M.R. Khalili, M. Soroush, A. Davar,O. Rahmani(Khalili et al. 2011)	The proposed FE method can serve as a benchmark for impact modeling of composite structures in future investigations.
3	Continuum damage modelling and progressive failure analysis of carbon fiber/epoxy composite pressure vessel-Liang Wang, Chuanxiang Zheng, Hongying Luo, Shuang Wei, Zongxin Wei(Wang et al. 2015)	1. Commercial finite element software ABAQUS is used. 2. The model is applied to predict the ultimate strength and complex failure behaviors of the aluminium-carbon/epoxy composite vessel, with the predicted results correlating well with experiments.
4	Numerical simulation and optimal design for composite high-pressure hydrogen storage vessel: A review-P.F. Liu, J.K. Chu, S.J. Hou, P. Xu, J.Y. Zheng(Liu et al. 2012)	FE simulation of composite pressure vessel
5	Trans-scale analysis of composite overwrapped pressure vessel at cryogenic temperature-MingFa Rena, Xin Chang, H.Y. Xu, Tong Li(Ren et al. 2017)	Analytical study
6	Structural design and experimental investigation on filament wound toroidal pressure vessels-Haixiao Hu, Shuxin Li, Jihui Wang, Lei Zu(Hu et al. 2015)	Ti alloy liner, aramid Fibers (Kevlar-49, Dupont)/ Epoxy Resin (E-44, Sinopec)

7	Experimental and analytical investigation of the cylindrical part of a metallic vessel reinforced by filament winding while submitted to internal pressure-A. Hocine, D. Chapelle, M.L. Boubakar, A. Benamar, A. Bezazi(Hocine et al. 2009)	Analytical studies
8	Design and Finite Element Analysis of FRP LPG Cylinder-Moyahabo Bradley Moketla & Mukul Shukla(Moketla and Shukla 2012)	Burst pressure = 3 MPa, The thickness of the cylinder = 3.5 mm (1.5 mm of liner and 2 mm of FRP composite layer)-FEA
9	Optimization of Composite Material System and Lay-up to Achieve Minimum Weight Pressure Vessel-Haris Hameed Mian&Gang Wang&Uzair Ahmed Dar& Weihong Zhang(Mian et al. 2013)	CLT (Classical Lamination Theory) used for comparison of results with FE results of composite pressure vessel, FE analysis of Metallic Al pressure vessel.
10	Numerical/experimental impact events on filament wound composite pressure vessel-Giovanni Perillo, Frode Grytten, Steinar Sørbø, Virgile Delhaye(Perillo et al. 2015)	1.Impact on composite pressure vessel studied using 3-D Fe model. 2.Predictive model was accurate by 5% error in case of impact energy.
11	Composite Pressure Vessels-Rao Yarrapragada K.S.S, R.Krishna Mohan, B.Vijay Kiran(K.S.S. et al. 2012)	1.Analytical model and FEM used for the minimum buckling load with/without stiffener composite shell of continuous angle ply laminas. 2. Windenburg and Trilling Equation: used for finding critical buckling load for composites. 3.Increase in shell thickness is shown to increase the buckling resistance of the composite shell.
12	Composite LPG Cylinders as an Alternative to Steel Cylinders: Finite Element Approach-Naser S. Al-Huniti and Osama M. Al-Habahbeh(Naser S. A-Huniti 2014)	FE analysis of composite LPG for impact load radial, axial load, and internal pressure are studied for steel and composite vessel.
13	Stress analysis of LPG cylinder with composites-M Dhanunjayaraju, TL Rakesh Babu(Dhanunjayaraju and Babu 2015)	FE analysis of different materials like steel, GFRP, and CFRP vessels, Weight of LPG cylinders can be saved.
14	Design and Analysis of Filament Wound Composite Pressure Vessel	1.CLT, matrix crack failure is used. 2.The hoop fibers maximum load-

	with Integrated-end Domes-M. Madhavi, K.V.J.Rao and K.Narayana Rao(Madhavi et al. 2009a)	bearing capacity only in Y-direction, and the helical fibers can contribute in both X and Y direction based on load-carrying capacity.
15	Design and analysis of full composite pressure-vessels- M.Kuhn,N.Himmel,M.Maier(M. Kuhn, N. Himmel 2000)	1.A full parametric analysis module has been developed. 2.Full FRP pressure vessels with plastic liners can be dimensioned and studied.
16	Numerical simulation and optimal design for composite high-pressure hydrogen storage vessel: A review-P.F. Liu, J.K. Chu, S.J. Hou, P. Xu, J.Y. Zheng(Liu et al. 2012)	FE analysis and optimization of composite vessels
17	Finite Element Modeling of a Lightweight Composite Blast Containment Vessel-Mohamed B. Trabia, Brendan J. O'Toole, Jagadeep Thota(Trabia et al. 2008)	Simulation results indicate that these models are within 20% deviation with respect to experimental ones.
18	Optimal Design for Compressed Natural Gas Composite Vessel by Using Coupled Model with Liner and Composite Layer-Jun-Ho Bae and Chul Kim(Bae and Kim 2013)	FEA of CNG composite pressure vessel was performed using the commercial code Ansys Workbench.
19	Development of an automated design system of a CNG composite vessel using a steel liner manufactured using the DDI process-J.C. Choi · Chul Kim · S.Y. Jung(Choi et al. 2004)	Non-linear Finite element analysis, by using ANSYS- composite pressure vessels.
20	Numerical Modelling of stress-strain behavior of Composite Overwrapped Pressure Vessel (COPV)-Egor Moskvichev(Moskvichev 2016)	COPV was developed using APDL (ANSYS Parametric Design Language)
21	Experimental Investigation and FE Analysis of CFRP Composites-Afroz Mehar, G.M.Sayeed Ahmed, G.Prassana Kumar, Md. Aaqib Rahman, M.A.Qayum(Mehar et al. 2015)	1.The experimental results of all the specimens for tensile test, flexural test was compared with ANSYS results. 2.Tensile and flexural results for numerical analysis are better than experimental results.
22	Structural design and experimental investigation on filament-wound toroidal pressure vessels-Haixiao Hu, Shuxin Li, Jihui Wang, Lei Zu(Hu et	The winding parameters can be accurately determined using the FEM-based method proposed in this paper. Analytical: progressive failure of

		filament wound cylindrical pressure vessels
23	Stress analysis in specimens made of multi-layer polymer/composite used for hydrogen storage application: Comparison with experimental results-Benoit Gentilleau, Maxime Bertin, Fabienne Touchard, Jean-Claude Grandidier(Gentilleau et al. 2011)	FE model has been developed to analyze multilayer composite–polymer technological specimens subjected to quasi-static tensile tests and fatigue tensile tests
24	Buckling of filament-wound composite cylinders subjected to hydrostatic pressure for underwater vehicle applications- Chul-Jin Moon, In-Hoon Kim, Bae-Hyeon Choi, Jin-Hwe Kweon , Jin-Ho Choi(Moon et al. 2010)	FE analysis of buckling load is done using commercially available software since all bucking modes are not similar to experimental ones. 2.The deformation that precedes the bucking of the cylinder can be studied.
25	Application of variable slippage coefficients to the design of filament wound toroidal pressure vessels-Lei Zu, Weidong Zhu, Huiyue Dong, Yinglin Ke(Zu et al. 2017)	1. The present design method is demonstrated by filament-wound carbon-epoxy toroidal pressure vessels with relative bending radii of 3–6, reflecting on the incredibly general design approach. 2. The resulting fiber trajectories and vessel mass are then determined and compared to each other in order to find the best distribution type of fiber slippage coefficients for winding a toroidal pressure vessel.

The Finite Element analysis of composite vessels is done to understand the behavior of vessels for a particular load and to compare critical results such as stresses, deformations with theoretical results. Different composite pressure vessels have different loading conditions as per applications, such as pressure vessels for sea water reverse osmosis (Kamal et al. 2016) which is subjected to FE analysis; results obtained are nearer to analytical results. The composite vessel is basically subjected to many types of loads, but low-velocity impact load observation is essential as such load can damage the vessel permanently. S.M.R Khalili *et al.*(Khalili et al. 2011) has done FE analysis of the low-velocity impact on cylindrical shells, and he has set a benchmark for this particular case study structural composites. Even though we do complete FE analysis of composite

pressure vessel used in various application, we need to understand each layer behavior in detail. By this way of analyzing, we can easily optimize the composite pressure vessel. In the aerospace industry, this kind of study is necessary, as per literature data of the researcher (Mian et al. 2013) has done FE analysis of laminated composite and compared various results with analytical outputs, which is carried as per CLT (Classical Lamination Theory). Most of the composite pressure vessels manufactured are made of using two materials one is out layer, which is called composite layer, and the inner layer is called as a liner. The behavior of the interface between these layers can be studied analytically by coupled model. This method has been adopted by Jun Ho Bae *et al.*(Bae and Kim 2013) for the analytical study of compressed Natural Gas composite vessels, and the results obtained are compared with FE results. It is found that only 6% error exists at liner and 9% error at composite layer stage. The weight of steel LPG cylinders can be reduced by using different composite materials. As per FE analysis of GFRP, CFRP LPG cylinder by M Dhanunjayaraju *et al.*(Dhanunjayaraju and Babu 2015), CFRP is the best alternative to existing steel LPG cylinder as it saves up 75-85% weight of the vessel. In order to understand the filament wound composite pressure vessel as per different windings such as hoop and helical, we need to adopt failure criteria such as matrix crack failure, progressive failure. Based on these criteria, fiber oriented in hoop directions can have the maximum load-bearing capacity in that direction only, Whereas fibers that are orientated in helical directions can bear load in all other directions also. A case study has been done (Kandasamy et al. 2016) as per the above case, and the results are analyzed. The full parametric analysis of composite CNG vessel (M. Kuhn, N. Himmel 2000) has been studied for various composite materials such as Aramid Fiber Reinforced Plastic, GFRP, CFRP, and results of FE analysis are compared with the existing steel cylinder.

Even though we have developed the composite pressure vessel as an alternative to steel vessels, we need to understand the various damage behaviour of these composite vessels so that preventive measures can be adopted in advance. As per the literature study (Wang et al. 2015)*,* continuous damage model and progressive failure analysis of carbon fiber/ epoxy composite pressure vessel is studied in ABAQUS software. We found that the

ultimate strength and predicted results of these criteria are almost nearer to the experimental one. The composite vessels are used for underwater applications are basically subjected to buckling load. Hence it necessary to study the buckling load behavior of composite vessels. FE analysis of underwater composite pressure vessels subjected to hydrostatic pressure is done by (Moon et al. 2010). Buckling load is excreted on the vessel; whichever load produces the deformation, that load behavior is studied, and necessary modifications are made to the vessel. Most of the hydrogen fuel storage composite vessels are made of filament wound composites. But in order to study the stress analysis of hydrogen high-pressure composite vessel, the specimens of this composite material are prepared and are subject to quasi-static tensile and fatigue test, the experimental results obtained are compared with FE results (Gentilleau et al. 2011). The FE analysis and fabrication of Composite LPG cylinder as per the various standards is a very difficult task because we have to cover every aspect of standards depending on countries' requirements. But a genuine attempt has been made by Moyahabo Bradley Moketla *et al*.(Moketla and Shukla 2012). Here, burst pressure for composite LPG cylinder is around 3 MPa; total vessel thickness is 3.5mm (1.5 mm HDPE liner and 2 mm FRP). The impact load on any composite vessel leads to interlaminar damage or may be delamination. Hence it is necessary to understand the behavior of composite vessels under such circumstances. According to a Literature study (Perillo et al. 2014), impact load on composite pressure vessels can be studied experimentally or numerically and compared with an analytical solution using puck and failure theories. These theories evaluate the interlaminar damages such as matrix cracking, fiber failure. The cohesive zone theory can be used for modeling delamination. Over the numerical results are in good agreement with experimental data.

2.2.5 Literature survey based on mechanical characterization and hygrothermal ageing

Table 2.5 List of research articles based on mechanical characterization and hygrothermal ageing

S.No.	Paper Title, Author	Mechanical characterization and hygrothermal ageing effects
1	Influence of hydrothermal ageing on the compressive behaviour of glass fiber/epoxy composite pipes (composite structures 2017)(Fitriah et al. 2017)	1.Tap water ageing, at 80°C for 500,1000,1500hr. 2. Testing at RT, 45°C, 65°C, and SEM images 3.Overall strength reduces, but 45 WA is good compared to ±55° and ±65° as fibers are almost in the loading direction.
2	Variation of the mechanical properties of E-glass/epoxy composites subjected to hygrothermal aging (Sage journal 2015)(Dogan and Atas 2015)	1. fabricated using vacuum bagging, ageing at 95°C for 1200h in the climate test chamber for 70°C humidity. 2. Tensile, compression, shear, drop wt impact are major load studies. Transverse moduli E2 affected due to material degradation, and shear moduli is least affected.
3	The modelling of hydrothermal aging in glass fiber reinforced epoxy composites (IOP science 1982)(Search et al. n.d.)	1.Analytical model such as Fickian model to study the effect of heat on the diffusion of water molecules in the composites
4	Investigation of thermal-oil environmental ageing effect on mechanical and thermal behaviour of E-glass fiber/epoxy composites (Springer nature 2018)(Akderya 2018)	1.The GEC studied for hot oil ageing effect on mechanical, thermal, and internal properties by varying temp from -10°C till 140°C for a varied period of 0-1080h. 2.Tensile, TGA, DTA, and SEM are determined and compared for variation in properties. 3.Low temp has improved the properties with time and vice versa w.r.t to high temp in all cases.
5	Effect of sea and distilled water conditioning on the overall mechanical properties of carbon	1.The study involves sea and distilled water treatment of CNTs at RT and studied for effect on various properties such as hardness, flexural,

	nanotube/epoxy composites (sage 2015)(Bal and Saha 2015)	and Tg. 2. Comparison with unexposed samples reveals that the properties and Tg are reduced due to the effect of both seas and distilled water but in different ways.
6	Changes in mechanical properties of GFRP composite after exposure to warm seawater (sage 2016)(Ronagh and Saeed 2016)	1.The GE panels are divided into 3 groups such as oven curing at 60C for 16h, 2nd is 60days, and last group 4 months in a sea water ageing. 2.The tensile test conducted for all with tensile modulus is least affected by SW and ultimate tensile strain, shear modulus are effected little higher. Overall reduction in properties is least.
7	Experimental Characterization of CFRP by NOL Ring Test (material today-2019)(Charan et al. 2019)	Here the CFRP, i.e., 700T carbon fiber NOL ring test, is more reliable than the unidirectional tensile test in the case of rocket ring cases.
8	Experimental study on compressive behaviour and failure analysis of composite concrete confined by glass/epoxy ±55° filament wound pipes (composite structures-2018)(Gemi et al. 2018)	1.Here, GE pipe confines the concrete under axial compression load to strength and ductility. 2.Comparison between confined and unconfined concrete pipes shows improved strength by 2.85 times average value.
9	Theoretical and FE analysis of epoxy composite pressure cylinder used for aerospace applications (material today-2019)(Rajendra Prasad and Syamsundar 2019)	1.This paper mainly focuses on the study of high-pressure composite pressure vessels used in aerospace and automobiles for varied material and internal pressure. 2.The outcome is FRPs have high specific strength compared to metals at varied internal pressure data.
10	Burst strength and impact behaviour of hydrothermally aged glass fiber/epoxy composite pipes(materials and design 2016)(Hawa et al. 2016)	1.Estimation of low-velocity impact (5J, 7.5J, and 10J) on tap water aged at 80C for 500-1500h of GE pipe (55 WA) samples. 2.The aged samples with high impact energy (10J) have lower burst strength. Confirmed by SEM also.
11	Use of split-disk tests for the process parameters of filament wound epoxy composite tubes (polymer testing-2005)(Kaynak et al. 2005)	1. The HTS is determined for specimens made of 2 different epoxies, five different fibers, five different winding angles. 2.The use of different epoxies has no difference

		or impact, but carbon fiber has a better impact than glass fiber, the winding angle larger than 60 has an increase in structural performance.
12	Mechanical properties of offshoring polymer composite pipes at various temperatures (Composite part-B: 2018)(Benyahia et al. 2018)	1.The GE pipe with 55WA is studied for varied temp from -40C to 80C for offshoring applications. 2.thermal ageing is studied in a SERVONTAN climatic chamber for 8h for different temps, and a uniaxial test is carried out. The mech prop decreases with an increase in temp, and the material becomes rigid with a decrease in temperature.
13	Material characterization of filament-wound composite pipes (composite structures-2018)(Toh et al. 2018)	1.The tensile and compression test are performed on laminated and GE pipe and estimated with homogenization theory. 2. Reverse mode of finding the ply properties using the properties of filament wound pipe and also using the FE simulation for validation of bulk properties obtained.
14	On the effect of the ply stacking sequence on the failure of composite pipes under external pressure (marine structure-2020)(Silva et al. 2020)	1.Here, the experimental tests are performed and compared with analytical and numerical prediction values. 2.Good agreement found among all exp, analytical and numerical outcomes. 3.Parametric analysis is done to understand the effect of ovality, stacking sequence on failure pressure of the composite pipe.
15	Effects of hydrothermal ageing on the behaviour of composite tubes under multiaxial stress ratios (composite structures-2016)(Krishnan et al. 2016)	1.GE tube ageing at 80°C for 1500h and tested for varied 5 stress ratios. 2. The effect of ageing can be seen on failed samples in an SEM micrograph in the form of debonding b/w fiber and matrix, access uptake of moisture by matrix leading osmatic matrix cracking and hence damage.
16	Higher performance carbon fiber reinforced thermoplastic composites from thermoplastic prepreg technique: Heat and	1. High-performance CFRTPCs are studied for tensile and three-point tests due to the effect of hot air and hot water ageing for varied temp and time periods.

	moisture effect (composite part B:2018)(Ma et al. 2018)	2. Hot water immersion has influenced the matrix, which led to a reduction in interfacial bonding between fiber and matrix. Another ageing has no influence.
17	Failure of a sag water pipe triggered by aging of the GFRP composite relining (Engineering failure analysis-2018)(Ch et al. 2018)	The GFRP section failure due to load propagation or imbalance from steel pipe portion till core part of material took almost 12 years of ageing which was detected after due to some leakage problem. Detail investigation with bending study and all.
18	Hoop strength characterization of high strength carbon fiber Composites (Composites 1992)(Etemad et al. 1992)	Experimental and computational investigation to find the basic mech prop and hoop strength of ultra-high carbon fiber composites are studied.
19	Moisture effects on the thermal and creep performance of carbon fiber/epoxy composites for structural pipeline repair (composites part: B-2013)(Keller et al. 2013)	1.CFRP composites are studied for flexural creep after having been exposed to water for a period of 18 months and flexural test performed in DMA. Time-temperature superposition was used to generate master curves. 2.The activation energy is almost unaltered for an immersed period of 11-18 months when compared with non-immersion. Also,16% UTS is enough for the design life of 50 years from TTS prediction.
20	Effectiveness of using fiber-reinforced polymer composites for underwater steel pipeline repairs (composite structures-2013)(Islam et al. 2013)	1.Metals have been used in underwater applications in long-distance areas for a vast period of time. The repair of steel pipes under a harsh corrosion environment is always challenging. Hence FRPCs provide easy patchwork in repairing steel pipe in underwater applications. 2.This paper provides details for in-air, on the ground, and underwater repair guides using FRPCs. The feasibility, shortcomings of FRPCs are also discussed.
21	Apparent hoop tensile strength prediction of glass fiber-reinforced polyester pipes (sage 2013)(Rafiee	1.Most industries use the hydraulic failure pressure method for finding apparent HTS. But as per this paper is developing sequential failure

		modeling for predicting apparent HTS, which is also integrated with classical lamination theory and progressive damage modeling. 2.Experimental study carried out to validate the developed model, and a very good agreement is observed between experimental outcome and developed sequential failure model.
22	Lepox L-12 detail data from suppliers(Sheet and Business 2017)	Epoxy resin and hardener different properties list at RT and higher temperatures.
23	Standard Test Method for Apparent Hoop Tensile Strength of Plastic or Reinforced Plastic Pipe (ASTM D2290)(ASTM Standard 2016)	Detail procedures along with dimensions are listed in this file.
24	Atul Ltd. TECHNICAL DATA SHEET Polymer Division Lapox L-12 K-6(Sheet and Business 2017)	Various properties are listed in the materials properties section in the paper are taken from the supplier
25	Modified split disk test for characterization of FRP composites(Journal of structural engineering-2017)(Ramesh et al. 2017)	1.Comparison of CFRP and GFRP tensile strength between split disk test and laminated uniaxial test specimens. 2.Found that laminated uniaxial test specimen has better tensile strength than split disk test sample. Also, the ultimate strain value is higher in uniaxial test samples.
26	Mechanics of composite materials by Kaw, Autar K.(Kaw and Group 2006)	A Text Book
27	Detection of Hydrothermal Aging in Composite Materials (1974)(Kaelble 1974)	To old data to cite and useful only for studies
28	Effect of Hydrothermal Ageing on Glass Fiber Reinforced Plastic (GFRP) Composite Laminates exposed to Water and Salt Water (IJCET 2013)(Rao 2013)	1.The aim is to study the effect of the different environments to find their influence on properties. 2. hydrothermal ageing has led to a reduction in tensile and flexural properties. Sea water has made higher degradation than normal water.
29	Effects of hygrothermal history on the structural performance of	1.Typical hydrothermal ageing tests were carried out on all composite laminates.

	aerospace composite materials: preliminary experiments and mass diffusion models (ICCM 2017)(Canale 2018)	2.The stiffness and tensile strength are unaffected by ageing. But if exposing period increases, then there is the possibility of a reduction in tensile strength.
30	Flexural and Hydrothermal Aging Behaviour of Silk Fabric/Glass Mat Reinforced Hybrid Composites(fibers and polymers 2016)(Zhao et al. 2016)	1.Here unsaturated polyester resin is used, and a 3-point bend test is carried out for both aged and unaged samples. 2.With immersion, both flexural and impact properties improved initially, and after reaching saturation point, the strength started decreasing as immersion time increases.
31	hydrothermal ageing mechanism of natural fiber reinforced composite in hot water (IMECE 2012 ASME proceedings)(Liao et al. 2012)	1.Because we all know that NFRP has low cost, ease of access, acceptable strength, biodegradability are few properties that drag us towards them. 2.Even though we know that JFRP hygroscopic in nature, we needed to study the probable holding time for NFRP, which is almost 24hours max.
32	Hydrothermal Aging effect on flexural properties of GFRP laminates (Indian journal of material science and engineering 2013)(Rao and Hussain 2013)	1.GFRP samples are subjected to ageing in a water medium at varying temperatures and time periods. 2.THe strength has decreased from 23% to 70% 45°C exposers and 60% to 77% for 60°C exposers. The main reasons for degradation are moisture absorption and temperature exposure time.
33	Strength Prediction Method for Unidirectional GFRP after Hydrothermal Aging (advanced composite material 2011)(Kotani et al. 2011)	1.The global load-sharing model is used to compare the experimental results. 2.Material degradation of fiber and fiber/matrix are predicted and are in good agreement with experimental results.
34	Hygrothermal ageing effect on mechanical properties of FRP laminates (AIP conference proceedings-2015)(S. Larbi, R. Bensaada 2015)	1.The Carbon/epoxy and glass fiber/vinyl ester are studied for a three-point bend test after ageing in sea water and de ionized water at 40C. 2.The significant loss of mechanical properties is observed.
35	Hygrothermal durability and failure	1.Here, 2D woven mats of carbon/polyester,

		glass/isopolyester, and gel-coated glass/isopolyester reinforced composites are exposed to 60°C and 70°C with 95% RH for a period of 100h.
	modes of FRP for marine applications (Sage 2012)(Santhosh et al. 2012)	2.The samples are withdrawn periodically and weighed for moisture absorption, and tested for variations in mechanical properties such as UTS, flexural strength, ILSS.
		3. A greater resistance against degradation is observed in the case of Carbon/isopolyester. SEM study was done to know degradation in detail.
36	Hygrothermal Studies on GFRP Composites: A Review (Matec web of conference 2018)(Shettar et al. 2018)	1.Hydrothermal ageing effect on GFRP composites is elaborated as per various tests done by many researchers. 2.Effect of cold soaking, boiling, thermal shocks, climate chamber usage, and their benefits, and lastly, ageing effects on fibers, matrix, and combined effects are discussed.
37	Mechanical properties of filament wound pipes: effects of winding angles (quality of life 2015)(Naseva et al. 2015)	1.Here, three different winding angles are proposed. 2.The bigger winding angle leads to higher HTS.

Mechanical characterization studies by various researchers(Dogan and Atas 2015; Hamed et al. 2007; Rafiee 2016; Toh et al. 2018; Zhao et al. 2016) have mainly focused on the particular material grade and fixed composition with respect to their application point of view. Hygrothermal ageing effect on the various natural, GFRP, and CFRP laminated composites was explored by many researchers(Dogan and Atas 2015; Fitriah et al. 2017; Kotani et al. 2011; P. Sampath Rao, M. Manzoor Husain 2012; Rao and Hussain 2013; Ronagh and Saeed 2016). Based on open literature, it is found that the research work was limited to single material composition, fixed experimental time period, and single working fluid (tap water, sea water, etc.) as in the case of hygrothermal studies.

2.3 Summary of literature review and motivation

Most of the research works were focused on FE studies between steel and polymer composites in pressure vessels. It is found that GFRP, CFRP are the two most suitable materials (alternative) for polymer composite cylinders as per various researchers. The composite pressure vessels have liners which is the innermost layer in any polymer composite vessels. Hence, different liners such as HDPE, Aluminium, polyethylene are being suggested by many researchers as per requirements. The filament winding technique is suggested for the fabrication of composite pressure vessels based on open literature. Mechanical characterization studied by various researchers was mainly focused on the particular material grade and fixed composition with respect to their application point of view. Hygrothermal ageing effect on the various natural, GFRP, and CFRP laminated composites was explored by many researchers. But research work was limited to single material composition, fixed experimental time period, and single working fluid (tap water, sea water, etc.) in most of the cases.

Motivation

There is scope for research in the field of composite pressure vessels. To study FE analysis of composite pressure vessels, for a varied range of material compositions (such as fiber volume fraction, winding angle, stacking sequence). Also, experimental studies at the lab scale to study the hygrothermal ageing effects by varying working environments to observe its effect on mechanical properties. These research gaps motivated to frame the research objectives to study in the field of composite pressure vessels.

2.4 Objectives and scope of the present work

Objectives

1. To design and analyze the filament wound GFRP cylinder and compare its properties with steel and Aluminium 6061 T6 cylinders.
2. To perform FE analysis of GFRP cylinder (with/without liner) with 4 volume fractions (0.45, 0.55,0.65, 0.75), 7 winding angles (WA or φ) (±45°, ±50°, ±55°, ±60°, ±65°, ±70°,

±75°), and 6 stacking sequences (SS1, SS2, SS3, SS4, SS5, SS6).

3.To optimize the volume fraction, winding angle, and stacking sequence from FE analysis.

4.To fabricate GFRP cylinder and cut the coupons and test them for various mechanical-physical and tribological properties with and without hygrothermal ageing.

Scope of present work

1.a) The finite element analysis of GFRP, Low Carbon Steel(LCS), and Aluminium 6061 T6 cylinders are carried out using analysis software.

b) The results obtained from the finite element analysis are compared among each other(all 3 case materials) along with their maximum specific strength(MSS).

2. a) The GFRP cylinder, which is selected as the best material for pressure vessel application based on outcomes of FE (Finite Element) analysis and MSS, need detailed understanding and hence, the effect of variations of filament winding process parameters on the outcomes of finite element analysis of GFRP cylinder is elaborated.

b) The filament winding process parameters such as fiber volume fractions (0.45, 0.55,0.65, 0.75), winding angles (WA or φ) (±45°, ±50°, ±55°, ±60°, ±65°, ±70°, ±75°), and stacking sequences (SS1, SS2, SS3, SS4, SS5, SS6) effects are combined together which has led to a total of 336 FE simulations (with and without PVC liner).

3. a) All 336 FE simulation results are tabulated, and only FE simulation results(168) along with PVC liner (poly vinyl chloride) are selected for optimization. This is because the effect of PVC liner on FE analysis outcome is negligible.

b) The multi-criteria decision making(MCDM) tool VIKOR method is used in order to optimize the obtained FE simulation results (with PVC liner). The main motive behind optimization is to find the best composition (best volume fraction, winding angle, stacking sequence) among the existing 168 attributes.

4. a) The GFRP cylinder is fabricated as per the best composition as suggested by the VIKOR method.

b) The fabricated GFRP cylinder is cut, and test coupons are prepared for mechanical-physical-tribological characterization studies.

c) Some of the cut GFRP test coupons are subjected to hygrothermal ageing studies in specific environmental conditions for a period of 1080 Hours.

d) The most important properties such as hoop tensile strength, ultimate tensile strength, ultimate compressive strength, and ultimate flexural strength for both aged and unaged cases are recorded and analyzed in detail.

2.5 Summary

The contributions from various researchers in the area of pressure vessel cylinder from different applications, fabrication methods, materials, numerical and experimental point of view are briefly discussed. The overall outcomes from the literature study have motivated in defining the objectives for current research work. In order to achieve the set objectives, a methodology has been defined. Here step by step procedure is planned, which is discussed in detail in a subsequent chapter. The few important highlights of current research objectives are FE analysis of composite pressure vessel cylinder, experimental studies on filament-wound GFRP vessel. These two topics are the main highlights of the following methodology section.

CHAPTER 3

METHODOLOGY

3.1 Overview

This chapter describes the flow chart and material properties used in the present investigation. The finite element analysis of cylindrical pressure vessel with different materials such as LCS (Low Carbon Steel), Al 6061 T6 (Aluminium), and GFRP (Glass Fiber Reinforced Polymer) and varied fabrication process parameters such as volume fraction, winding angle, and stacking sequence are discussed. The MCDM (Multi-Criteria Decision Making) optimization method used in the current research work is also highlighted. This chapter deals with the fabrication of filament wound GFRP pressure vessel cylinder using filament winding technique. The detailed study on coupon preparation for physical, tribological, and mechanical tests as per respective ASTM standards is explained. Further hygrothermal ageing studies on few selected samples are also explored.

3.2 Flow of work

Here the methodology of workflow is plotted in the form of a block diagram, as shown in Figure 3.1. The step-by-step research work is executed as per the flow chart given in Figure 3.1.
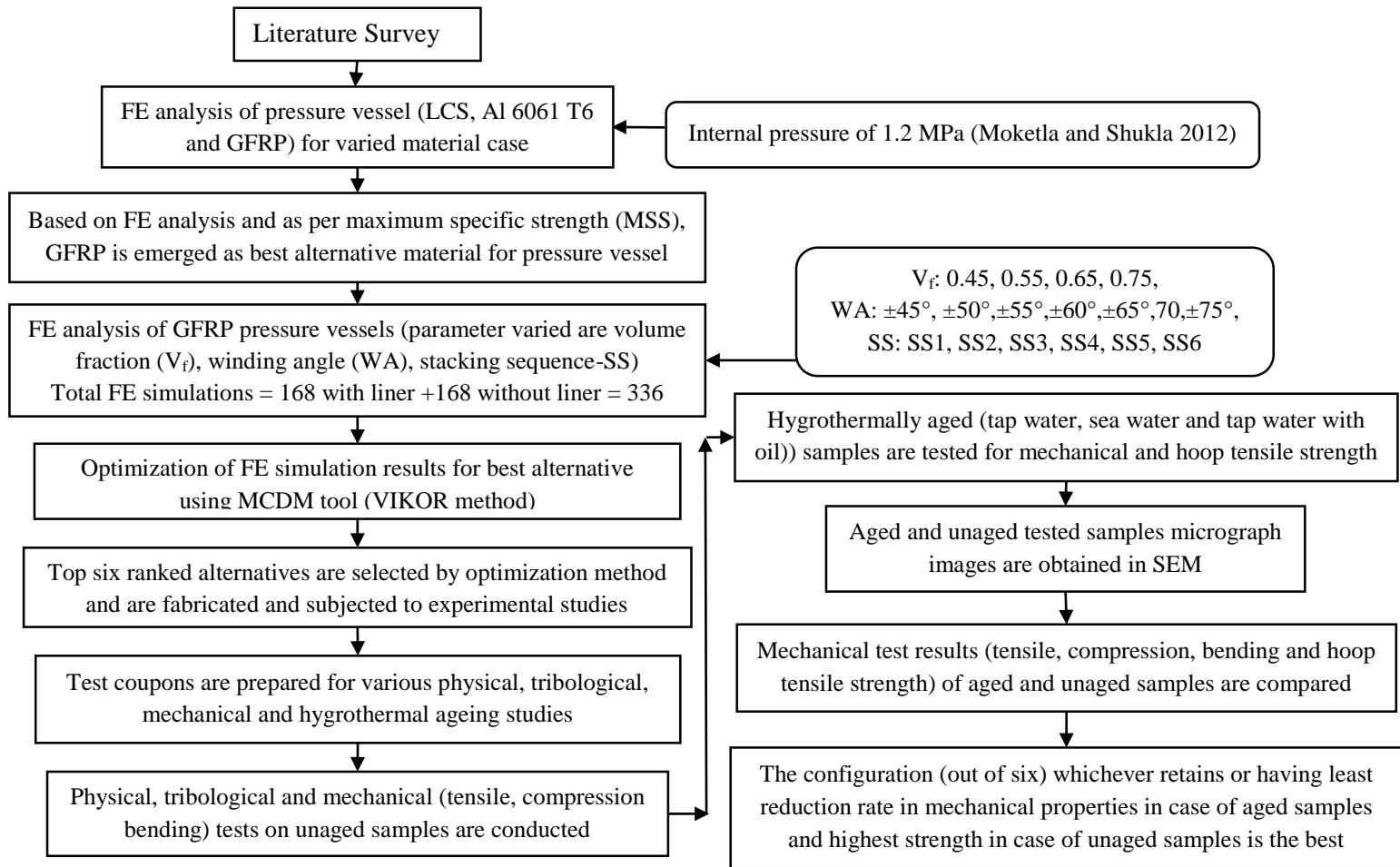
Figure 3.1 Methodology flow diagram

3.3 Materials used for proposed filament wound composite pressure vessels

Table 3.1 is highlighting the various properties of GFRP and PVC (Poly Vinyl Chloride) liner. The GFRP material properties are obtained by literature and the rule of mixture method. The PVC liner properties are obtained from the local material supplier (S.N Trading Company Bengaluru).

Table 3.1 Properties of material used in FE simulations

Material Property \ Material Type	GFRP				PVC liner	
Fiber volume fraction (V_f)	0.45	0.55	0.65	0.75	Density in kg/m^3	1.49
E_1 in GPa	40.1	48.3	56.4	64.6	Yield Strength in MPa	52
E_2 in GPa	6.4	7.27	7.96	8.05	Young's Modulus in GPa	3.3
E_3 in GPa	6.4	7.27	7.96	8.05	Elongation in % strain	0.4-0.8
μ_{12}	0.255	0.245	0.235	0.225	Impact strength in KJ/m	200
μ_{13}	0.255	0.245	0.235	0.225	Poisson's ratio	0.38
μ_{23}	0.49	0.53	0.59	0.69	Shear Modulus in GPa	1
G_{12} in GPa	16.7	20.1	23.5	26.9	Flexural Modulus in GPa	3
G_{13} in GPa	16.7	20.1	23.5	26.9	UTS in MPa	52
G_{23} in GPa	2.15	2.38	2.5	2.38	Rockwell Hardness	1-70

3.4 FE analysis of pressure vessel

The FE (Finite Element) analysis of cylindrical pressure vessel is carried out with the following dimensions:

Dimensions of the proposed cylinder,

Diameter, D = 206 mm, R = 103 mm, Height, H= 180 mm, Thickness t = 4 mm

Steps involved in FE analysis are:

- ➢ Pre processing
- ➢ Solution
- ➢ Post processing
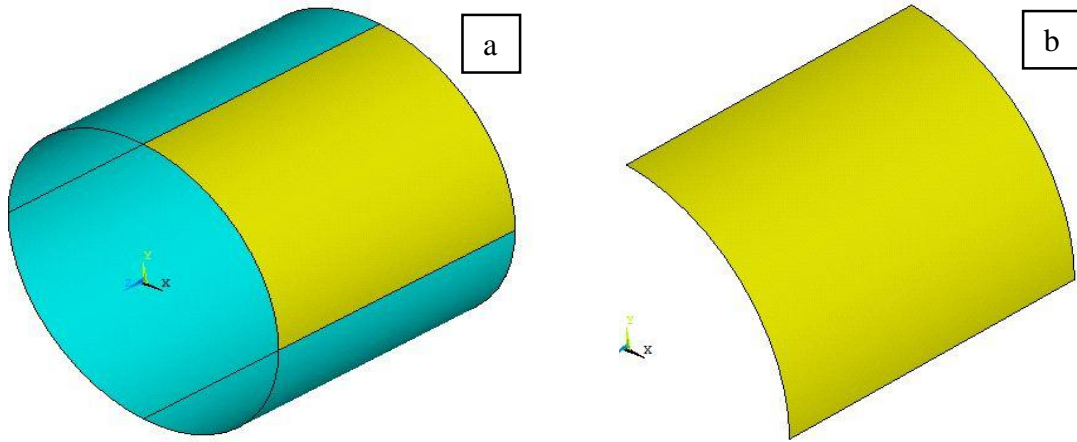
Full model view of pressure vessel with ¼th section highlighted will be used in FE analysis

1/4th Section of full Model
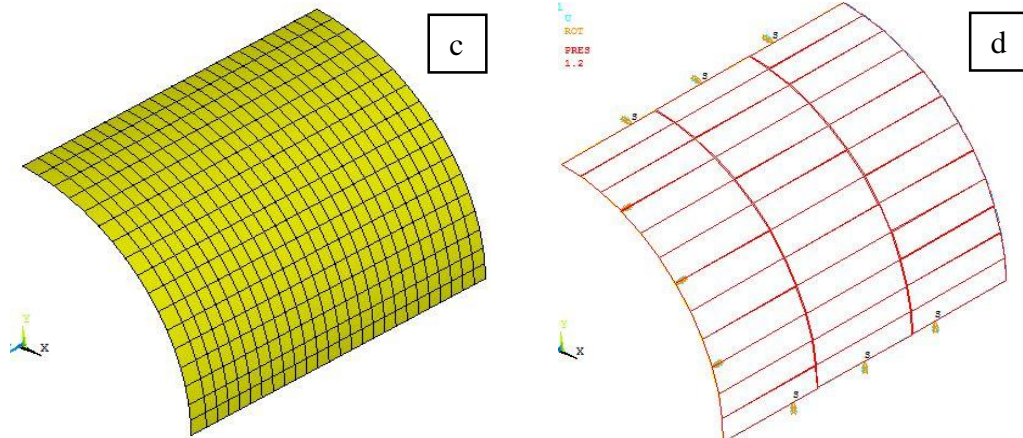
Meshed Model

Applying Boundary Condition and internal pressure

Figure 3.2 Highlighting different steps involved in FE simulation

Pre processing

This step involves the modelling of the product, assigning the element type, meshing, applying the boundary conditions and loads.

Solution

The model prepared in the previous step is used to get a solution by running the FE simulation using a solver in ANSYS academic software.

Post-processing

The various results obtained after FE simulation are observed and are interpreted. The suitable conclusions are drawn out of obtained results.

3.4.1 Modelling of pressure vessel for varied material (LCS, Al6061 T6, GFRP)

The basic steps involved in FE analysis of GFRP, LCS, and Al 6061 T6 cylinders are as shown in Figure 3.2. Figure 3.2(a) is showing the full FE model of a cylindrical pressure vessel. Figure 3.2(b) indicates the 1/4th section of the full model to be used for FE analysis instead of a full cylindrical vessel. The same FE model is used for LCS, Al 6061 T6, and GFRP cylinders. The material properties, which are tabulated in Table 3.1(GFRP) and Table 3.4(LCS, Al 6061 T6), are assigned to respective material (as per 3 different cases) models. Figure 3.2(c) indicates free meshing of the model using a meshing tool. The same meshing model is followed for all three material cases. Figure 3.2(d) indicates the distribution of boundary conditions and internal pressure of 1.2 MPa (Ashok, T. et.al.) applied on the FE model. Here load distribution and boundary conditions remain the same for all three cases.

3.4.2 Modeling of pressure vessel for varied winding angle

In this FE analysis, most of the steps are similar to that of the GFRP, LCS, and Al 6061 T6 vessel study. Here the study is carried out by keeping the fiber volume fraction $V_f = 0.55$, stacking sequence ($\pm\varphi°_2/90°_2/\pm\varphi°_2$) constant, and varying the winding angle ($\pm0°$, $\pm45°$, $\pm55°$, $\pm90°$) different FE simulation results are recorded to optimize the winding angle.

3.4.3 FE analysis of GFRP pressure vessel cylinder for varied filament winding process parameters such as volume fraction (V_f), winding angle (WA), and stacking sequence (SS)

Finite element simulation of GFRP composite cylindrical pressure vessel is studied. During this study, by varying the most influencing process parameters such as fiber volume

fraction (V_f), filament winding angle(WA), and stacking sequence(SS), the variations and effect of each process parameter on the strength of the pressure vessel is predicted. Table 3.2 highlights the list of all possible combination input parameters required in the case of FE simulation. Using all these combinations, about 168 FE simulations have been analyzed to obtain the required results. Further, to estimate the effect of PVC liner on strength of the vessel, again 168 FE simulations are carried out along with PVC liner.

Table 3.2 List of all FE simulations carried out (FE simulations template)

Input parameters are: Fiber volume fraction, $V_f = (0.45, 0.55, 0.65, 0.75)$, Filament winding angle, WA(φ) = ($\pm 45°$, $\pm 50°$, $\pm 55°$, $\pm 60°$, $\pm 65°$, $\pm 70°$, $\pm 75°$), Stacking sequence, SS = (SS1, SS2, SS3, SS4, SS5, SS6) SS1 = $(90°_2/\pm\varphi°_2/90°/\pm\varphi°_2/90°/90°_2)$, SS2 = $(90°_4/\varphi°_2/90°_2/-\varphi°_2/90°_4)$, SS3 = $(90°_2/\pm\varphi°_2/90°_2/\pm\varphi°_2/90°_2)$, SS4 = $(90°_2 /(\pm\varphi°/90°)_3/\varphi°/90°_2)$, SS5 = $(90°_2 /(\varphi°/90°)/(\pm\varphi°/90°)_2/(90°/\varphi°)/90°_2)$, SS6 = $(90°_2/\varphi°_2/90°/(-\varphi°_4)/90°/\varphi°_2/90°_2)$			
FE Simulations	V_f	WA(φ)	Stacking sequence, SS
1	0.45	$\pm 45°$	SS1
2	0.45	$\pm 45°$	SS2
3	0.45	$\pm 45°$	SS3
4	0.45	$\pm 45°$	SS4
5	0.45	$\pm 45°$	SS5
6	0.45	$\pm 45°$	SS6
Similarly Continued for other parameter combinations till all 168 FE simulations completed			
The 168 FE simulations are repeated for GFRP composite pressure vessel without PVC liner			
Important Outputs obtained after each FE simulation:			
1. Von Mises stress, 2. Hoop stress			

Figure 3.3 Graphical representation of all possible 168 FE simulation

The graphical representation of all possible FE simulations is shown in Figure 3.3. In simple words, for $V_f = 0.45$ with a single winding angle ($\pm 45°$) and six stacking sequences leads to six different specifications for six FE simulations. If we consider all seven winding angles and six stacking sequence, which leads to 42 FE simulations for $V_f = 0.45$ case. Similarly, if we repeat the analysis for the other three fiber volume fractions (0.55,0.65,0.75), about 126 cases (42 simulations for each V_f) are obtained. Overall, 168 (42+126) FE simulations are carried out without considering PVC liner. Another 168 FE simulations are carried by considering PVC liner to understand the effect of liner on the strength of GFRP composite pressure vessel cylinder. The other parameters such as vessel dimensions, element type, boundary conditions, and loading remain constant throughout all FE simulation cases.

Figure 3.4 indicating, the sample pictures of six different stacking sequences used in the current study. The winding angle $\pm 55^0$ is used to alter the helical winding angle (φ). Whereas $\pm 90^0$ is used to alter hoop winding angle. The hoop winding is provided at the beginning, and the end portion of all six stacking sequences helps in avoiding fiber pull out

48

and also provides uniformity in load distribution compared to helical wound filaments(Madhavi et al. 2009b). The main purpose of short listing only six stacking sequences is as the selected six different stacking sequences cover all possible combinations of the hoop and helical windings, which are responsible for variations in the strength of vessel as studied in different literature data. In Figure 3.4, layer 1 is a PVC liner with orientation of 0^0 angle and material is designated as 2.
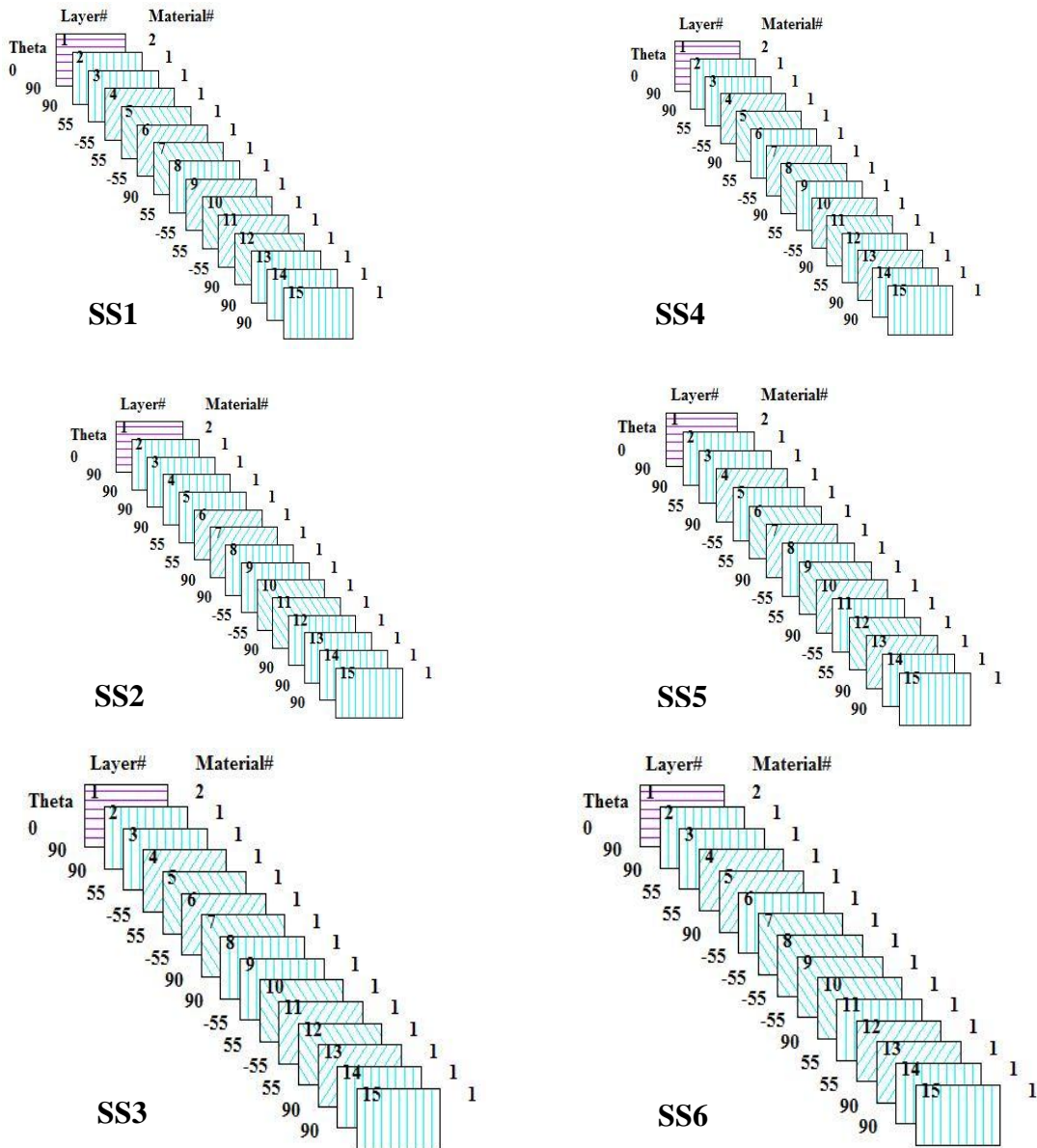
Figure 3.4 Different stacking sequences used in the present study

3.4.4 Comparison of FE analysis of cylindrical pressure vessel for varied composite materials

In this section, FE analysis of cylindrical pressure vessel is carried out for fixed dimension and varied material properties. The list of material properties is tabulated in Table 3.4. The important results of this study are von mises stress, hoop stress, and maximum specific stress (MSS) recorded and compared based on varied material properties.

Table 3.3. FE modelling details with dimensions of pressure vessel

Dimensions and boundary condition and loading details of pressure vessel				
Dimensions	Model	Boundary conditions	Element type and meshing	Loading
Diameter = 206 mm	full pressure vessel is modelled	UX, UY, UZ =0,	Shell 8-node 281	Internal pressure of 1.2 MPa
Cylinder length = 180 mm				
Thickness = 4 mm			Free mesh	

Table 3.4. Material properties list

V_f	E_1 in [GPa]	E_2 in [GPa]	E_3 in [GPa]	μ_{12}	μ_{13}	μ_{23}	G_{12} in [GPa]	G_{13} in [GPa]	G_{23} in [GPa]
GFRP-Glass fiber reinforced polymer									
0.45	40.1	6.44	6.44	0.255	0.255	0.49	16.7	16.7	2.15
0.55	48.3	7.2	7.2	0.245	0.245	0.53	20.1	20.1	2.38
0.65	56.4	7.9	7.9	0.235	0.235	0.59	23.5	23.5	2.50
CFRP-Carbon fiber Reinforced polymer									
0.45	105	6.52	6.52	0.3	0.3	0.52	10.6	10.6	2.15
0.55	128	7.42	7.42	0.3	0.3	0.56	12.7	12.7	2.38
0.65	151	8.15	8.15	0.3	0.3	0.63	14.8	14.8	2.50
AFRP-Aramid fiber reinforced polymer									
0.45	57.7	6.46	6.46	0.327	0.327	0.50	2.07	2.07	2.15
0.55	69.7	7.36	7.36	0.333	0.333	0.55	2.24	2.24	2.38
0.65	81.8	8.07	8.07	0.339	0.339	0.61	2.41	2.41	2.50

	Modulus of Elasticity, E in [GPa]		Poisson s ratio, μ		Shear Modulus, G in [GPa]		
Metals (Kaw and Group 2006)							
LCS	207		0.3		83		
Al 6061 T6	69		0.33		27.5		

The FE modeling of composite pressure vessels is done in commercially available FE analysis software. The pressure vessel dimensions and other data related to the present proposed FE model are listed in Table 3.3. In the present study, three composite materials with input parameters such as fiber volume fraction, winding pattern, and winding angle are used at three different levels. The variation of fiber volume fraction can be observed in material properties list in Table 3.4.

The FE modeling of composite pressure vessels and metallic pressure vessels requires material properties, which are listed in Table 3.4. Most of the properties listed in Table 3.4 are being calculated as per the rule of mixture for respective fiber volume fractions. The fiber and matrix properties are taken from literature resources (Kaw and Group 2006).

3.5 Optimization using multi-criteria decision making (MCDM) tool VIKOR Method

In this step, all FE simulation results or outcomes are studied by using an optimization tool called the VIKOR method. It's a MCDM method that helps in deciding the most influencing winding parameters on an outcome of FE simulation of GFRP pressure vessel. This method is applied for both with liner and without liner FE simulation results. The ranking is assigned to all FE simulation outcomes after required analytical evaluations. The top-ranked (maximum rank of 6th) FE simulations are considered for further experimental studies.

3.5.1 Basic Information and Steps involved in VIKOR Method: (Sasanka and Ravindra 2015)

The VIKOR method is a multi-criteria decision making (MCDM) or multi-criteria decision analysis method. It was originally developed by Serafim Opricovic (Opricovic 2004) to solve decision problems with conflicting and no commensurable (different units) criteria, assuming that compromise is acceptable for conflict resolution, the decision-maker wants a solution that is the closest to the ideal, and the alternatives are evaluated according to all established criteria. VIKOR ranks alternatives and determines the solution named compromise that is the closest to the ideal.

51

The idea of a compromise solution was introduced in MCDM by Po-Lung Yu in 1973(Yu 1973) and by Milan Zeleny(ZELENY 1974). S. Opricovic("Opricovic, S" 1990) had developed the basic ideas of VIKOR in his Ph.D. dissertation in 1979, and an application was published in 1980(LUCIEN DUCKSTEIN 1980). The name VIKOR appeared in the form of Serbian language: VIseKriterijumska Optimizacija I Kompromisno Resenje(VIKOR), that means Multicriteria Optimization and Compromise Solution, with pronunciation: VIKOR. ("Opricovic, S" 1990) The paper in 2004 contributed to the international recognition of the VIKOR method along with others on extended in 2007 and extension of VIKOR method in 2009 (Opricovic 2004, 2007; Sayadi et al. 2009).

The MCDM problem is stated as follows: Determine the best (compromise) solution in multicriteria sense from the set of J feasible alternatives A_1, A_2, ...A_J, evaluated according to the set of n criterion functions. The input data are the elements f_{ij} of the performance (decision) matrix, where f_{ij} is the value of the i th criterion function for the alternative A_j.

VIKOR method steps

Step 1. Establish the decision matrix.

Structure of the decision matrix can be expressed as follows:

$$X = \begin{array}{c} \\ A_1 \\ \vdots \\ A_i \\ \vdots \\ A_m \end{array} \begin{array}{ccccc} SN_1 & \cdots & SN_j & \cdots & SN_n \\ \begin{bmatrix} SN_{11} & \cdots & SN_{1j} & \ldots & SN_{1n} \\ & \vdots & \vdots & & \vdots \\ SN_{i1} & \cdots & SN_{ij} & & SN_{in} \\ & \vdots & \vdots & & \vdots \\ SN_{m1} & \cdots & SN_{mj} & \ldots & SN_{mn} \end{bmatrix} \end{array}$$

Where,

A_1 = first alternative,

A_i = ith alternative,

A_m = 168th alternative.

and SN_{11} = Von mises stress in the first alternative(FE simulation) in MPa,

SN_{1j} = Hoop stress in the first alternative(FE simulation) in MPa,

SN_{1n} = Longitudinal stress in the first alternative(FE simulation) in MPa,

SN_{i1} = Von mises stress in the ith alternative(FE simulation) in MPa,

SN_{ij} = Hoop stress in the ith alternative(FE simulation) in MPa,

SN_{in} = Longitudinal stress in the ith alternative(FE simulation) in MPa,

SN_{m1} = Von mises stress in the mth alternative(FE simulation) in MPa, = 168th alternative(FE simulation).

SN_{mj} = Hoop stress in the mth alternative(FE simulation) in MPa, = 168th alternative.

SN_{mn} = Longitudinal stress in the mth alternative(FE simulation) in MPa, = 168th alternative(FE simulation).

matrix columns indicate the corresponding SN ratios due to the different objective functions or outcomes.

Step 2. Determine the normalized decision matrix.

In order to remove the units of decision matrix, the normalized values can be calculated as f_{ij} represents the normal quality loss of jth outcome in the ith FE simulation(alternative).

$$f_{ij} = \frac{SN_i^{\ j}}{\sqrt{\sum_{i=1}^{m}(SN_i^{\ j})^2}} \quad i = 1,2,\dots,\dots m; j = 1,2,\dots,n; \text{---(1)}$$

Step 3: Determine the ideal and negative ideal solutions.

As a minimization problem is dealt with in this, the ideal solution A^* and the negative ideal solution A^- are computed as follows:

$$A^* = \{min f_{ij} | i = 1,2,\dots,m\} = \{f_1^*, f_2^*,..f_j^*,..f_n^*\}\text{-----------------------------------(2)}$$

$$A^- = \{max f_{ij} | i = 1,2,\dots,m\} = \{f_1^-, f_2^-,..f_j^-,..f_n^-\}\text{---------(3)}$$

Step 4: Calculate the utility measure and the regret measure.

The utility measure and the regret measure for each non-dominated solution can be expressed as:

$$S_i = \sum_{j=1}^{n} w_j(f_j^* - f_{ij})/(f_j^* - f_j^-)\text{---------------------(4)}$$

$$R_i = max j \,[w_j(f_j^* - f_{ij})/(f_j^* - f_j^-)]\text{------------------(5)}$$

where S_i, $R_i \in [0,1]$, 0 denotes the best and 1 denotes the worst situations. w_j is the weight of the jth outcome (objective function).

Step 5: Calculate the VIKOR index.

The VIKOR index can be calculated as follows:

$$Q_l = \alpha \left[\frac{S_i - S^*}{S^- - S^*}\right] + (1 - \alpha)\left[\frac{R_i - R^*}{R^- - R^*}\right]\text{---(6)}$$

where $\alpha \in [0,1]$ is a weighting factor and is usually selected to be 0.5.

Step 6: Rank the order of preference.

The alternative solution with the smallest VIKOR value is the best solution.

It is worth mentioning that the computations can be done with different weights and then compare them. For example, we set the weights to (0.5, 0.25, 0.25), but we may also try by 0.25, 0.5, 0.25) or (0.25, 0.25, 0.5). Other weights can also be examined to compare the results. Then a better decision is made based on the results.

Here, MCDM tool such as the VIKOR method helps in deciding the most influencing process parameters on the results of FE simulation of GFRP pressure vessel. In this process, the ranking is assigned to all FE simulation alternatives after analytical evaluation (based on defined formulae for data analysis steps). The top rank is assigned to the lowest VIKOR index value, and subsequent rankings are followed. Here, as per our requirement, we have selected the top six ranked alternatives (composition) for experimental studies. Figure 3.5 illustrates the selection of top-ranked attributes based on the VIKOR method.
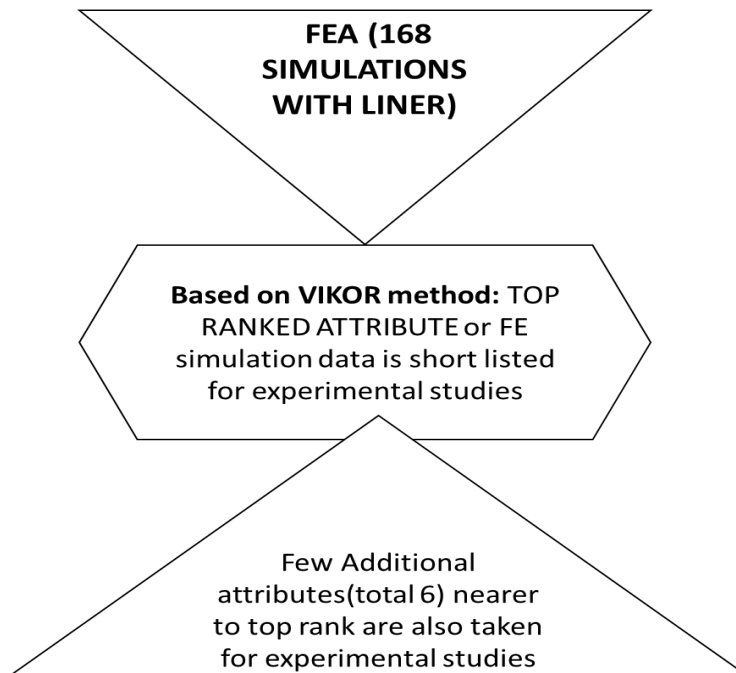
Figure 3.5. Schematic representation of a selection of top-ranked composition based on the VIKOR method

3.6 Experimental Studies

3.6.1 Fabrication of GFRP composite pressure vessel cylinders

In this section, the composite pressure vessel cylinders are fabricated along with PVC liner for 6 different compositions as optimized by using by VIKOR method. Table 3.5 is highlighting the list of cylinders fabricated along with their respective specification and product ID. In this section, the materials required for fabrication are procured from the local market (Epoxy Resin-M.S. Polymer and Formulators, Bengaluru, Glass Fiber-Link Composites, Belagavi) and cleaned before the start of the fabrication process. A semi-automatic filament winding machine is used for fabricating composite cylinders. In this machine, the winding angle and start-stop positions of the resin bath are feed in the control panel before the beginning of actual fabrication (Since the resin bath is moving/linear motion from right to left and vice versa to cover the required length of PVC liner with filament winding).

The filament winding machine parameters such as spindle speed, carriage speed (resin bath/container), carriage movement limitation, filament tension are set as per our requirement during dry run. There are two types of filament winding methods exist such as wet winding and dry winding (as shown in Figure 3.6 (g)). The PVC mandrel is cleaned from all the dust, oil, and other contaminants before mounting on the filament winding machine. A dry run (dry winding) is carried out in order to ensure defined specification and smooth running of the fabrication process. All necessary fabrication parameters are set once, and a dry filament winding is carried out on PVC mandrel. The dry winding helps in finding the errors before actual fabrication. The epoxy resin with hardener weighed on a weigh scale of 1 mg as per requirements and poured into a resin bath. In any filament winding process, there exist three different winding techniques such as helical, hoop, and polar winding.
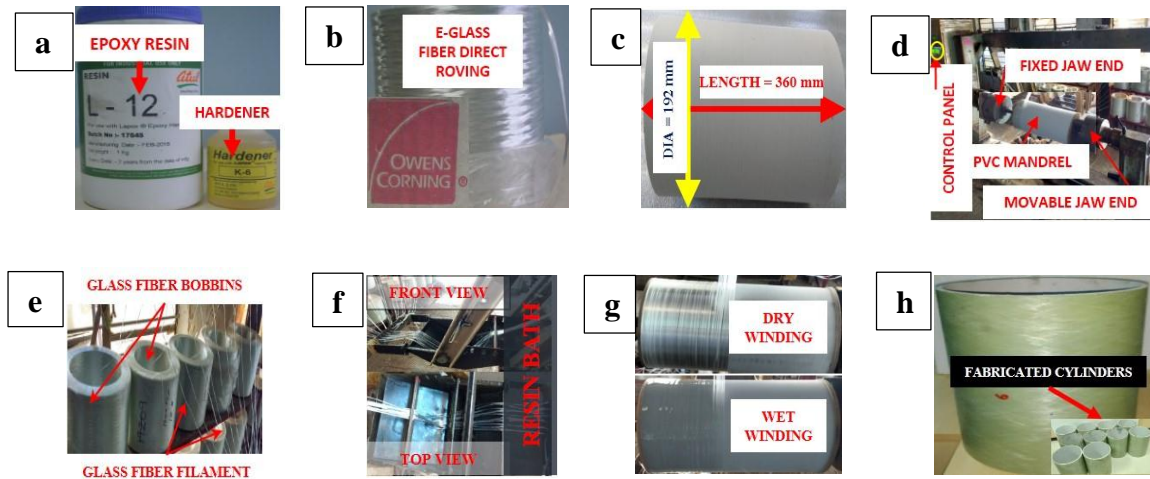
Figure. 3.6 (a) Epoxy resin with hardener, (b) E-Glass fiber direct roving(1200TEX), (c) PVC mandrel, (d) Filament winding setup, (e) Glass fiber filament bobbins, (f) Resin bath, (g) Dry winding and wet winding, (h) Fabricated GFRP pressure vessel cylinders

Table 3.5 Highlighting the fabricated product code along with respective specification details.

S.NO.	Product ID	Volume fraction, Vf	Winding Angle (WA)	Stacking Sequence (SS3) ACTUAL STACKING SEQUENCE
1	055WA55SS3(P1)	0.55	±55°,	$(\pm55°_2/90°_2/(\pm55°_2)$
2	055WA60SS3(P2)	0.55	±60°	$(\pm60°_2/90°_2/(\pm60°_2)$
3	065WA55SS3(P3)	0.65	±55°,	$(\pm55°_2/90°_2/(\pm55°_2)$
4	065WA60SS3(P4)	0.65	±60°	$(\pm60°_2/90°_2/(\pm60°_2)$
5	075WA55SS3(P5)	0.75	±55°	$(\pm55°_2/90°_2/(\pm55°_2)$
6	075WA65SS3(P6)	0.75	±65°	$(\pm65°_2/90°_2/(\pm65°_2)$

Around 45-50 minutes are required to complete the whole fabrication process. The whole product is kept at room temperature curing for 24 hours. Figure 3.6 (a) to (h) highlighting the various pictures of the fabrication process.

3.6.2 Preparation of test coupons

The samples are cut as per respective ASTM standards. The CNC cutting tool is used for cutting test coupons. Figure 3.7 illustrates various test coupons.
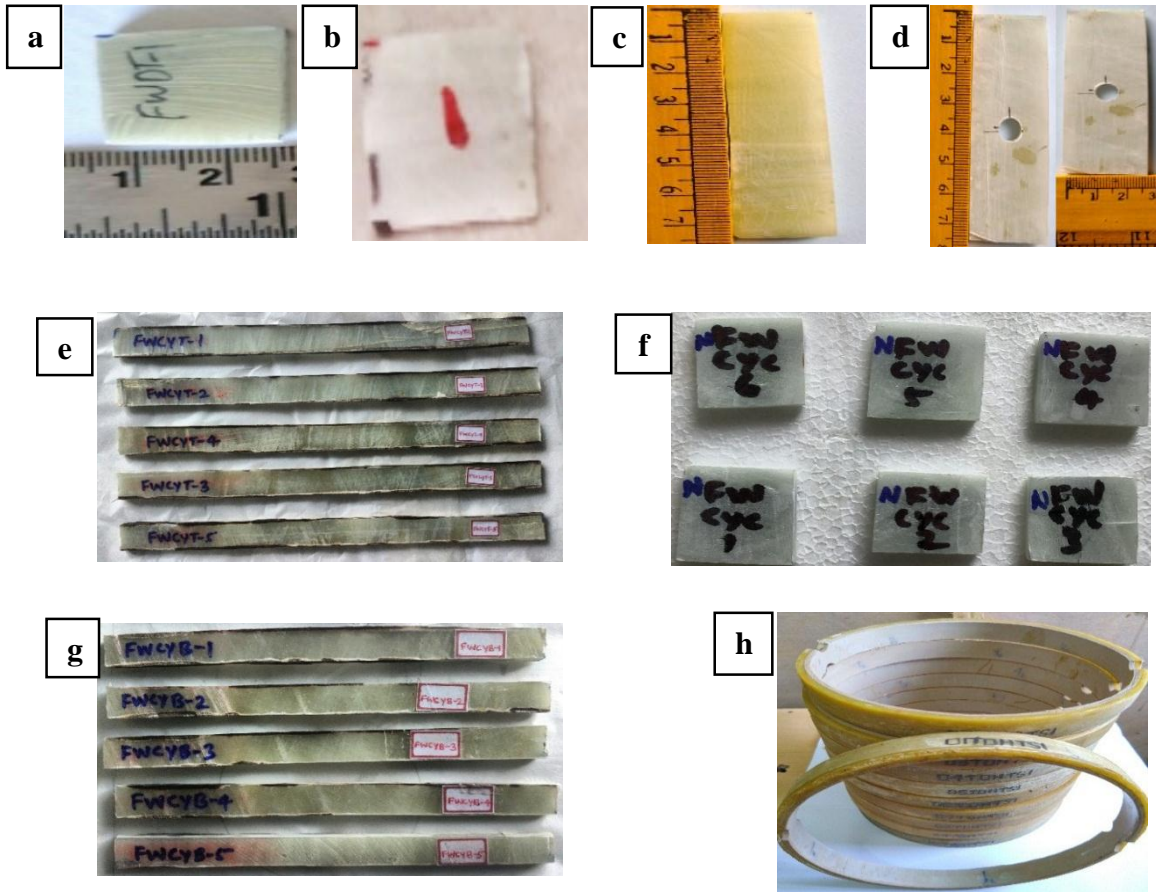
Figure 3.7 Images of GE test coupons for physical, tribological, and mechanical characterization studies: (a) Density test sample, (b) Ignition loss test sample, (c) Water absorption test sample, (d) Wet abrasive slurry erosion test sample, (e) Tensile, (f) Compression and (g) Bending test sample, (h) Split disk test sample

3.6.3 Testing of samples for Mechanical, Physical, and Tribological Characterization

3.6.3.1 Mechanical Characterization

The filament wound GFRP composite test coupons are subjected to various mechanical tests such as tensile, compression, and bending tests as per respective ASTM standards. The test coupons are cut as per ASTM D3039, D3410, D7264, respectively. The actual test sample for tensile, compression bending and hoop tensile are shown in Figure 3.7(e), (f), (g), and (h), respectively. In each case, five samples are tested for required mechanical properties.

3.6.3.2 Physical Characterization

Density Test

The density of material plays an important role in any engineering applications; as density of the material increases, the effort required to perform certain tasks such as transportation, lifting of the product will also increase in general. The rule of mixture method is adopted for calculating theoretical density (ρ_t). Whereas analytical weigh balance of capacity 1kg with a sensitivity of 1mg is used for experimental observation. Here five samples are subjected to density test as shown in Figure 3.8. The fabrication of filament wound GFRP composite vessel involves many steps. During these steps, there is a possibility of air entrapment, which leads to voids in the finished product. The presence of void content will have a considerable impact on various strengths of the vessel. To study void content percentage, we have a relation as shown in equation (7).

Figure. 3.8 Density test sample

$$\text{Void Content } (\%) = \frac{\rho_t - \rho_a}{\rho_t} \times 100 \text{---(7)}$$

Where, ρ_a = Apparent density in kg/m^3.

ρ_t = Theoretical density in kg/m^3

Ignition Loss Test

ASTM D2684-18 is used to carry out an ignition loss test on cured reinforced resins. This test helps in finding the exact fiber to resin ratio after deduction of void content and also gives a clear idea of the complete combustion of resin which is a carbonaceous material. Here a specimen of size 25 x 25 x any thickness in mm is subjected to heating in a muffle furnace at a temperature of around 500°C to 600°C in a ceramic or alumina crucible for the period of around 30 to 45 minutes which is normally dependent on the thickness of

material. The later specimen is cooled in a desiccator to room temperature and weighed on weigh balance of 1 mg. The % weight of ignition loss is calculated using equation (8). Where, ω_i = Initial weight of sample in grams, ω_r = Weight of residue in grams. Figure 3.9 illustrates about test sample, muffle furnace, and crucible used during the experiment.

Figure 3.9 Ignition test set up: (a) Ignition test sample weighed before the test, (b) Muffle furnace(burning of samples inside furnace), (c) Alumina crucible(sample kept in a furnace with this crucible)

$$\text{\% weight of ignition loss} = \left(\frac{\omega_i - \omega_r}{\omega_i}\right) \times 100 \text{ ---(8)}$$

Water Absorption Test

The water absorption test is carried out as per ASTM D570-98 on polymer composites in order to find the relative rate of water absorption when immersed in a water bath container for a specified period of time. There exist two water (distilled) mediums, such as boiling water, normal water. In boiling water, the specimen can be kept up to a maximum of 2 hours. Whereas in the case of normal water media, there are different time periods are specified in ASTM standards. In the current study, we are using three sets of samples in different water media such as samples vertically immersed/placed in distilled water for varied time periods; in the second set, up samples are immersed in a sea /saltwater bath container for a predefined time period. In the last set, samples are placed in a boiling distilled water container for two hours. The samples are weighed on an analytical weigh the balance of a maximum 1 mg accuracy before and after immersion in a water bath. The sample is freed from any dust, oil, and sharp edges before start of the experiment. After every interval of time, each sample is individually taken out from the container, and excess water is gently wiped out using a dry cloth before weighing. The same procedure is

repeated till a saturation point is attained. The water absorption percentage can be calculated using equation (9). The actual samples for the current test and water absorption test setup are as shown in Figure 3.10(a) and (b), respectively.
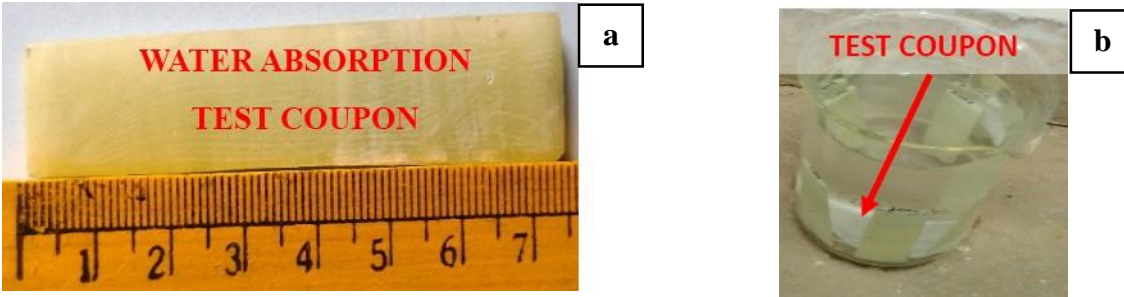
Figure. 3.10 Water absorption test: (a) Filament wound GFRP test coupon, (b) test set up

% increase in weight of sample $= \left(\frac{\omega_f - \omega_i}{\omega_i}\right) \times 100$ --(9)

3.6.3.3 Tribological Characterization

In the present study, the slurry erosion or wet sand erosion testing method is adopted in order to understand the tribological behaviour of filament wound GFRP composite. The wet slurry erosion test is carried out on a slurry erosion tester set up manufactured and supplied by DUCOM instruments at FIST laboratory, mechanical engineering department, NITK, as shown in Figure 3.11(a), (b), and (c) as per ASTM D75-95. The highly influencing parameters such as slurry concentration (250 g, 500 g, 750 g), sand particle size (400μ, 800μ, 1200μ), spindle speed (500 rpm,1000 rpm,1500 rpm) are used for optimizing the number of experiments. The design of experiments has many optimization techniques; one of them is Taguchi factorial design. Again, Taguchi design has many alternative tools. In the present study, the L9 design is selected as we have three variables with 3-level of variation. Here nine experiments as suggested by the L9 tool are successfully conducted, and various outcomes are tabulated. The wet abrasive slurry is prepared by using three different sets of sand particles and sand concentrations using the fixed quantity of distilled water (1litre). The sand particles used in the current erosion test are collected from a nearby river place and are properly dried and sewed using a wide range

of BSS graded sand particle standard sewing mesh. The weight of the specimen before and after test is measured using an analytical weigh balance of capacity of 1 mg. The erosion rate is calculated using equation (10). The actual sample used in the slurry erosion test is shown in Figure 3.11(d).
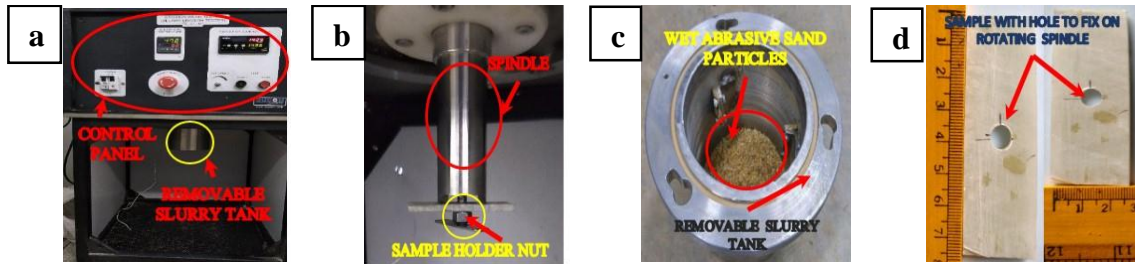
Figure. 3.11 Wet abrasive slurry erosion test set up: (a) Slurry erosion tester, (b) Specimen held at spindle, (c) Sand particles for slurry preparation, (d) GFRP test coupon

$$\text{The erosion rate } (\%) = \left(\frac{\omega_i - \omega_f}{\omega_i}\right) \times 100 \text{--(10)}$$

Where, ω_i = Initial weight of the sample (before slurry erosion test) in grams

ω_f = Final weight of the sample (after slurry erosion test) in grams

3.6.4 Hygrothermal ageing study

The hygrothermal ageing study is carried out in three different mediums. The three mediums, tap water (TW), seawater (SW), and tap water with oil (TWWO), are maintained at a constant temperature of 80°C throughout the experimental time period. The experiment is carried out in a hot bath chamber. The container is constantly maintained with a sufficient quantity of tap water, seawater, and tap water with oil. The experiment is carried out for 45 days' time period (it covers roughly 1000 working hours). The samples are placed in a SS (Stainless Steel) tray before placing them in a hot bath chamber. Each SS tray is having an equal number of samples (90), which include tensile, compression, and bending. The sample is taken out for reading for every defined interval of time and placed back in the chamber immediately.
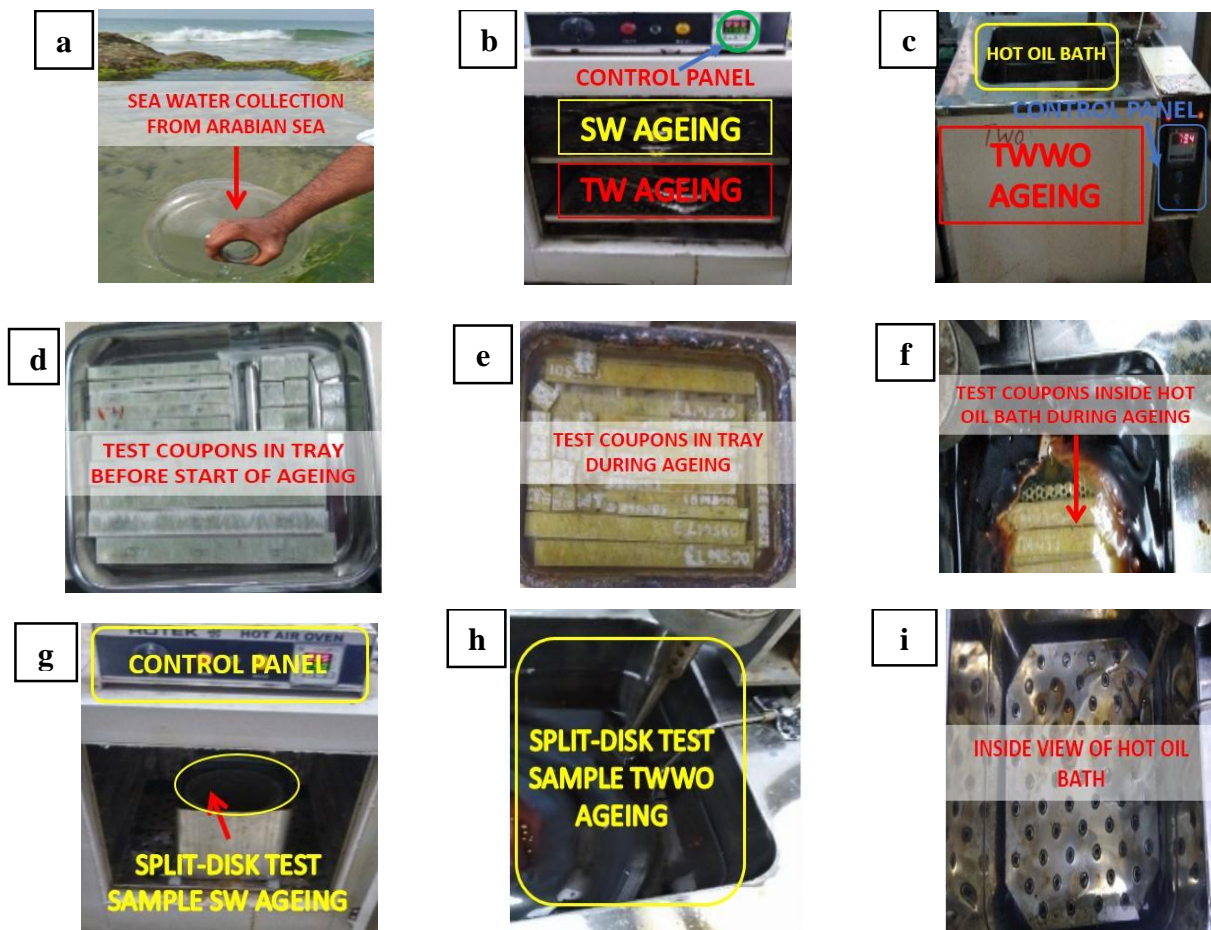
Figure 3.12 Hygrothermal ageing: (a) Seawater collection, (b) Samples placed in a hot air oven, (c) Hot oil bath and (d) Samples in SS tray, (e) Samples in a try after few days of ageing, (f) Samples in hot oil bath during TWWO, (g) Split disk test sample for SW ageing, (h) Split disk test sample for TWWO ageing, (i) Inside view of a hot oil bath

After the first 15-day, one set of samples from all three chambers (seawater, tap water, and tap water with oil) are taken out for testing. The same is repeated for 30 days and 45 days also. Figure 3.12 highlights few images of the hygrothermal ageing setup. The raw material for seawater ageing is taken from the nearby arabian sea and used only after testing it for various constituents. The tap water with oil ageing has 15% oil, and the rest is tap water. The oil used is a lubricating SAE procured from the local market. The samples are cleaned thoroughly before the start of ageing study. Each sample is weighed at regular intervals. The samples are gently cleaned with separate paper towels before weighing.

62

3.6.5 Hoop tensile stress studies on GFRP ring samples
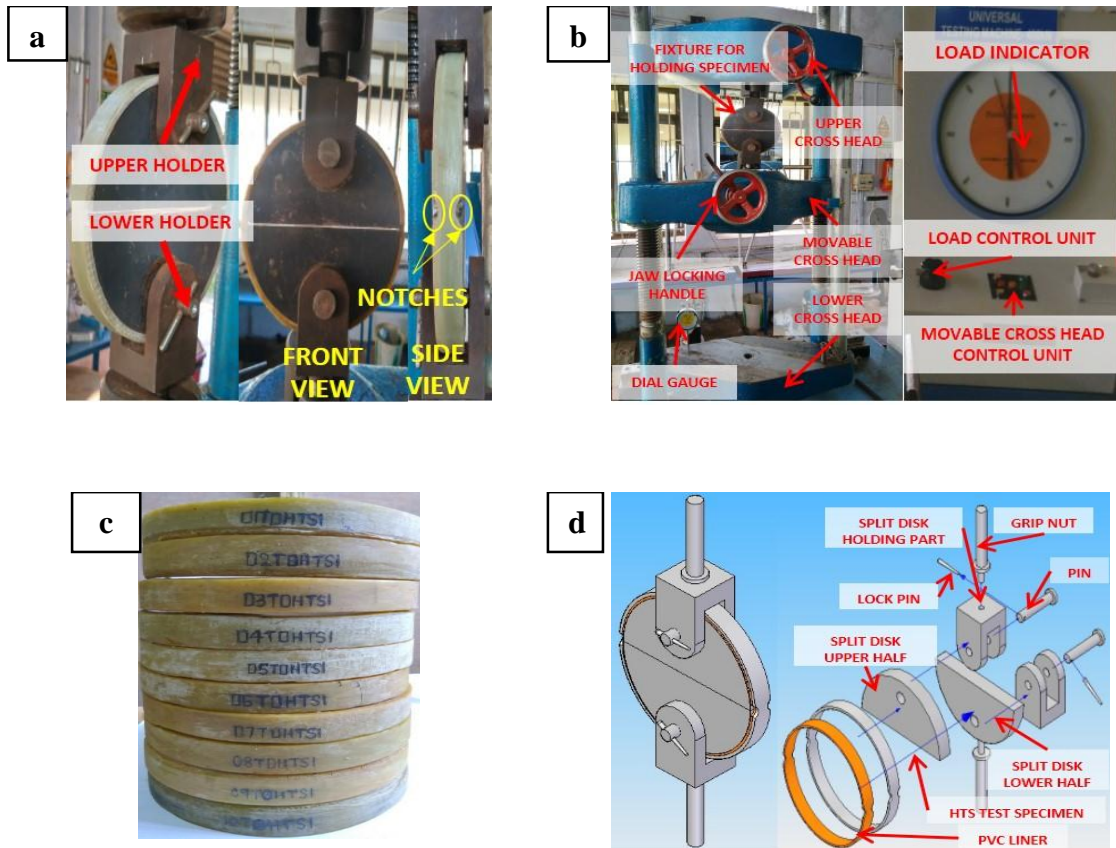
Figure 3.13A HTS test set up: (a) HTS sample with front and side view, (b) UTM of capacity 400 kN, (c) HTS samples before test and (d) CAD model of HTS test fixture

The hoop tensile Strength (HTS) is a primary mechanical property in the case of cylindrical vessels. The HTS or split disk test is conducted as per ASTM D2290 in a UTM machine as shown in Figure 3.13A (b). The fixture used to hold HTS test sample is shown in Figure 3.13A (a). Figure 3.13A (c) highlighting about HTS samples to be tested. Figure 3.13A (d) illustrating the CAD assembly view along with exploded view for better understanding of different parts of CAD model.
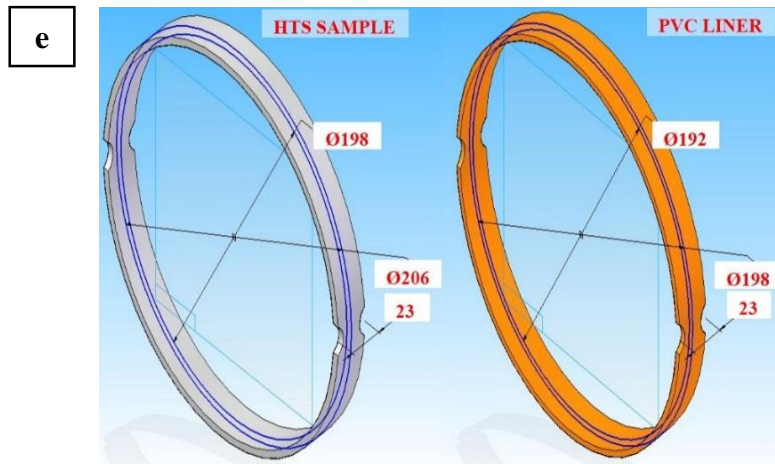
Figure 3.13B (e) Dimensions of hoop tensile test sample

The CAD model of HTS test sample along with all dimensions as per ASTM 2290 is shown in Figure 3.13B (e) The HTS tested samples are further subjected to fractography study to investigate the actual cause of failure. The main purpose of the post-failure analysis is to understand actual failure mechanisms at the micro-level using Scanning Electron Microscope (SEM) images.

3.6.6 Study of failure modes

The mechanical tested samples are subjected to fractography study to investigate the actual cause of failure. By manual examination and visualization, few samples are selected. The main purpose of the post-failure analysis is to understand actual failure mechanisms at the micro and nano level using scanning electron microscope (SEM). The different mechanical tests have different failure mechanisms whose various SEM images are analyzed. scanning electron microscope (SEM) is used for fractography study is shown in Figure 3.14.

Figure 3.14 Scanning electron microscope @MME NITK

3.7 Summary

Methodology, FE analysis, optimization using the VIKOR method, experimental studies are few highlights of this chapter. In the FE analysis, 3 different ways of FE simulations were studied, such as comparison based on varied pressure vessel cylinder material and winding angle, variations in 3 important fabrication parameters (fiber volume fraction (4), winding angle (7), stacking sequence (6)). The material characterization, hydrothermal ageing, and HTS examination using split disk test are few highlights of this chapter. Results obtained from FE simulations, experimental studies are briefly discussed in the subsequent chapter. SEM images of tested samples are also discussed for correlation of results in the same chapter.

CHAPTER 4

RESULTS AND DISCUSSIONS

4.1 Overview

This chapter covers results obtained from various FE analysis of cylindrical pressure vessel to experimental studies on filament-wound GFRP test coupons. Here, FE analysis of cylindrical pressure vessel with different materials such as LCS, Al 6061 T6, and GE and FE analysis of filament wound GFRP pressure vessel cylinder for varied filament winding process parameters (fiber volume fraction, winding angle, and stacking sequence) results are discussed in details. In case of experimental studies, the outcomes of physical, tribological, and mechanical characterization of filament wound GFRP test coupons are interpreted in detail. Further, the effect of hygrothermal ageing on mechanical properties is discussed with the help of various plots and data in table form. Detailed discussion on the effect of ageing hoop tensile strength is systematically elaborated. Lastly, various plots and results of FE analysis comparative study among GFRP, CFRP, and AFRP are discussed in detail.

4.2 Results of FE analysis of pressure vessels

4.2.1 FE analysis results for alternative materials and varied winding angle in case of GFRP composites

In this section, two important FE analysis results are plotted and discussed in detail. Figure 4.1(a) and Figure 4.1(c) highlights the comparison of FE simulation results and maximum specific strength (MSS) among three different materials used. Figure 4.1(b) and Figure 4.1(d) are highlighting about the comparison of FE results and MSS value based on the varied winding angle in the case of GFRP material. As shown in Figure 4.1(a), the FE results of LCS material is higher compared to the other two materials, but as per Figure 4.1(c), the MSS of GFRP material is higher. This is due to its lesser weight to higher strength ratio and better directional property. Hence it is a guiding factor for further studies for GFRP material as an alternative to LCS in the case of pressure vessel cylinders.
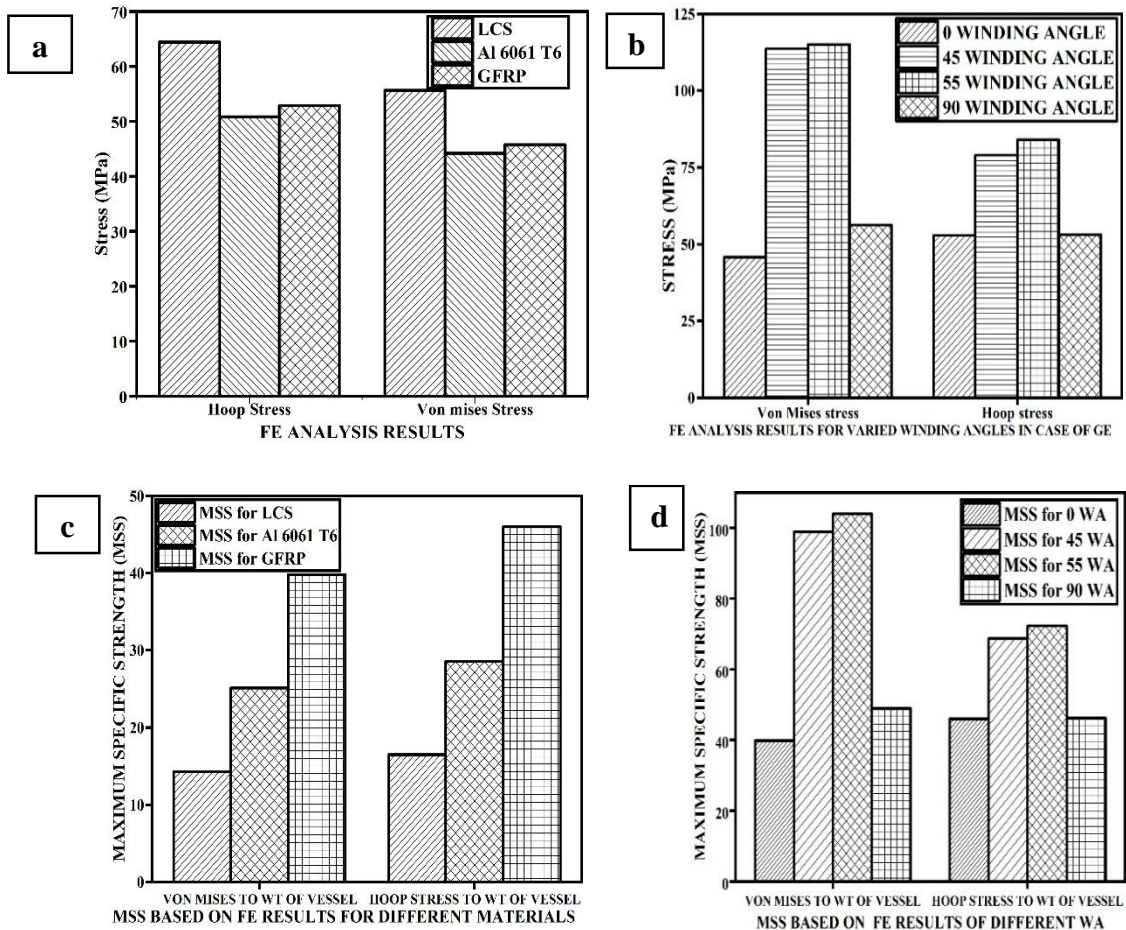
Figure 4.1 FE and MSS results: (a) Stress vs. Material, (b) Stress vs. WA, (c) MSS vs. Material, and (d) MSS vs. WA

The Figure 4.1(b) clearly highlighting that winding angles such as ±45° and ±55° are giving better results compared to 0° and 90° winding angles. Hence FE results clear showing that the fibers oriented other than 0° and 90° have more resistance against applied internal pressure. Similar trends are observed in case of MSS results, as shown in Figure 4.1(d). A small variation in MSS value is observed between ±45° and ±55° winding angles, which is negligible. The winding angles 0° and 90° have resistance against applied pressure only in one direction, whereas fibers with ±45° and ±55° winding angles can withstand load in more than one direction. Hence helical wound fibers are more responsible for variation in strength compared to hoop wound fibers in any filament wound FRP composite pressure

vessel cylinder. The stress and MSS value obtained after the FE study for varied winding angle is providing enough information and suggesting for further detailed investigation by varying other influencing parameters such as fiber volume fraction, stacking sequence.

4.2.2 Results of FE analysis of composite pressure vessel

As per winding parameters, we have 4 volume fractions, 7 winding angles, and 6 stacking sequences which leads to 168 FE simulations. Since we have a liner, the effect of the liner on the stress pattern is needed to be studied. Hence total of 336 FE simulations are carried out on pressure vessel cylinder (cylindrical pressure vessel with liner having 168 FE simulations and without liner having 168 FE simulations). In this section, important FE simulation results such as von Mises stress and hoop stress are compared in all varied winding process parameters with liner (PVC) and without liner. The FE results obtained for varied fiber volume fraction, winding angle, and stacking sequence are tabulated in Table 4.1, Table 4.2, Table 4.3, respectively. Here the effect of various winding parameters on stress pattern is clearly visible as we can clearly see that in Table 4.1, the stresses in the vessel is increasing with an increase in fiber volume fraction marginally. The PVC liner vessels have marginally higher stress values (~19%) compared to vessels without liner. This small difference may be due to the presence of PVC liner, which imparting resistance against applied internal pressure. Similar variations are observed in Table 4.2 and Table 4.3. The stress values gradually start increasing from 0.45(45%) to 0.75(75%) fiber volume fraction. Hence the effect of variation in fiber volume fraction on FE analysis results is moderate. Below 45%, the stress value further decreases drastically, and the stress value reaches peak value after a further increase in fiber volume fraction beyond 0.75. But practically, increasing the fiber content beyond 75% is not a feasible option. Figure 4.2 (a) highlights FE results for varied fiber volume fractions. The highest and lowest von mises stress value of 53.88 MPa and 40.81 MPa are recorded in the case of 75% V_f and 45% V_f respectively. The highest and lowest hoop stress value of 50.34 MPa and 41.39 MPa are recorded in the case of 75% V_f and 45% V_f respectively. In the case of pressure vessels without liners, there is a small drop in stress values recorded, as shown in Table 4.1.

Table 4.1 FE analysis outcomes for varied volume fraction (with/without liner)

S. No	Volume fraction	Von Mises stress in MPa		Hoop stress in MPa	
		With liner	Without liner	With liner	Without liner
1	0.45	40.81	32.65	41.39	37.11
2	0.55	45.64	33.36	44.82	37.74
3	0.65	49.91	33.95	47.66	38.23
4	0.75	53.88	35.00	50.34	39.09

*Fixed Winding angle WA (±55°) and Stacking sequence (SS3)

The stress values gradually start increasing from 0.45(45%) to 0.75(75%) fiber volume fraction. Hence the effect of variation in fiber volume fraction on FE analysis results is moderate. Below 45%, the stress value further decreases drastically, and the stress value reaches peak value after a further increase in fiber volume fraction beyond 0.75. But practically, increasing the fiber content beyond 75% is not a feasible option as it leads to poor wettability.

Table 4.2 highlights the FE results obtained for varied winding angles in filament wound GFRP pressure vessel cylinder. The highest and lowest von Mises stress value of 47.74 MPa and 39.57 MPa is obtained for ±45° and ±75° winding angle respectively. Similarly, the highest and lowest hoop stress value of 45.29 MPa and 42.09 MPa are recorded for ±45° and ±75° winding angle respectively. It can be observed from Figure 4.2 (b) that the influence of variation in winding angle on von Mises and hoop stress is less compared to fiber volume fraction. Also, there exists the least influence of PVC liner on FE results in varied winding angle cases.

Table 4.2 FE analysis outcomes for varied winding angle (with/without PVC liner)

S.No.	Winding angle (WA)	Von Mises stress in MPa		Hoop stress in MPa	
		With liner	Without liner	With liner	Without liner
1	±45°	47.74	31.39	45.29	35.26
2	±50°	46.88	32.29	45.08	36.39
3	±55°	45.64	33.36	44.82	37.74
4	±60°	44.12	34.63	44.43	39.34
5	±65°	43.00	36.08	43.88	41.17
6	±70°	41.47	37.67	43.11	43.16
7	±75°	39.57	39.24	42.09	45.12

*Fixed volume fraction (0.55) and Stacking Sequence (SS3)

Here, six stacking sequences are used in the FE model in order to study their influence on FE analysis results. Table 4.3 highlights about FE results of the GFRP pressure vessel cylinder with /without liner for six different stacking sequences along with fixed fiber volume fraction ($V_f = 0.55$) and winding angle ($\pm55°$) as primary input parameters. The highest and lowest von Mises stress of 46.06 MPa and 42.71 MPa are recorded for SS5 and SS2, respectively. Similarly, the highest and lowest hoop stress of 46.09 MPa and 43.61 MPa are observed in SS5 and SS2, respectively. The FE results obtained for varied stacking sequence cases are tabulated in Table 4.3, and the bar chart is plotted in Figure 4.2 (c). It is clearly visible from the current study that the effect of variation in stacking sequence on FE results is less compared to other two parameters (fiber volume fraction, winding angle). The main reason for the influence of varied fiber volume fraction, winding angle, and stacking sequence on von Mises and hoop stress is difficult to highlight just based on FE analysis results. However, among the existing present data from 336 FE simulations, the best and most influencing parameters can be predicted by using one of the optimization techniques called MCDM tools such as the VIKOR method is used in the present work.

Table 4.3 FE analysis outcomes for varied stacking sequence (with/without PVC liner)

S. No	Stacking sequence (SS)	Von Mises stress in MPa		Hoop stress in MPa	
		With liner	Without liner	With liner	Without liner
1	SS1	44.02	31.49	43.66	36.24
2	SS2	42.71	39.34	43.61	44.63
3	SS3	45.64	33.36	44.82	37.74
4	SS4	45.33	32.89	45.13	37.40
5	SS5	46.06	34.76	46.09	39.53
6	SS6	45.37	32.34	44.73	36.63

* Winding angle WA ($\pm55°$), volume fraction (0.55)

Bar Charts are plotted in Figure 4.2 (a), Figure 4.2 (b), and Figure 4.2 (c) as per data tabulated in Table 4.1, Table 4.2, and Table 4.3 to compare the different outcomes of FE simulations (with/without liner) for varied winding process parameters.
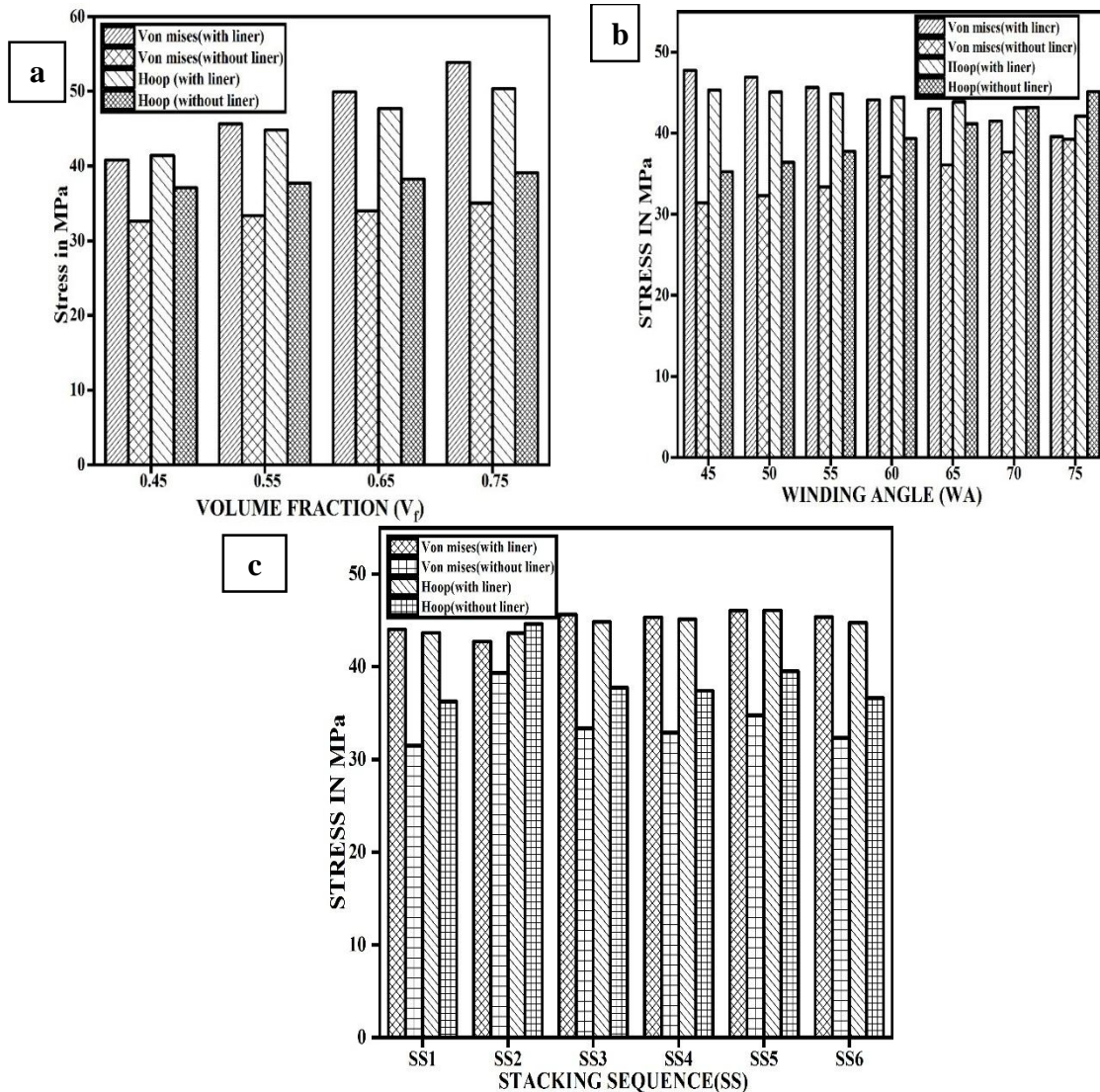
Figure 4.2 FE simulation results for varied winding process parameters (with PVC/without liner): (a) Volume fraction vs. Stresses (with/without liner), (b) Winding angle vs. Stresses, and (c) Stacking sequence vs. Stresses (with/without liner)

4.2.3 FE simulation results images

Figure 4.3A and Figure 4.3B illustrate various FE simulation results. The red portion indicates the stress pattern in the vessel, which varies from one stacking sequence to the other. The von Mises and hoop stresses are affected by varied stacking sequence (SS), whereas the longitudinal stress is unaltered in most of the cases. Hence the longitudinal stress is not considered in comparative studies.

71

STACKING SEQUENCE	VON MISES STRESS DISTRIBUTION	HOOP STRESS DISTRIBUTION
90° 14 90° 13 90° 12 -55° 11 55° 10 -55° 9 55° 8 90° 7 -55° 6 55° 5 -55° 4 55° 3 90° 2 90° 1 **SS1**	38.2202 39.8119 41.4035 42.9952 44.5869 46.1786 47.7703 49.362 50.9537 52.5454	33.27 34.6411 36.0121 37.3832 38.7543 40.1253 41.4964 42.8675 44.2385 45.6096
90° 14 90° 13 90° 12 90° 11 -55° 10 -55° 9 90° 8 90° 7 55° 6 55° 5 90° 4 90° 3 90° 2 90° 1 **SS2**	33.7463 35.6503 37.5543 39.4584 41.3624 43.2664 45.1705 47.0745 48.9785 50.8826	30.5659 32.0984 33.6308 35.1632 36.6956 38.228 39.7605 41.2929 42.8253 44.3577
90° 14 90° 13 55° 12 -55° 11 55° 10 -55° 9 90° 8 90° 7 -55° 6 55° 5 -55° 4 55° 3 90° 2 90° 1 **SS3**	39.8646 41.8922 43.9198 45.9474 47.975 50.0026 52.0302 54.0578	34.6344 36.3886 38.1429 39.8972 41.6515 43.4057 45.16 46.9143
90° 14 90° 13 55° 12 90° 11 -55° 10 55° 9 90° 8 -55° 7 55° 6 90° 5 -55° 4 55° 3 90° 2 90° 1 **SS4**	35.7393 37.3668 38.9942 40.6217 42.2492 43.8767 45.5042 47.1317 48.7592 50.3867	31.1623 32.5872 34.0121 35.4369 36.8618 38.2867 39.7116 41.1365 42.5614 43.9862

Figure 4.3A FE simulation results along with stacking sequences(SS1-SS4)

STACKING SEQUENCE	VON MISES STRESS DISTRIBUTION	HOOP STRESS DISTRIBUTION
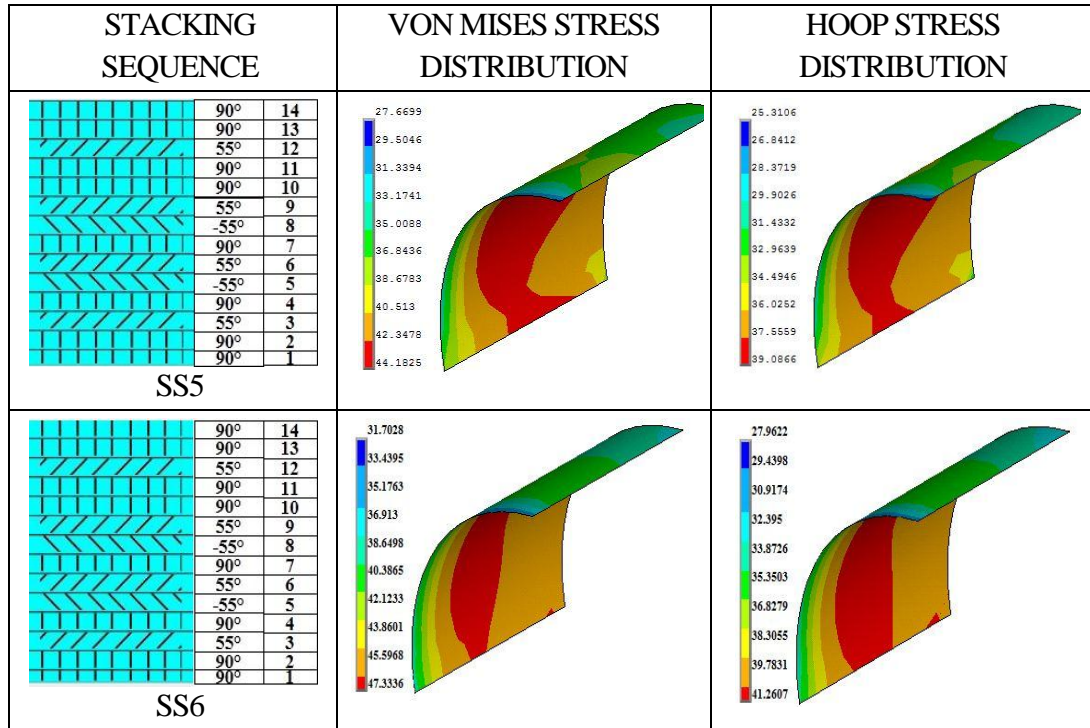
Figure 4.3B FE simulation results along with stacking sequences (SS5-SS6)

4.3 Outcomes of VIKOR Method

This is an MCDM tool that is applied to all FE simulation outcomes. As per FE analysis studies, we found that most of the results on GFRP vessels with PVC liners have a small edge over vessels that are without liners. Hence, it is decided that the VIKOR method can be used on FE simulation results (168 FE simulations based on 4-fiber volume fraction, 7-winding angle, 6-stacking sequence) of GFRP vessel cylinder with liner only. The main aim of this tool is to find the best suitable winding specifications in order to fabricate a GFRP pressure vessel. The steps involved are already discussed in the earlier part of the report. As per the various steps, the rankings are assigned for all 168 simulations. Based on the availability of resources for experimental studies and also based on the cut-off Q index value (0.03), we found that only 6 specifications hold good. Table 4.4 is highlighting the top-ranked specifications as per Q index values.

Table 4.4. The final alternatives which are suitable for the fabrication of pressure vessel as per Q index values

S. No.	Volume fraction, V_f	Winding angle, φ	Stacking Sequence (SS)	Alternative	Von Mises, MPa	Hoop Stress, MPa	Q	Rank
1	0.55	±60°	SS3	63	44.12	44.43	0.0091	1
2	0.55	±55°	SS3	57	45.64	44.82	0.0097	2
3	0.65	±60°	SS3	105	48.19	47.37	0.020	3
4	0.65	±55°	SS3	99	49.91	47.66	0.021	4
5	0.75	±65°	SS3	153	49.99	49.77	0.027	5
6	0.75	±55°	SS3	141	53.88	50.34	0.029	6

4.4 Results obtained from experimental studies

The details about products fabricated and subjected to various testing are listed in Table 4.5A.

Table 4.5A products fabricated and subjected to various testing

S. NO.	Product ID	Volume Fraction, V_f	Winding Angle (WA)	Stacking sequence type (SS3) ACTUAL STACKING SEQUENCE	Physical tests	Tribological test	Mechanical tests
1	055WA55SS3 (P1)	0.55	±55°,	$(\pm55°_2/90°_2/\pm55°_2)$	1. Density test, 2. Ignition loss test, 3. Water absorption test	Wet slurry erosion wear test	1.Tensile, 2. Compression, 3. Bending 4.Hoop tensile test
2	055WA60SS3 (P2)	0.55	±60°	$(\pm60°_2/90°_2/\pm60°_2)$			
3	065WA55SS3 (P3)	0.65	±55°,	$(\pm55°_2/90°_2/\pm55°_2)$			
4	065WA60SS3 (P4)	0.65	±60°	$(\pm60°_2/90°_2/\pm60°_2)$			
5	075WA55SS3 (P5)	0.75	±55°	$(\pm55°_2/90°_2/\pm55°_2)$			
6	075WA65SS3 (P6)	0.75	±65°	$(\pm65°_2/90°_2/\pm65°_2)$			

4.4.1 Physical, tribological and mechanical test results of filament wound GFRP test coupons

In this section, characterization studies on filament-wound GFRP test coupons are discussed in detail. The test coupons are prepared from fabricated GFRP cylinders, and coupon dimensions are marked on the cylinder to cut sufficient numbers as per respective

ASTM standards.

Table 4.5 Consolidated physical characterization results

	Physical Characterization					
Density test	Theoretical density in kg/m3	Experimental density in kg/m^3			Void content (%)	
	1.915	1.813			5.74	
Ignition	Initial weight (W$_i$) in grams	Final weight (W$_f$) in grams			Ignition loss (%)	
	5.8734	4.2458			27.71	
Water absorption test	Time Period (Hours)	Water Absorption (Grams)			Water Absorption (%)	
		Distilled	Sea	Boiling	Distilled	Sea	Boiling
	0	14.994	12.441	8.35	0	0	0
	2	15.004	12.451	8.37	0.06	0.088	0.239
	4	15.004	12.451	-	0.06	0.088	-
	8	15.022	12.457	-	0.166	0.136	-
	16	15.022	12.461	-	0.196	0.168	-
	32	15.044	12.471	-	0.332	0.248	-
	64	15.044	12.471	-	0.332	0.248	-
	Type of water	Water absorption (grams) at time T in week					
		0	1st	2nd	3rd	4th	5th
	Distilled	14.994	15.044	15.052	15.056	15.062	15.054
	Sea	12.44	12.476	12.486	12.49	12.498	12.5
		Water absorption (%) at time T in week					
	Distilled	0	0.333	0.386	0.412	0.453	0.399
	Sea	0	0.288	0.368	0.4	0.464	0.479

The detailed discussion about physical, tribological, and mechanical characterization studies results are explained in subsequent paragraphs. All characterization studies are conducted as per their respective ASTM standard method. Few important plots are shown in the respective test results discussion section. In all tests, the sufficient number of samples or test coupons are examined, and in results Table 4.5, Table 4.6, and Table 4.7 average value is highlighted in few test result columns.

4.4.1.1 Detail discussion on Physical Characterization studies

Density test

The density test was conducted on randomly selected five samples, and the average is considered as the final apparent density of the material. The presence of void content in the the specimen is calculated as per equation 1, and the results are tabulated in Table 4.5. Table 4.5 Consolidated physical characterization results The void content percentage is calculated using equation (5). The average void content percentage of 5.74 observed in filament wound test coupons. The air entrapment during the fabrication process, non-uniform distribution of resin, and glass fiber rovings are some of the possible reasons for non-uniform void content. Further, during fabrication of filament wound GFRP vessel, there is always the possibility of air entrapped as there exists a minute gap between subsequent windings and layers. Since we have alternative layers of hoop and helical windings to obtain required stacking sequence hence there exists variation in void content at different locations of the vessel. One more probable reason for varied void content is the non-uniform squeezing of excess resin during the fabrication process. Since the excess resin squeezing process is a manual process, hence possible human errors can't be ignored. The density test and void content results are tabulated in Table 4.5. The overall outcomes of the density test are highlighted in the bar chart, as shown in Figure 4.4. The bar chart illustrates the comparison between the theoretical and experimental density of the proposed composite material along with percentage variation in void content. The theoretical density of GFRP material is calculated using the rule of mixture (ROM).
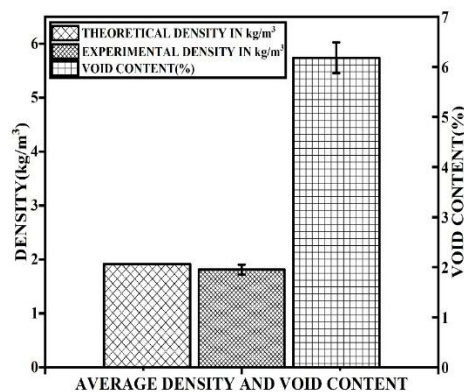
Figure. 4.4 Comparison of experimental and theoretical density and void content (%)

Ignition loss test

The ignition loss test is conducted on five randomly selected filament wound GFRP test coupons as per ASTM D2584-18 to know the fiber to resin ratio. The outcome of this test is percentage ignition loss i.e., amount of carbonaceous material (epoxy resin in this case) burnt for a specific period of time. In order to avoid fiber burnout, the combustion process is stopped after nearly 95% - 99% of epoxy resin is burnt, and the residue (glass fiber roving) is weighed.
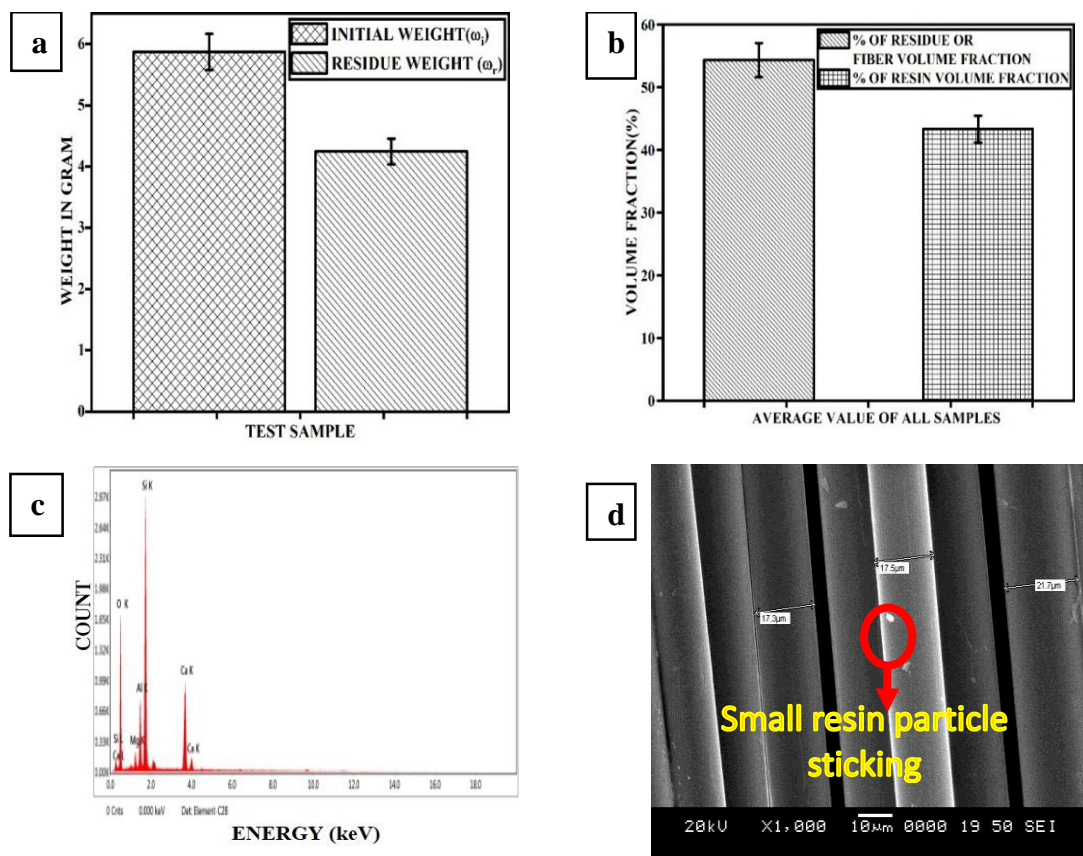
Figure 4.5 Illustrates about the various plots and sem image concerned with ignition loss test: (a) Variation in weight of the sample before and after test, (b) Fiber and resin volume fraction in %, (c) Energy Dispersive X-Ray analyzer plot used for elemental identification in ignition loss residue and (d) SEM image of ignition loss tested GFRP sample

The percentage ignition loss is calculated by using equation 2 as discussed in the methodology section, and results are tabulated in Table 4.5. The bar chart is plotted to

know the average amount of resin burnt with respect to residue in grams, as shown in Figure 4.5(a). As per analytical calculation and visual inspection, we can clearly observe the existence of some unburnt resin particles on glass fiber roving's.

Figure 4.5(b) is highlighting the variation in the percentage volume fraction of residue(fiber) and resin. There exists a small percentage of variation of volume fraction between burnt resin and residue(fiber). Further, the existence of resin particles on fiber roving's is justified by SEM image (incite of EDX plot) of tested samples. The energy dispersive X-ray analyzer is clearly indicating the presence of resin particles on fiber roving's, as shown in Figure 4.5(c) along with the SEM image. From the above studies, we can conclude that the filament wound GFRP composite has fiber to resin ratio of nearly 55:45.

Water absorption test

Normally moisture absorption is carried out in order to find resistance offered against the flow of water inside the material in various working environments. The suitability and limitation of GFRP composite in vast applications under high moisture environmental conditions detailed examination were needed. Even though many researchers have already studied this area as a case study, we definitely need re-examination in order to fulfill our requirement. The main objective of this test is not only to observe the moisture absorption capability, but we have also gone through a few mechanical tests after the water absorption test. Detailed discussion on this matter is further given in the subsequent section of mechanical characterization. There are three different types of waters used in this study such as distilled, seawater, and boiling distilled water. Five samples of each category are tested for water absorption in separate containers. The distilled and seawater tests are carried at room temperature for two different time slabs, such as hourly (2, 4, 8, 16, 32, 64) and weekly (week-1, week-2, week-3, week-4, week-5). Whereas boiling distilled water absorption test is conducted in a hot oil bath container for constant temperature (boiling water at 100˚C) for a 2-hour period as per ASTM standard D570-98 (ASTM D570 2014). It is observed in Figure 4.6(a) that water absorption has become almost uniform after 12-hours in the case of distilled and seawater tests. Whereas in the case of boiling distilled

water test, there is water absorption of around 0.239% after 2-hours of time period, which is highlighted in Table 4.5. The uniform water absorption in the case of distilled and seawater is mainly due to presence of uneven voids, which have certainly influenced the flow pattern of water molecules inside the samples. The water absorption observed in all three tests is significantly low as GFRP composites are non-hydrophilic. Hence, we needed a longer time period of water absorption test to judge on moisture absorption characteristics of filament wound GFRP composites.
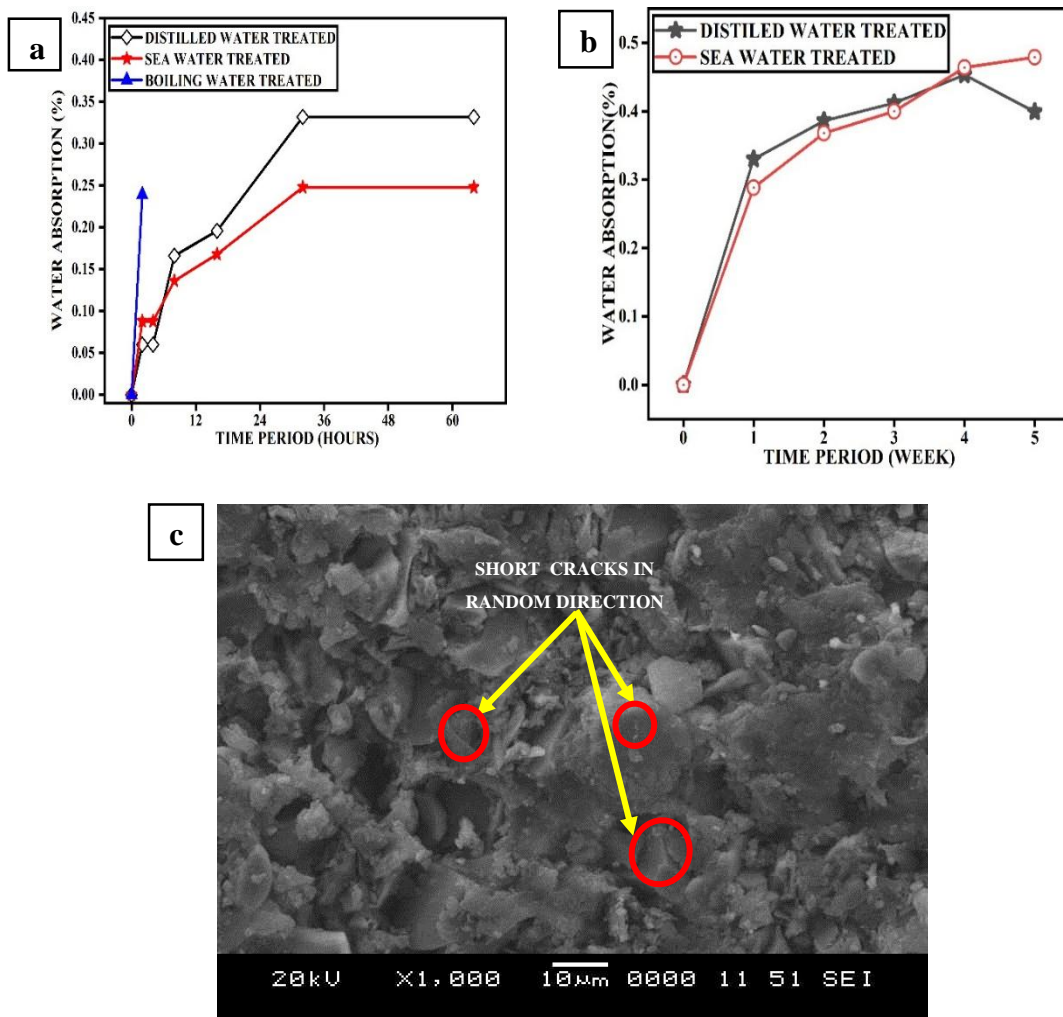
Figure 4.6 Highlighting about various results plotted after water absorption test: (a) Time period (hour) vs. Water absorption in %, (b) Time period (week) vs. Water absorption in % and (c) SEM image of water absorption tested sample

79

Hence a little longer, such as five weeks of water absorption examination, was performed. But even after 5 weeks of exposure to the water surface, there exists a negligible percentage of water absorption. The boiling > sea > distilled is the order of highest to lowest quantity of water absorbed in respective water absorption tests. The amount of water absorbed in the boiling water test is larger compared to the amount of water absorbed in case of seawater exposure and distilled water exposure. The least amount of water absorbed in case of distilled water indicated that the migration of salt could be driving higher water absorption. In the case of boiling the temperature gradience, the bursting of matrix cracks to create larger cracks that encourage greater absorption might have enhanced the absorption. Evidence of large number of cracks could be noticed in the SEM micrograph of a filament wound GFRP sample that was exposed to boiling water is shown in Figure 4.6(c). The impact of water absorption examination on filament-wound GFRP composite various mechanical properties are further studied and discussed in detail in the mechanical characterization results section. The comparison of water absorption percentage after five weeks of examination between distilled and seawater tests is as shown in Figure 4.6(b).

4.4.1.2 Detail discussion on Tribological Characterization studies

Slurry erosion test

The slurry erosion test is conducted on filament-wound GFRP composite in order to explore erosion wear property. There are two types of erosion wears exist such as wet and dry sand slurry erosion. Here we have focused only on wet sand slurry erosion wear. Since the GFRP vessels are subjected to various working environments during their application periods, one of the main applications is processing, transportation of different chemicals, materials where the study of wear characteristics of vessels becomes crucial. In the present work, we are examining the wear property by coupon level tests as per ASTM D75-95.

The number of experiments needed to be conducted is decided by the design of experiments (DOE) tool by using the Taguchi L9 method in a Minitab software. The results obtained from the wear test are tabulated in Table 4.6. Figure 4.8(a) clearly shows that the erosion rate is increasing uniformly with an increase in the size of the sand particle. Whereas with

80

an increase in sand concentration in a slurry container there is an uneven increase in erosion is observed, as shown in Figure 4.8 (b). As we can see, that for 250 g, the erosion rate is much lesser compared to 500 g and 750 g of sand concentration. The probable reasons for such variation in erosion rate are the influence of other less important parameters such as the shaft speed and time is taken for completion of a defined set of revolution for respective sand concentrations.

Table 4.6 Tribological characterization results

Tribological study of filament wound GFRP composite						
Slurry erosion test	S.No.	Sand particle size, and BSS std.	Weight of sample before the test in grams	Weight of sample after test in grams	Weight loss (%)	Sand particle size in microns
	1	Course, 14	13.00	11.75	9.67	1200
	2	Medium, 18	15.78	15.15	4.35	800
	3	Fine, 36	11.13	10.99	1.27	400
	S.No.	Sand conc. in slurry in grams	Weight of sample before the test in grams	Weight of sample after test in grams		Erosion rate (%)
	1	250	13.71	13.41		2.19
	2	500	13.09	12.23		6.57
	3	750	13.11	12.25		6.56

The decreasing order of erosion rate of 9.67 % > 4.25 % > 1.27 % for respective sand particle size (1200 μ > 800 μ > 400 μ) is observed. Similarly, for sand concentration of 750 g > 500 g > 250 g the erosion rate of 6.57 % > 6.56 % > 2.17% is observed.
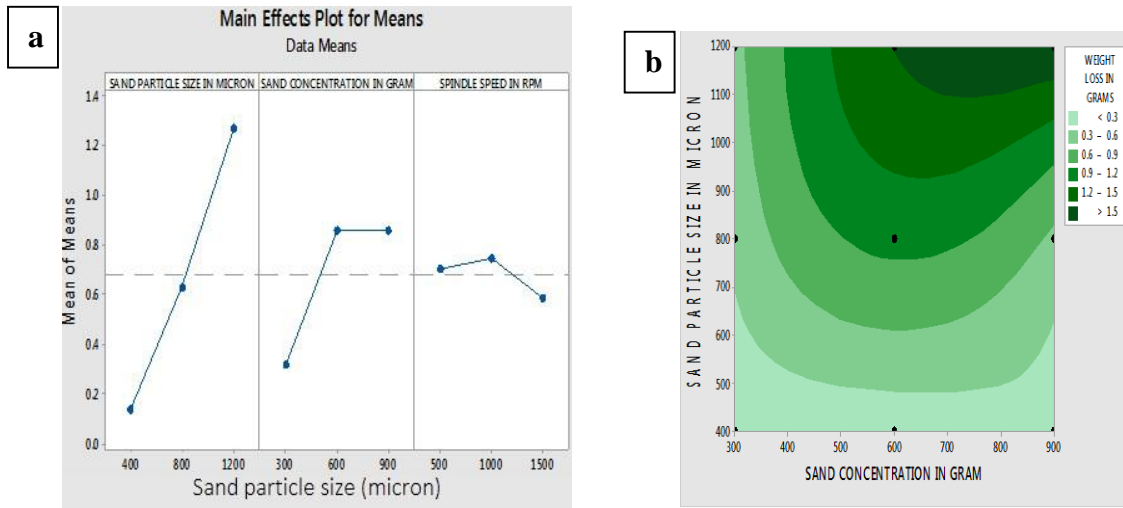
Figure. 4.7 (a) Main effect plot(sand particle size vs mean of means, sand concentration vs mean of means, Spindle speed vs mean of means); (b) 2D contour plot
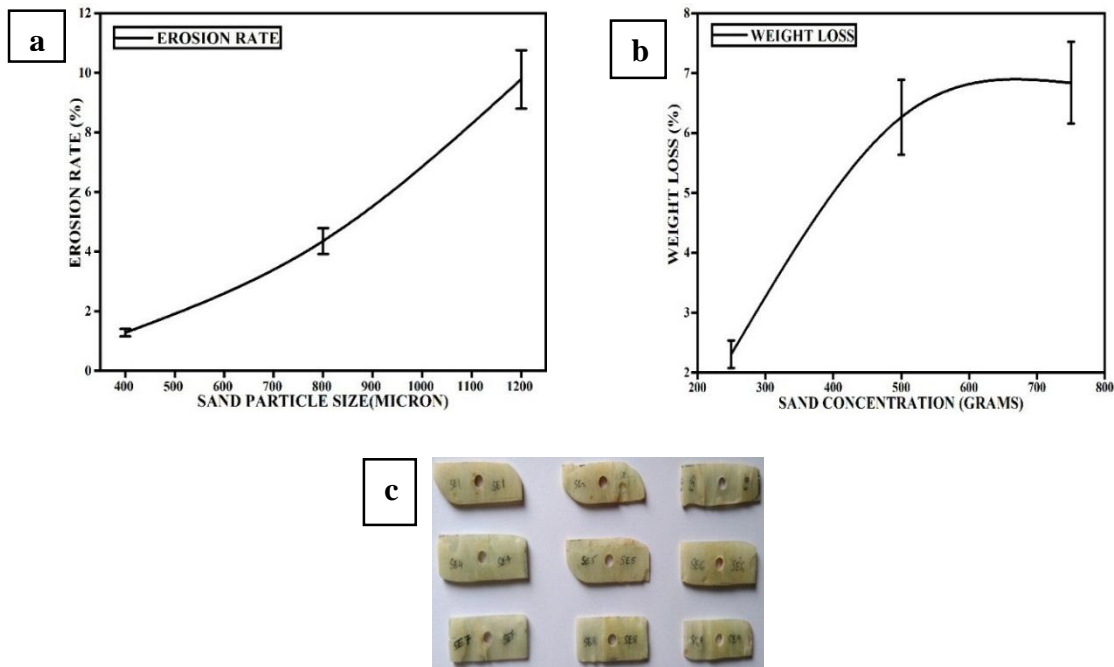
Figure 4.8 Illustrates the plots for wet slurry erosion rate based on varied and particle size and its concentration and also about erosion tested samples: (a) Sand particle size vs. erosion rate, (b) Sand concentration vs. erosion rate and (c) All samples tested for wet slurry erosion

Regression Equation

Weight Loss in grams = - 0.870 + 0.001413 Sand particle size in micron-----------------(11)

+ 0.000900 Sand concentration in gram - 0.000120 Spindle speed in rpm

From the fraction factorial Taguchi L9 method and regression analysis studies, the main effect plot and 2D contour plot are obtained as shown in Figure 4.7 (a) and (b), respectively. We can clearly observe that the significance of sand particle size on the erosion rate or weight loss is much higher than the other two parameters. The main reason could be the friction between large-sized sand particles and samples is more effective; the longer period of sand particles edges sharpness could be one of the reasons for the higher erosion rate.

4.4.1.3 Detailed discussion on Mechanical Characterization studies

Tensile test

The tensile test is conducted on filament-wound GFRP composite (five) test coupons as per ASTM D3039(ASTM 2014). The outcomes are tabulated in Table 4.7. The primary mode of failure is fiber pull-out. The highest tensile strength is observed in FWCYT2 as 10.12 MPa and lowest in FWCYT1 as 8.78 MPa.

Table 4.7 Consolidated mechanical characterization results

Mechanical Characterization		
Tensile test as D3039	Ultimate Tensile Strength in MPa	Tensile Modulus in GPa
	11.17	44.67
Compression test as per D3410	Ultimate compressive strength in MPa	
	51.50	
Flexural test as per D7264	Flexural strength in MPa	Flexural modulus in GPa
	43.6	7.32
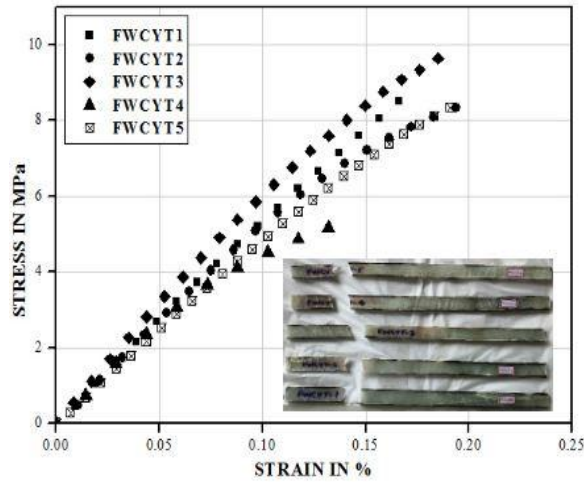
Figure. 4.9 The Stress vs. Strain graph is plotted for outcomes of filament wound GFRP samples tested under tensile load; image of samples failed due to tensile load is highlighted inside the graph

Compression test

The compression test on filament-wound GFRP composite is conducted as per ASTM D3410(Method 2017) for a set of five test coupons.
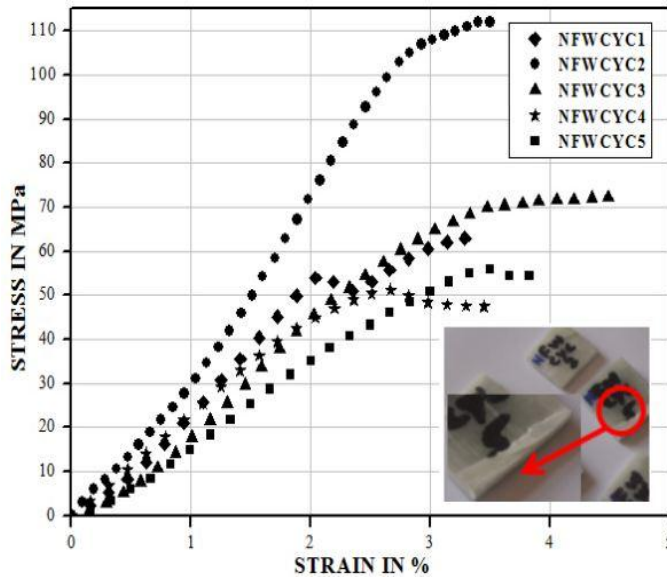
Figure 4.10 The Stress vs. Strain graph is plotted for outcomes of filament wound GFRP samples tested under a compression load; the image of samples that failed due to compression load is highlighted inside the graph

The compression tested GFRP sample fails mainly due to micro buckling, micro crack, fiber breakage, matrix crack. The maximum compressive strength is observed in NFWCYC2 with the value of 109.65 MPa, and a minimum compressive strength of 50.25 MPa is observed in NFWCYC1. This variation in stress value is mainly due to the presence of void content, improper distribution of fibers, which is also due to a cluster of matrix or fibers. All these can be clearly observed in SEM images of tested samples at the fractography analysis section. The graph of stress versus strain is plotted as shown in Figure 4.10, and a failed sample is highlighted in a circle.

Flexural test

The five test coupons of filament wound GFRP composite is subjected to flexural test examination as per ASTM D7264(ASTM International 2007). These specimens have failed due to fiber breakage after the application of a 3-point bending load. The top layer fibers on the specimen have failed due to compressive load, whereas the bottom layer fibers have failed due to tensile load.
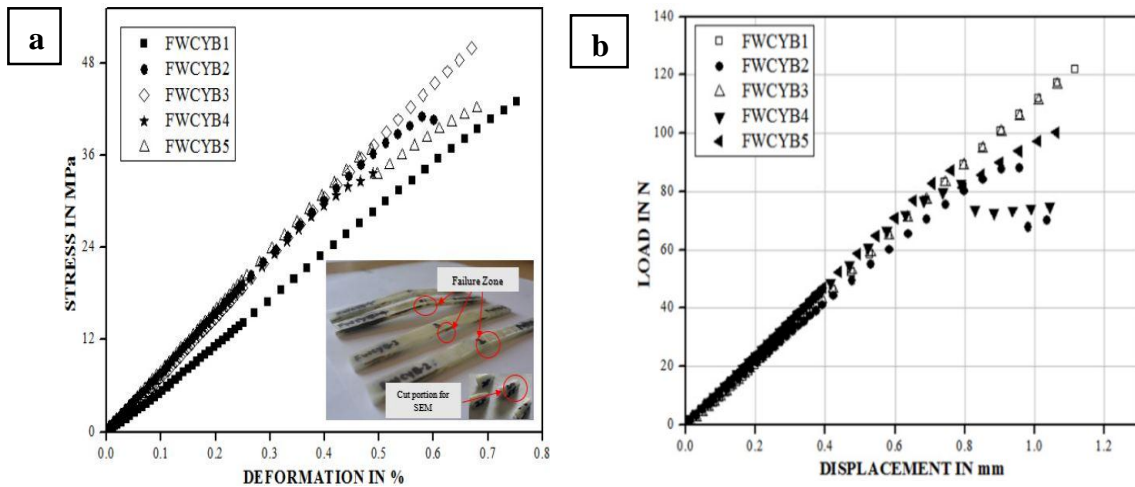
Figure 4.11 (a) Stress vs. Deformation, (b) Load vs. Displacement graphs are plotted for outcomes of flexural test conducted on filament-wound GFRP samples, the failed samples image is also highlighted in the plot

The major outcomes of this experiment are flexural modulus and flexural strength, which

are tabulated in Table 4.7. The highest and lowest flexural strength of 55.1 MPa and 33.8 MPa in FWCYB3 and FWCYB4 are noted, respectively. Similarly, about 7.82 GPa and 5.86 GPa flexural modulus was observed in FWCYB5 and FWCYB1, respectively. The stress versus deformation along with failed samples and along with failed zones are shown in Figure 4.11(a). The variation in stress value is mainly due to misalignment of different fiber layers of filament wound samples, uneven distribution of epoxy resin which may lead to poor bonding between fibers and matrix. The presence of void content is also having a major influence on varied stress values. The load versus displacement is plotted as shown in Figure 4.11(b), which highlights the influence of load variation on different fibers displacement. Further failed samples are subjected to fractography analysis to investigate the different causes or modes of failure.

Overall outcome and comparative study of mechanical characterization of filament wound GFRP composites with earlier research work

As per literature studies, there exists enough research data on laminated GFRP composites, and after comparing the mechanical properties, such as tensile, compression, and flexural, with proposed filament wound GFRP composites, it is found that the proposed filament wound GFRP composites are not superior to laminated GFRP composites due to many aspects. As per some of the key observations, the composite fabrication method, during the fabrication process, some of the important compositions of material such as fiber volume fraction, the fiber or woven fabric orientation, stacking sequence to suit the necessity of application are the deciding factors of composite material property. From various results as per the literature review, there is hardly a little literature focusing on filament wound composites with different angular orientations (i.e., varied winding angles and stacking sequence in parallel). Hence from observation of various outcomes of mechanical characterization, filament wound GFRP composites have been found to possess inferior properties compared to GFRP laminates. A further property of filament wound GFRP material can be enhanced by adopting suitable modifications in the existing fabrication method and also making special changes in the existing physical feature, such as increasing

the thickness of test coupons in case of filament wound GFRP material.

Failure Analysis

The Scanning Electron Microscope (SEM) is used for examining or fractography analysis of various failed or tested filament wound GFRP samples. The failure analysis is helpful in investigating primary reasons for respective mode or type of failure during various tests. A typical SEM equipment made of JOEL JSM 6380LA at MME@NITK Surathkal used for fractography studies.

Failure analysis of tensile tested samples

The fractography study of failed tensile tested samples is carried out with the help of SEM images. From Figure 4.12 (a) and (b), we can clearly judge why there is a variation in tensile strength exist in spite of having the same material composition in all tested samples. As we can see in Figure 4.12 (b), which is exhibiting different modes of failure such as adhesive fracture, cohesive fracture, presence of voids, improper bonding among matrix material and fiber. The river flow pattern in Figure 4.12 (a) is an indication of resistance offered by the matrix against deformation under the application of tensile load. The fibers have failed due to shearing action, which can be observed in SEM images.
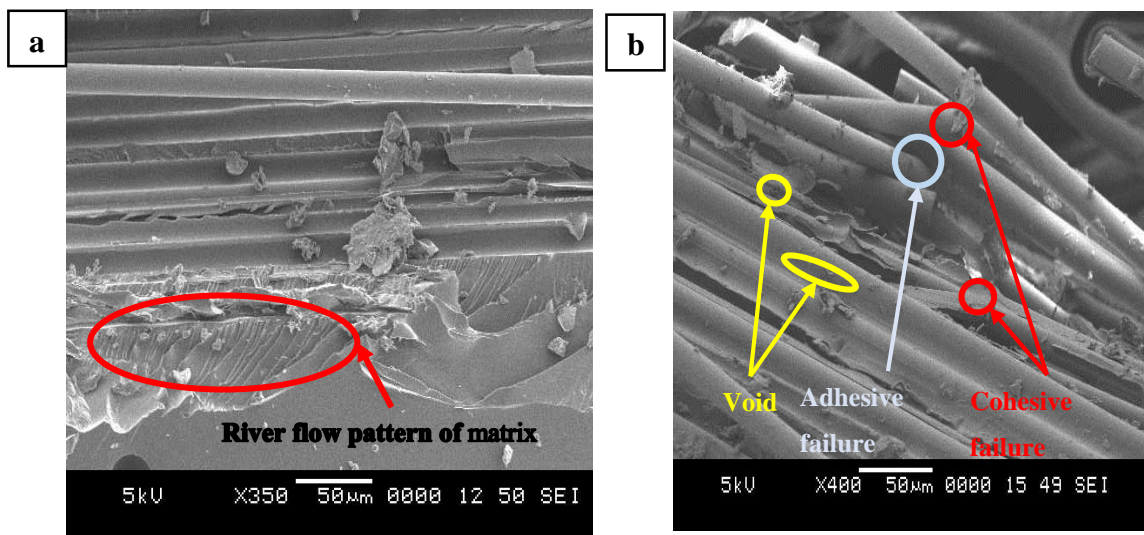
Figure. 4.12 SEM image of failed GFRP samples under the application of tensile load which are highlighting the various spots in micrographs: (a) River flow pattern of the matrix, (b) Presence of voids, adhesive and cohesive failure

Failure analysis of compression tested samples

The compression tested samples are subjected to fractography study in order to elaborate failure criteria by using various images obtained from Scanning Electron Microscope (SEM). The SEM images of the tested sample are taken at different points to study the behavior of fiber and matrix for the applied compressive load. Figure 4.13(a) is clearing showing different modes of failure due to compressive load on filament-wound sample. Figure 4.13(a) is highlighting the lateral splitting of fiber due to the high length to diameter ratio, poor interfacial bonding between fiber and matrix, and the presence of voids. The presence of void also leads to fiber buckling as the gap between fiber and matrix is high, which is clearly visible in Figure 4.13(b). The angular splitting of fibers in Figure 4.13(a) is a clear indication of the shear mode of failure.
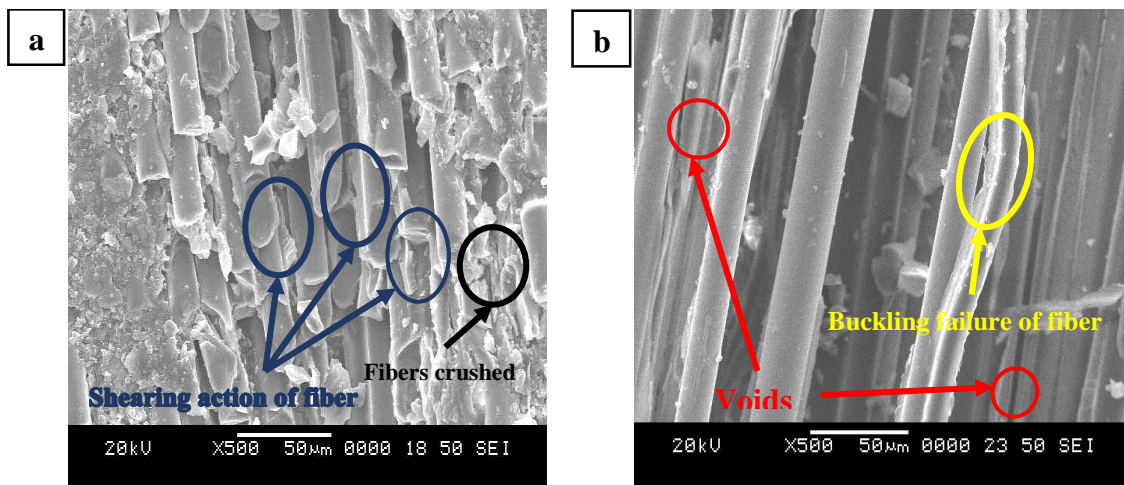
Figure 4.13 Some SEM images of failed GFRP samples that have failed due to compression load under compression test are highlighting modes of failure and presence of voids: (a) Shearing and lateral splitting of fiber, (b) Voids and buckling of fibers

Failure analysis of tested flexural samples

The bending tests have different failure criteria whose various SEM images are shown in Figure 4.14.
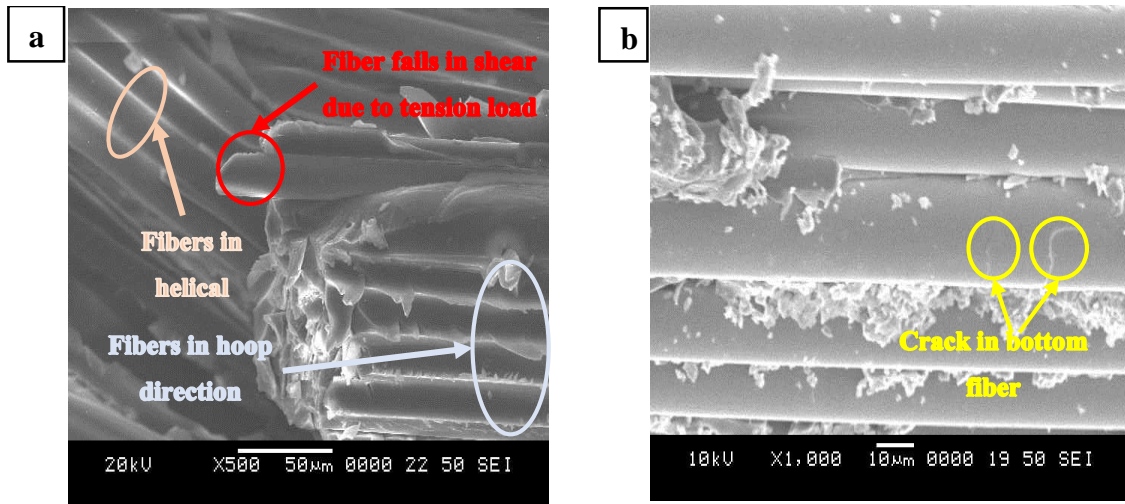
Figure 4.14 The various modes of failure occurred in GFRP samples under the influence of flexural load is highlighted in SEM micrographs with pointed arrows: (a) Hoop and helical fibers failed in shear, (b) Crack in bottom fiber due to tension
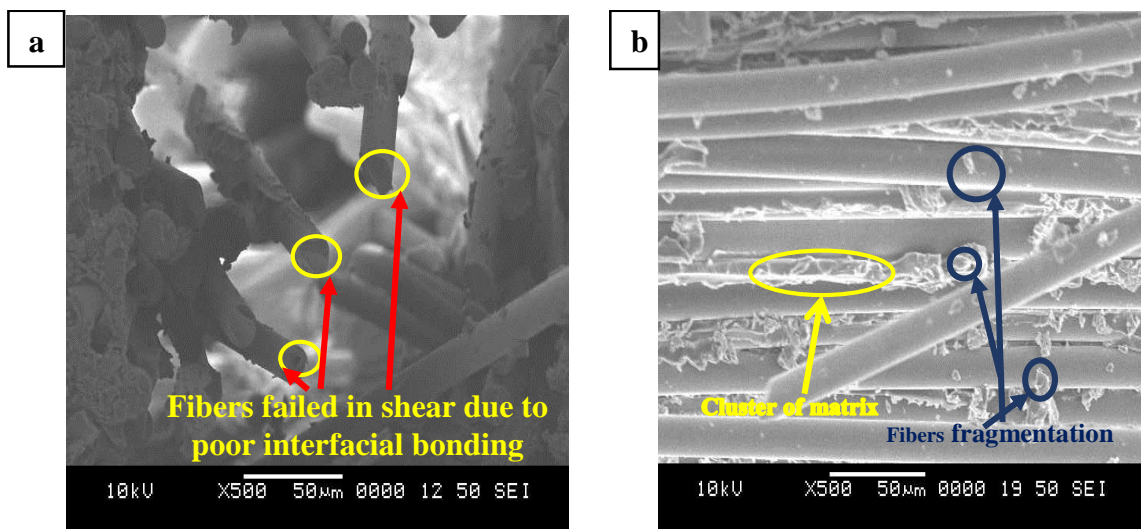
Figure 4.15 SEM images highlighting the failed samples internal pattern, which is helpful in judging the actual reason of failure after the sample was failed to flexural load: (a) Poor interfacial bonding between fibers and resin particles, (b) Fiber fragmentation

The hoop and helical direction fibers are clearly visible in the above Figure 4.14(a). The fibers in this flexural test have failed in different modes, such as the fibers which are at the

bottom half of the test sample in a 3-point bend test have failed in tension by shearing action, a sample of such fiber failure is highlighted in above Figure 4.14(b). At the same time, fibers at the uppers half have failed due to compression. Figure 4.14(b) showing crack generation in the fiber due to the applied load. This crack is leading to break the fiber anytime. The resin particles sticking on fibers can be observed in the form of white spots in Figure 4.14(b).

Since the resin distribution is not uniform, and as we know that resin or matrix plays a very important role in the transfer of load from one fiber to another, pre-peak load failure is one of the modes of failure that can be anticipated because of poor distribution of resin. Hence overall flexural strength of the material also gets reduced. Figure 4.15(a) has clearly highlighted the broken and blunt edges of fibers. The mode of failure is due to interlaminar shearing action between fibers and also due to the lack of matrix material surrounding the fibers to resist the compressive stresses which are generated due to bending load. Figure 4.15(b) has a cluster of matrix due to the adhesion of failed fiber surfaces. All these figures illustrate the failure of the GFRP specimen subjected to the three-point bend test. As per the literature study and ASTM standard D7264, any specimen failure due to tension in a bending test gives rise to the flexural strength of that specimen. Hence the tension side of the flexural test sample will be given more importance. Figure 4.15(b) showing fiber fragmentation due to friction between the matrix and failed fiber particles. The neatly arranged fibers, along with the uneven quantity of matrix material around fibers, is also shown in Figure 4.15(b). This uneven matrix quantity is mainly due to lack of adhesion between matrix and fibers, also due to manufacturing difficulties such as improper curing, presence of voids.

4.5 Hygrothermal ageing effect on fabricated GFRP pressure vessel

Table 4.8, Table 4.9, and Table 4.10 are highlighting the hygrothermal ageing results in tap water, seawater, and tap water with oil, respectively. A particular set of samples (in the present study bending test samples) are properly cleaned and weighed on a high precision weigh balance before the start of ageing study. The samples are now subjected to aging at different ageing mediums for a period of 15 days (i.e.10 samples for TW, 10 for SW, and

10 for TWWO ageing = 30 sample set). After 15 days of ageing, the sample are taken out from ageing mediums and cleaned gently using separate paper towels before weighing them on weigh balance. The weights of all samples before and after ageing are noted in a result column as per different ageing mediums. A similar procedure is followed for samples kept for 30 days and 45 days ageing periods. A similar method is followed for all other mechanical test coupon ageing studies.

Table 4.8 Effect of tap water (TW) ageing on GFRP test coupon's

S. No.	Product ID	Initial weight (any test sample)	Weight after 15 days	Weight after 30 days	Weight after 45 days
1	055WA55SS3(P1)	24.54	24.93	26.11	24.88
2	055WA60SS3(P2)	22.08	22.69	23.02	22.46
3	065WA55SS3(P3)	25.8	25.02	25.55	26.3
4	065WA60SS3(P4)	23.01	22.5	22.41	23.4
5	075WA55SS3(P5)	26.06	25.74	26.3	26.48
6	075WA65SS3(P6)	23.85	23.59	24.29	24.23

Table 4.9 Effect of seawater (SW) ageing on GFRP test coupon's

S. No.	Product ID	Initial weight (any test sample)	Weight after 15 days	Weight after 30 days	Weight after 45 days
1	055WA55SS3(P1)	22.76	24.03	25.74	22.98
2	055WA60SS3(P2)	22.22	22.9	22.45	22.45
3	065WA55SS3(P3)	25.57	25.15	25.75	25.82
4	065WA60SS3(P4)	22.68	23.05	22.31	22.93
5	075WA55SS3(P5)	25.94	26.77	26.63	26.15
6	075WA65SS3(P6)	22.81	23.85	23.61	24

As it can be observed from Table 4.8, the effect of tap water on filament-wound GFRP samples is not at a considerable level which is clearly visible in the form of weight before and after ageing in result Table 4.8. Overall, the weight of the sample is not varying even 1% of its initial weight. Table 4.8 and Figure 4.16 a) are clearly showing that product P1 is more influenced among 6 products by the tap water ageing process. The product P1 weight is varying by 6% from its initial weight. This may be due to the presence of void

and poor interfacial bonding between fiber and matrix, which has led to the entrapment of water molecules.

The ageing method used in the case of tap water hygrothermal ageing is repeated, i.e., the samples are thoroughly cleaned from oil, dust, and other water particle and weighed before the start of ageing. The seawater obtained from the nearby Arabian seashore is used instead of tap water as ageing media. In this ageing study, product P1 and P6 are more influenced compared to other products. The main reason could be the reaction between active chloride particles and matrix material at a constant temperature of 80°C for a longer period of time. Another reason could be the combination of highly concentrated chloride particle and non-uniform strength between fiber and matrix at elevated temperature has led to the accumulation of chloride particles. It is clearly observed from Table 4.9 and Figure 4.16 b) that product P1 and P6 have weight variations of 11% and 5% from their initial weight after seawater ageing.

Table 4.10 Effect of tap water with oil (TWWO) ageing on GFRP test coupon's

S. No.	Product ID	Initial weight (any test sample)	Weight after 15 days	Weight after 30 days	Weight after 45 days
1	055WA55SS3(P1)	21.67	22.9	22.74	21.99
2	055WA60SS3(P2)	22.23	22.78	23.28	22.62
3	065WA55SS3(P3)	24.89	25.31	25.12	25.34
4	065WA60SS3(P4)	23.06	22.64	23.1	23.47
5	075WA55SS3(P5)	26.81	26.87	26.23	27.24
6	075WA65SS3(P6)	23.89	24.45	23.82	24.32

The probable reason for the variation in weight is the entrapment of oil particles inside the void at elevated temperature. Since oil particles have two properties that differentiate it from tap water and seawater, i.e., cooling time is higher and are highly viscous in nature at room temperature. Hence entrapment of oil particles at 80°C at an early stage of ageing (15 days) and even after cooling, few oil particles remain present has led to higher variations in the weight of the sample at stage one (15 days ageing) itself. The tap water with oil ageing results are tabulated in Table 4.10, and a graph of the number of ageing days versus the weight of product is plotted in Figure 4.16 c). In the case of seawater and tap water

with oil, the small variation in strength can be clearly observed. The main reason could be a probable reaction of chloride particle with matrix material at high temperature, SAE oil molecules entrapment in the sample, which might have led to variation in the weight of the sample after ageing. At present, as per tap water ageing, the filament wound GFRP test coupons are least affected and hence might have retained the same strength as before ageing. The retaining of mechanical strength can be clearly understood only after mechanical testing and further SEM analysis of failed samples which will give a clear picture of material behaviour.
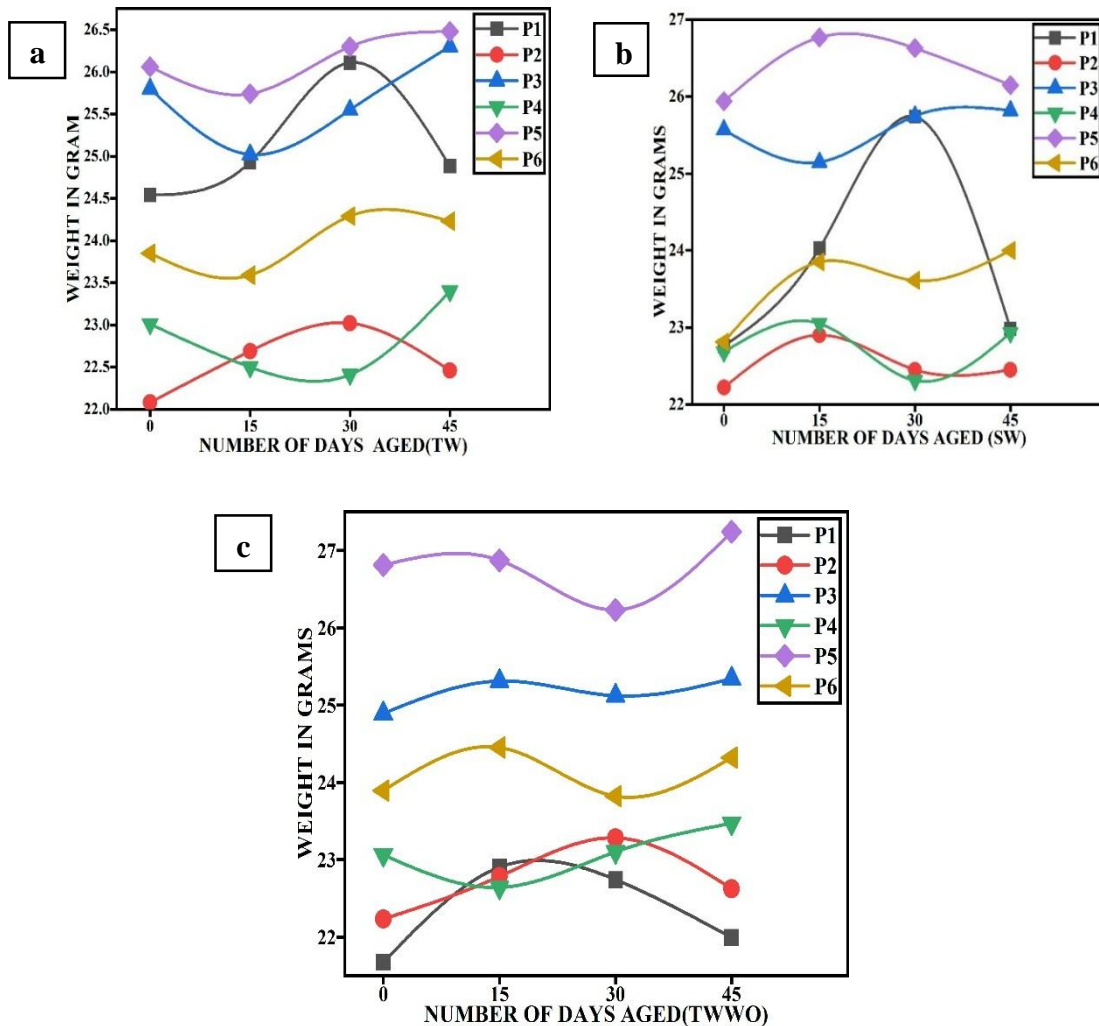
Figure 4.16 (a) Tap water ageing (product for ageing in days vs. weight of sample), (b) Seawater ageing (product for ageing in days vs. weight of sample), (c) Tap water with oil ageing (product for ageing in days vs. weight of sample)

93

4.5.1 Effect of hygrothermal ageing on mechanical properties of filament wound GFRP test coupons

The different hygrothermal ageing studies have different effects on the mechanical properties of filament wound GFRP test coupons. In this study, the mechanical properties such as ultimate tensile strength (UTS), ultimate compressive strength (UCS), and ultimate flexural strength (UFS) of aged samples are obtained by respective ASTM testing methods and are compared with unaged samples mechanical properties to understand the capability of property retention.

4.5.1.1 Hygrothermal ageing effect on ultimate tensile strength of filament wound GFRP test coupons

In this section, tensile test on aged (45 days at fixed temperature of 80°C) and unaged GFRP test coupons are conducted as per ASTM D3039. The Table 4.11 is highlighting about tensile test results of unaged and aged (TW, SW, TWWO) GFRP test coupons. As per the bar charts shown in Figure 4.17 (a) and Figure 4.17 (b) the product P3 and P5 have shown greater resistance against all 3 ageing mediums.

Table 4.11. Tensile test results of aged and unaged samples

Product ID	Ultimate tensile strength (UTS) in MPa			
	Unaged	Tap water (TW)	Sea water (SW)	Tap water with oil (TWWO)
055WA55SS3(P1)	34.8	20.4	19.2	22.3
055WA60SS3(P2)	27.4	25.8	23.6	27.1
065WA55SS3(P3)	**30.8**	**29.2**	**32.1**	**34.1**
065WA60SS3(P4)	32.7	27.2	27.2	26
075WA55SS3(P5)	**27.6**	**27.7**	**26.8**	**27.6**
075WA65SS3(P6)	29.4	25.6	25.1	21.3
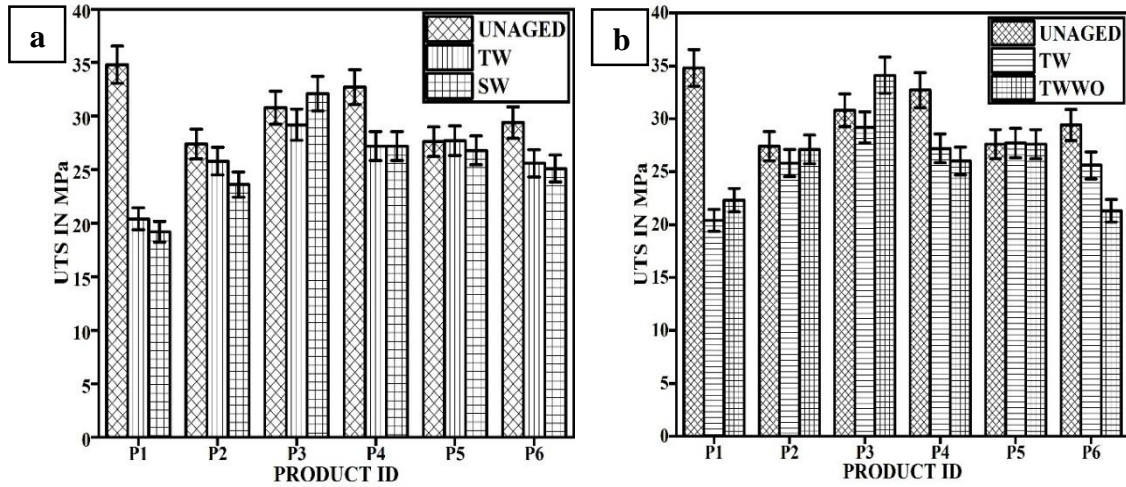
Figure 4.17 (a) UTS of Unaged-TW-SW, (b) UTS of Unaged-TW-TWWO

The retention capability of product P3 and P5 is highly appreciable and same are highlighted in the Table 4.11. The expected reason for retention in tensile strength could be strong interfacial bonding between fiber filament and matrix material at elevated temperature for longer period of time. The same has been justified in the SEM image analysis of failed aged and unaged tensile sample in later part of present work.

4.5.1.2 Hygrothermal ageing effect on ultimate compressive strength of filament wound GFRP test coupons

In the present study, a compression test is conducted on unaged and aged GFRP test coupons as per ASTM D3410. The results are tabulated in Table 4.12. From the Table 4.12 and Figure 4.18 (a) and (b), which clearly shows that product P3 and P6 have high retention capability compared to other products. The accumulation of chloride particles and SAE oil molecules at the key location of the sample, such as joining point/interfacial of fiber and matrix, at weak fiber filaments, which has led to improvement on bonding strength and hence overall compressive has improved after TW, SW and TWWO ageing.

Table 4.12. Compression test results of aged and unaged samples

Product ID	Ultimate compressive strength (UCS) in MPa			
	Unaged	Tap water (TW)	Seawater (SW)	Tap water with oil (TWWO)
055WA55SS3(P1)	118.63	72.99	96.46	65.68
055WA60SS3(P2)	63.02	103.54	112.34	129.03
065WA55SS3(P3)	**102.85**	**91.62**	**93.97**	**97.36**
065WA60SS3(P4)	70.4	88.41	81.83	117.74
075WA55SS3(P5)	72.82	88.12	90.87	89.62
075WA65SS3(P6)	**91.55**	**97.06**	**81.29**	**94.20**

The improvement in UCS in a few of products is mainly due to filling of voids, reinforcement to fiber and matrix bonding, and non-uniformity of load distribution to uniformity due to re-strengthening of fiber-matrix bonding strength to resist any applied compressive load.
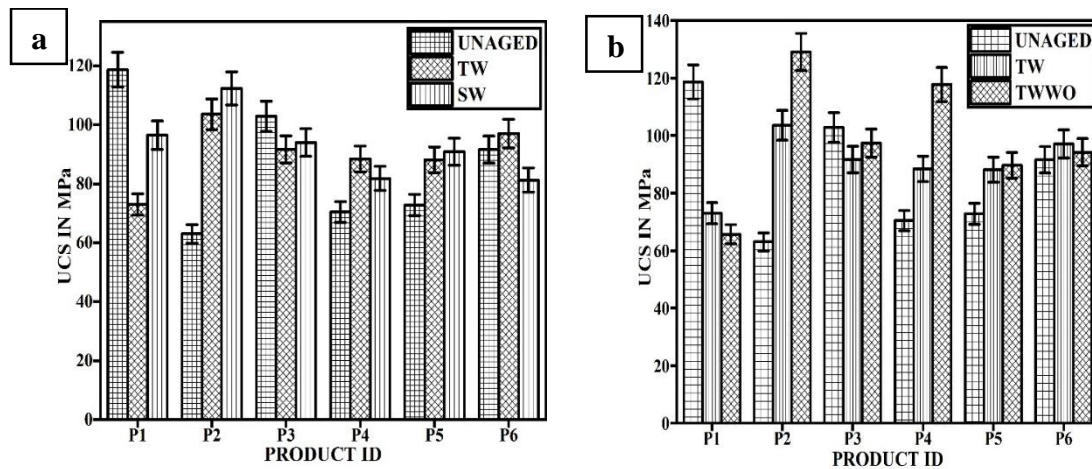
Figure 4.18 (a) UCS of Unaged-TW- SW, (b) UCS of Unaged-TW-TWWO

4.5.1.3 Hygrothermal ageing effect on ultimate flexural strength of filament wound GFRP test coupons

In this study, ultimate flexural strength (UFS) of unaged and aged GFRP test coupons are compared. The flexural test is conducted as per ASTM 7264. The results are tabulated in Table 4.13. Product P2 and P3 have shown the highest retention rate compared to other

products. The same can be clearly seen in Table 4.13 and Figure 4.19 (a) and Figure 4.19 (b). The primary reason for the highest retention rate could be the balance of fiber and matrix material bonding strength at the upper and lower part of GFRP test coupons. Another reason could be the lesser influence of ageing mediums such as seawater chloride particles and hot oil molecules on weaker and vulnerable portions of test coupons even at elevated temperature.

Table 4.13. Bending test results of aged and unaged samples

Product ID	Ultimate flexural strength (UFS) in MPa			
	Unaged	Tap water (TW)	Seawater (SW)	Tap water with oil (TWWO)
055WA55SS3(P1)	47.72	37.48	49.68	51.69
055WA60SS3(P2)	**55.52**	**49.23**	**47.79**	**56.37**
065WA55SS3(P3)	**75.58**	**70.49**	**73.97**	**64.52**
065WA60SS3(P4)	84.30	63.70	49.16	61.12
075WA55SS3(P5)	57.65	42.58	54.83	68.02
075WA65SS3(P6)	60.44	26.56	61.39	58.35
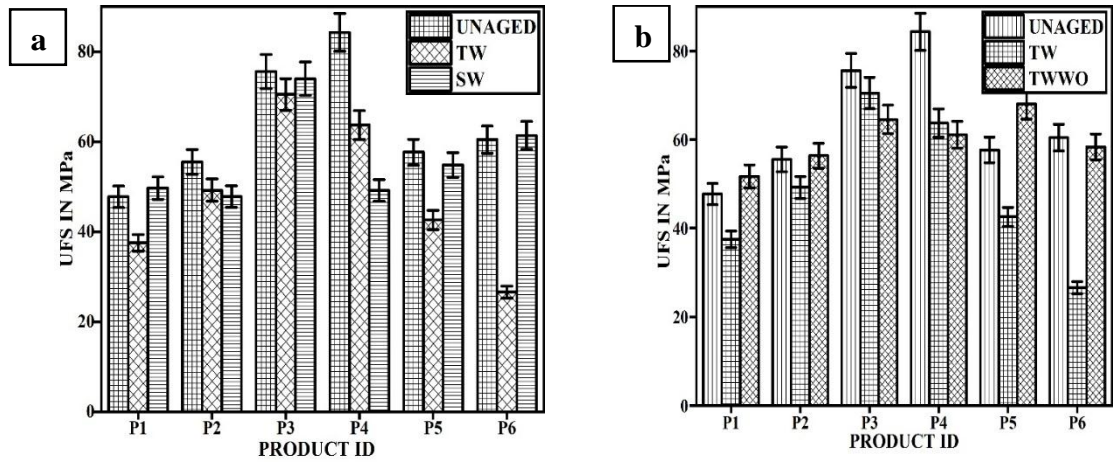
Figure 4.19 (a) UFS of Unaged-TW-SW, (b) UFS of Unaged-TW-TWWO

Further detailed examination of SEM micrographs of failed aged and unaged flexural tested samples is carried out to find the exact reason for the high flexural strength retention rate.

4.6 Results of HTS studies

4.6.1 Hoop tensile test results (split disk test)

Table 4.14 clearly indicates that the hygrothermal ageing with seawater (SW) and tap water with oil (TWWO) have a larger influence on the hoop tensile strength of GFRP test coupons after 45 days of ageing at a constant temperature of 80°C. The primary reason for this can be clearly understood by fractography studies.

Table 4.14 (a) Split disk test results of unaged samples

Case	Sample code	Failure Load in kN	Displacement in mm	HTS in MPa	HOOP STRAIN in %
Unaged	UP1	71	7.95	316.96	1.3125
	UP2	77	8.3	343.75	1.4234
	UP3	90.25	9.7	402.9	1.4287
	UP4	75.25	7.9	335.94	1.1913
	UP5	87.5	8.7	390.62	1.2094
	UP6	68	6.65	303.57	0.9398

Table 4.14 (b) Split disk test results of aged seawater samples

Case	Sample code	Failure Load in kN	Displacement in mm	HTS in MPa	HOOP STRAIN in %
SW aged	SWP1	68.75	11.98	306.92	1.2709
	SWP2	41.25	5.5	184.15	0.7625
	SWP3	34.25	4.6	152.9	0.5422
	SWP4	48.75	6.34	217.63	0.7718
	SWP5	45.5	5.49	203.12	0.6289
	SWP6	44.5	6.05	198.19	0.6150

The consolidated results of the HTS test or split disk test are tabulated in Table 4.14(a), 4.14(b), and 4.14(c) for unaged, seawater aged, and tap water with oil aged samples, respectively. The experimental study highlights failure load, HTS, maximum displacement before breakage of each unaged and aged sample.

Table 4.14 (c) Split disk test results of tap water with oil aged samples

Case	Sample code	Failure Load in kN	Displacement in mm	HTS in MPa	HOOP STRAIN in %
TWW O aged	TWWOP1	49.25	6.6	219.87	0.9104
	TWWOP2	42	5.75	187.5	0.7764
	TWWOP3	41	5.5	183.03	0.6491
	TWWOP4	37.5	5.02	167.41	0.5937
	TWWOP5	62.5	6.7	279.02	0.8638
	TWWOP6	43.75	5.1	195.31	0.6047

The important results are highlighted by bold letters in Table 4.14(a), (b), and (c), respectively. All the results tabulated in Table 4.14(a), 4.14(b), and Table 4.14(c) are rounded off to two decimals in case of HTS and 4 decimals in case of hoop strain.

4.6.2 HTS and Hoop Strain of unaged and aged samples

Here, the various plots are plotted in order to study the effect of hygrothermal ageing on filament-wound GFRP samples. The HTS vs. samples in Figure 4.20A (a) highlights the reduction in HTS of aged samples, the influence of heat on different composition samples based on the type of ageing are few major observations from the plot. Among two aged samples, SW samples have better HTS when compared to TWWO samples as per the scatter plot. But the polynomial fit curve showing that the mean value of SW samples HTS is nearer to TWWO aged sample. Similar kind of observations can be made from Figure 4.20B (c) for samples vs. hoop strain plots for both unaged and aged samples. Figure 4.20A (b) clearing showing that there is a gradual drop in HTS in the case of aged samples. The order of highest to lowest average HTS is 347.88 > 236.56 > 198.66 in MPa in unaged > SW aged > TWWO aged samples respectively. Similarly, the average hoop strain in the order of highest to lowest 1.24 > 0.85 > 0.71 in % is observed in the case of unaged > SW aged > TWWO aged samples. We can see that in SW samples, there is a reduction in HTS of about 32%. About 43% HTS reduction in the case of TWWO aged samples is observed. The main possible reasons for the drop in HTS value could be many. Few reasons for the reduction in HTS can be highlighted are, continuous exposure of resin particles present in

the samples to the high-temperature environment leads to erosion of resin or weakening of resin strength, uneven accumulation of chloride and oil particles at various locations in the sample, which intern is making samples internally week after room temperature cooling.

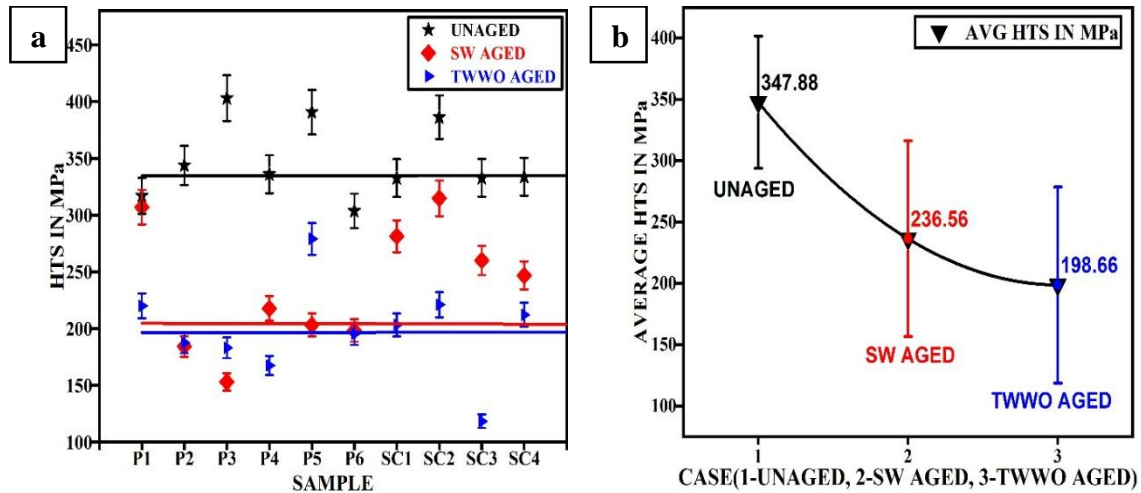Figure 4.20A (a) Product ID vs. HTS, (b) Unaged-aged vs. AVG HTS

Figure 4.20C e) is plotted for hoop strain vs. hoop stress for all three cases. The portion of points circled in black is the case of unaged samples, the points circled in red colour are SW aged samples, and lastly, the blue circled points highlight the TWWO aged samples.
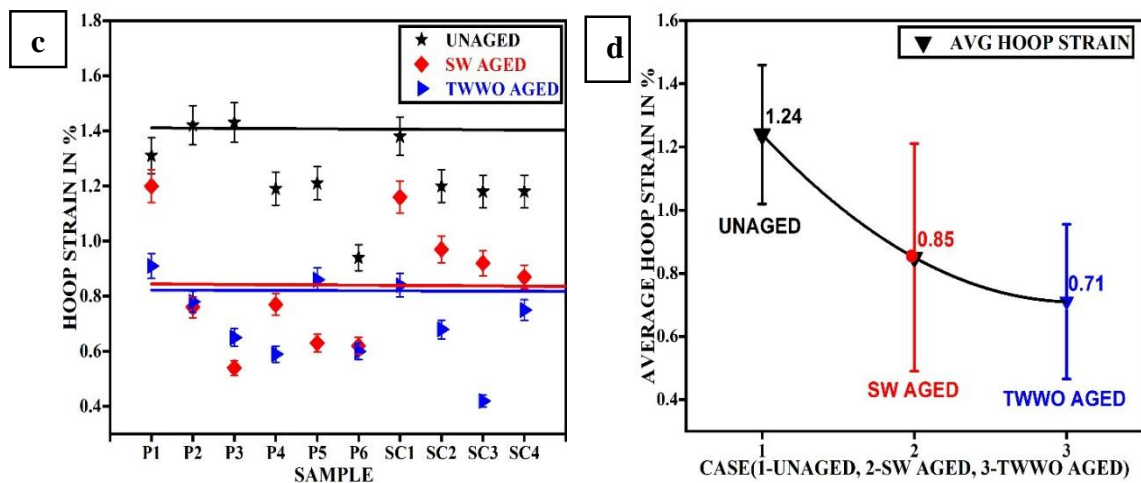
Figure 4.20B (c) Product ID vs. HTS, (d) Unaged-aged vs. AVG HTS

100
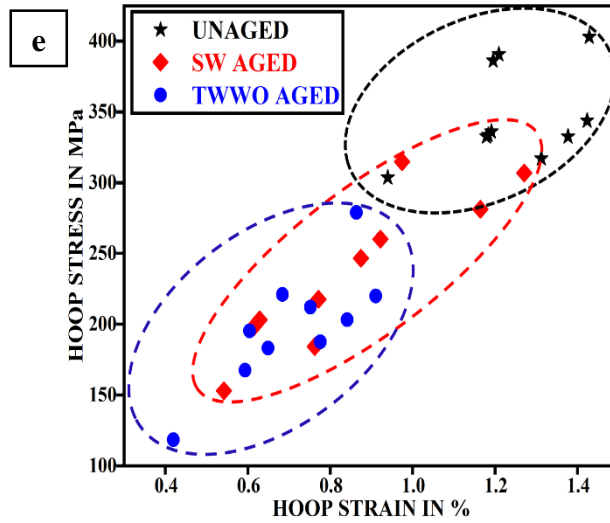
Figure 4.20C (e) Hoop Stress vs. Hoop Strain

The main significance of this plot is exploring the hygrothermal ageing effect on hoop stress and hoop strain of various filament wound GFRP composition samples. The scattering points in the case of unaged samples are less, as same can be seen in the plot in Figure 4.20C (e). This explains that the unaged samples are having a less or non-considerable influence on varied samples fabrication parameters. In the case of SW aged samples, the points are highly scattered. The highly scattered points indicating that there is a higher percentage variations effect due to hygrothermal ageing compared to just fabrication parameters. From the blue circled area, we can point out that TWWO aged samples are having an ageing effect in a little better-disciplined manner when compared with SW aged samples. Overall, the 6 different composition samples (with and without hygrothermal ageing) have been tested for hoop stress and hoop strain. The aged samples HTS has notably reduced when compared to unaged samples.

4.6.3 Influence of filament winding process parameters on HTS

The various parameters such as volume fraction, winding angle, and stacking sequence plays a very important role in the variation of HTS. The various plots in Figure 4.21A and Figure 4.21B highlight the influence of the above parameters on HTS. The influence on HTS due to variation in fiber volume fraction (V_f = 0.55 to 0.75) is plotted in Figure 4.21A

(a). In the case of unaged samples, the HTS has increased marginally from low volume fraction to high volume fraction. Hence, we can conclude from the above evidence that the addition of fiber content has strengthened the filament wound GFRP samples by about 10%. In the case of aged samples, overall, the HTS has dropped by around 50% with the increase in volume fraction. The main reasons for the reduction in HTS could be the effect of heat and the ageing fluid on filament-wound samples having varied fiber content, which were kept for a period of 45 days in a closed container. The resistance offered by SW aged filament wound samples for varied volume fractions on HTS is almost negligible. In the case of TWWO aged samples with the increase in fiber volume fraction, the increase in HTS has been observed. Figure 4.21A (b) highlighting the effect of variation of winding angle on HTS. The effect of variation in winding angle of unaged samples on their HTS is minimal. The maximum HTS of 350.44 MPa is recorded for winding angle 45°/55°/65° in case of unaged samples. The SW and TWWO aged samples have also experienced the variation in HTS due to varied winding angles. In case of the SW aged sample, fluctuation of HTS is more compared to TWWO aged samples. The maximum HTS of 285.34 MPa for winding angle 45°/55°/65° is observed in case of SW aged samples. At the same time, a maximum of 227.15 MPa HTS is recorded in TWWO aged samples.
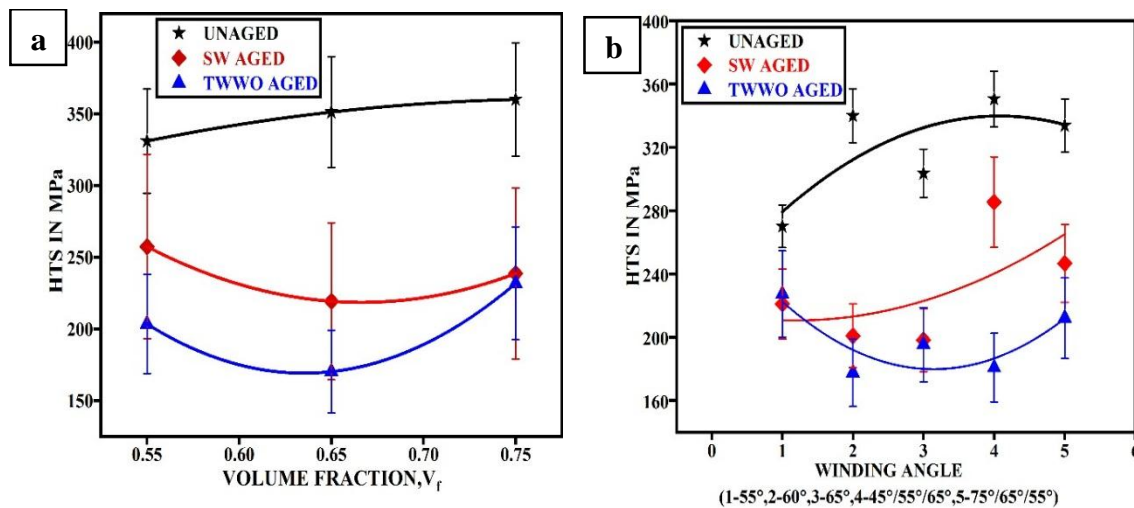
Figure 4.21A Effect of varied fiber volume fraction, winding angle on HTS: (a) Volume fraction vs. HTS, (b) Winding angle vs. HTS

From the plot in Figure 4.21A (b), we can clearly highlight that the effect of winding angle on SW aged samples is more among all aged and unaged samples. Figure 4.21B (c) highlights the effect of stacking sequence on the aged and unaged samples. The unaged samples are having a lesser effect of variation in stacking sequence compared to aged samples. The stacking sequence SS2(45°/55º/65°) is having the highest HTS in all three stacking sequence cases.

The drop in HTS for SS3 case is clearly visible in Figure 4.21B (c) in all cases. The probable reason for this common effect, i.e., increases (highest HTS) at SS2 and drops in HTS at SS3, are very simple. The continuous variation in layers to obtain the required thickness of the cylinder is limited, i.e., at some level, the resistance capacity of fiber and resin placed in a pre-defined manner are limited due to the possibility of forced voids, gaps, and entrapment of air particles during the fabrication process, accumulation of chloride particles, oil particles in case of aged samples are few reasons for variations in HTS.
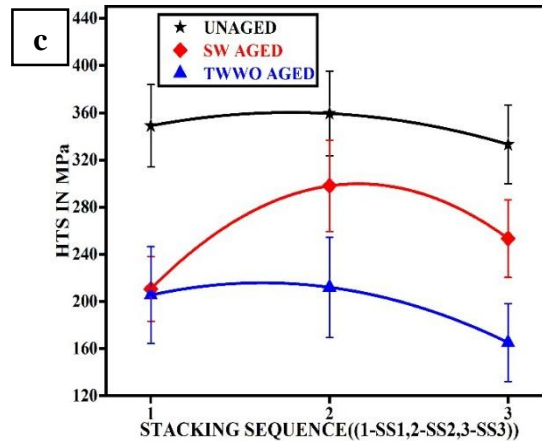
Figure 4.21B Effect of varied stacking sequence on HTS: c) Stacking sequence vs. HTS

Overall unaged samples have better HTS compared to aged samples. The simple and most important factor other than fabrication parameters for the reduction in HTS is the effect of seawater and tap water with oil on filament-wound GFRP samples. A few more reasons in detail among them could be the application of heat (80°C) and its duration (45 days). Due to this situation, the ease of entrapment of active seawater particles, active tap water with oil molecules inside the filament wound samples is high. Hence the damage to the samples was already done before the split disk test. In the case of among unaged samples, the HTS

103

is varying due to improper distribution of fiber and matrix composition, poor interfacial bonding, fiber fragmentation, cluster of fiber and matrix are few reasons.

4.6.4 Damage analysis and fractography study

In this section, failed samples of HTS tests are investigated for modes of failure. The microstructure of a few of the failed samples is examined using the scanning electron microscope. The SEM images will provide information pertaining to the actual cause of failure due to applied hoop load. Figure 4.22 (a), (b), and (c) highlights the HTS test sample before the test for unaged, SW aged, and TWWO aged, respectively. Whereas Figure 4.22 (d), (e) and (f) highlights the HTS test sample after the test for unaged, SW aged, and TWWO aged, respectively.

The few failed split disk (HTS) test samples are shown in Figure 4.22 (d), (e), (f), and Figure 4.23 (a) and (b). Overall, three types of failure modes are observed in the HTS test, and they are 1) Conical mode failure at the notch provided, 2) Delamination from PVC liner, which leads to an imbalance in the sample followed by random failure at notch section, and 3) Random angular failure other than cup and cone.
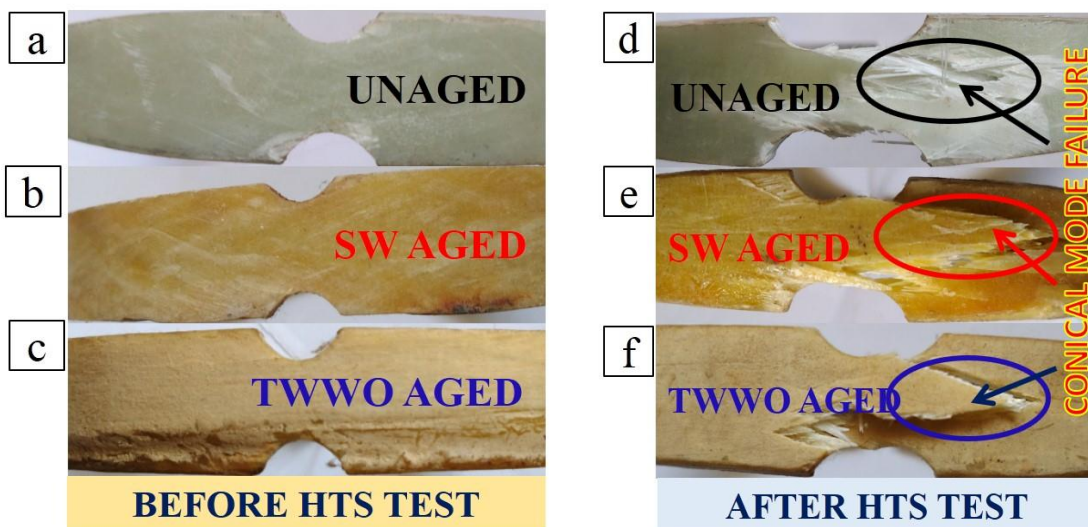
Figure 4.22. All unaged and aged samples are shown in (a) Unaged, (b) SW aged and (c) TWWO aged are before HTS test and (d) Unaged, (e) SW aged and (f) TWWO aged are after HTS test.
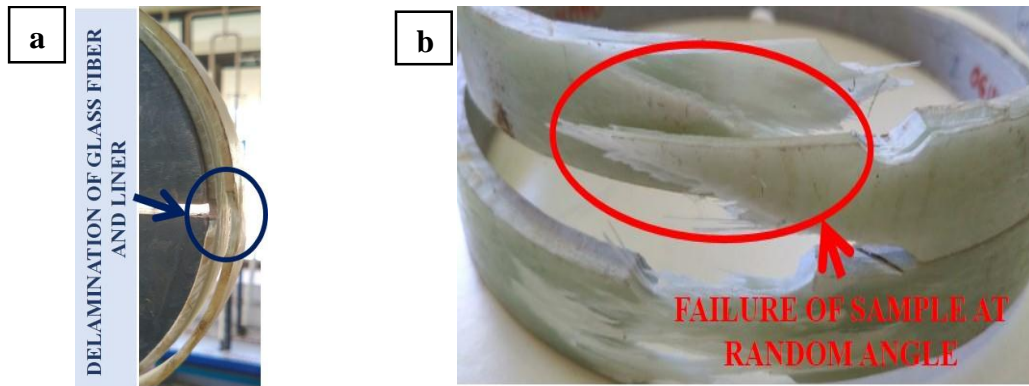
Figure 4.23. Failed GFRP sample after HTS test (a) Delamination from liner lead to early failure, (b) Sample failed outside notch provided

The failure points are highlighted in Figure 4.23 (a) and (b) for the above said two types of failure. The conical mode failure is highlighted in Figure 4.22 (d), (e) and (f) for unaged, SW aged, and TWWO aged, respectively.

Figure 4.24 illustrates a few failed samples SEM micrographs. Figure 4.24A (a) clearly highlights fiber-matrix debonding, which led to the fiber rupture in the case of unaged HTS test samples.
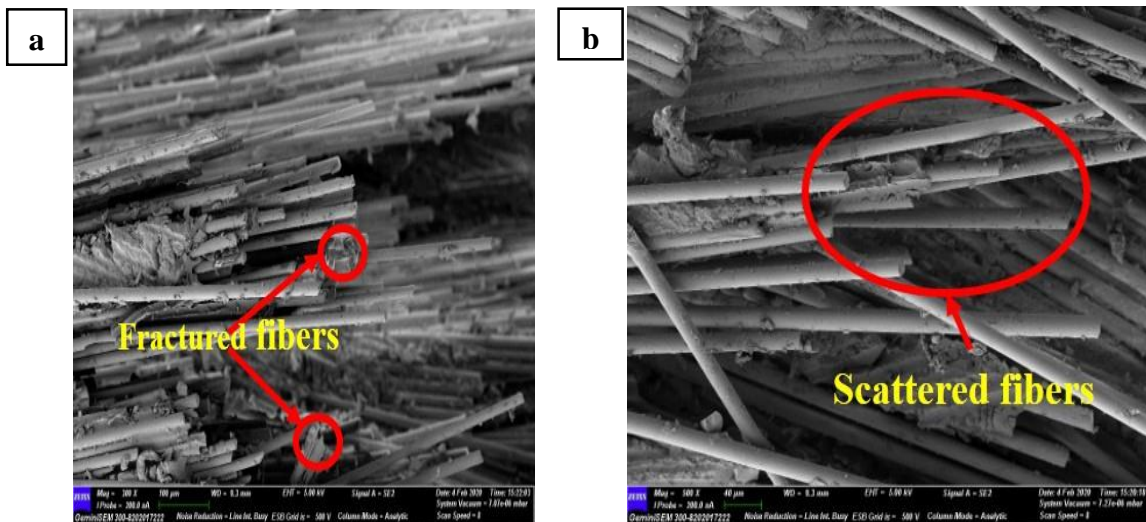
Figure 4.24A. SEM micrograph images of failed HTS test samples: (a) Ruptured fibers, (b) Fibers scattered after breakage
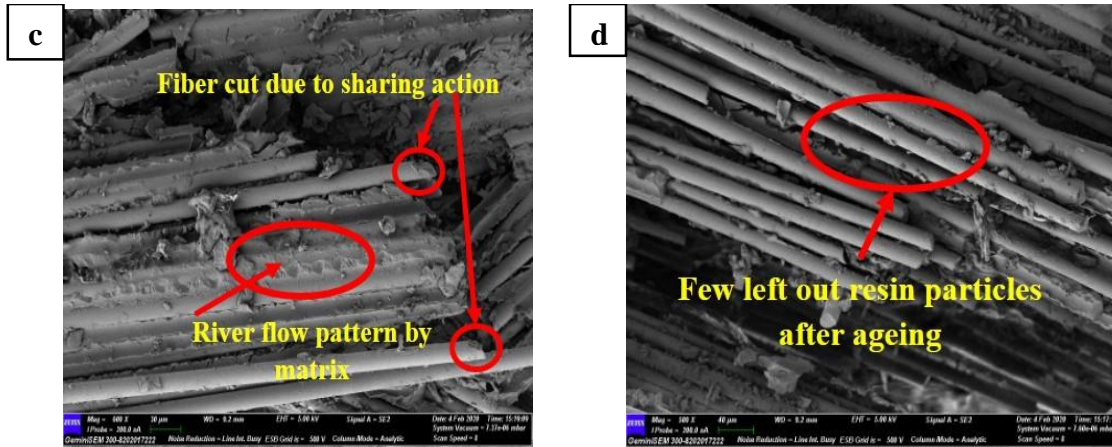
Figure 4.24B. (c) the river flow pattern of matrix and (d) Non-uniform distribution of matrix after ageing

In Figure 4.24A (b), the fibers are scattered due to the non-availability of sufficient matrix material to resist the applied load. This situation has arrived due to the effect of seawater ageing, and it has promoted adhesive and cohesive failure. Figure 4.24B (c) Highlights the resistance offered by the matrix against applied load. It also shows the fiber's failure due to sharing action (45° angle). In the case of Figure 4.24B (d), the lack of matrix can be clearly observed in the case of tap water with an oil-aged HTS failed sample. Hence due to the shortage of matrix material between the fibers, the interfacial bonding has reduced, which has led to the failure of aged samples before reaching the actual peak load.

4.6.5 SEM images of tensile failed samples (Before and after ageing)

In Figure 4.25A (a), Figure 4.25A (b) and Figure 4.25B (c) the effect of tap water, seawater ageing on product P1, P2, and P6 in case of tensile, compression, and flexural strength is in considerable range. Especially in case of products P1 and P2, seawater ageing is high. In case of product 6, the tap water ageing is high. The main cause of this is clearly discussed in SEM image studies.
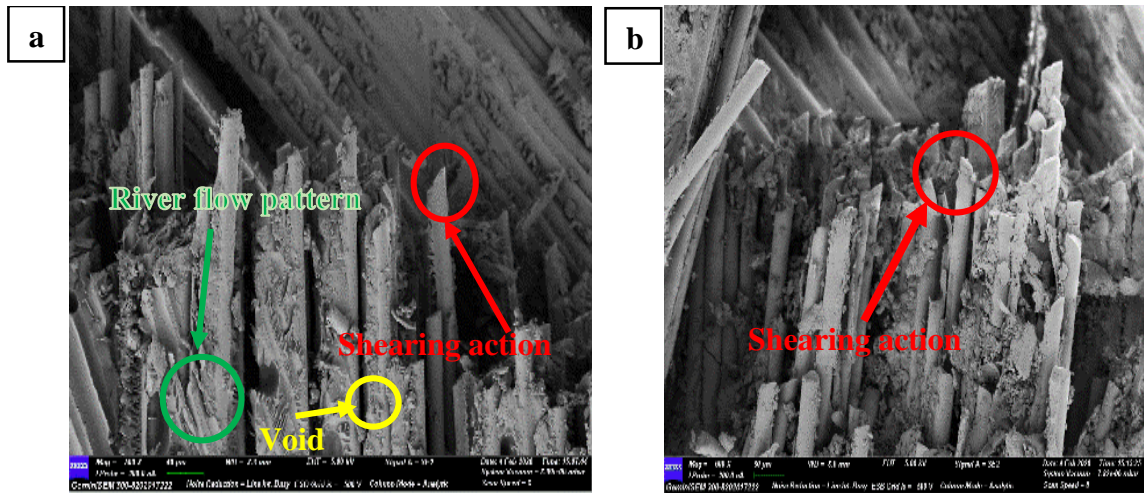
Figure 4.25A. (a) and (b) Unaged tensile sample

From Figure 4.25B (d), Figure 4.25C (e) and Figure 4.22C (f), after comparing unaged, ageing by tap water, tap water with oil samples. Product P1, P2, and P6 have greater influence among other products due to ageing. From Figure 4.25D (g) and Figure 4.25D (h) hoop tensile strength of unaged and seawater aged samples are compared and similarly hoop tensile strength of unaged and tap water with oil. Here the effect of ageing can be clearly seen in all products except in product 1.
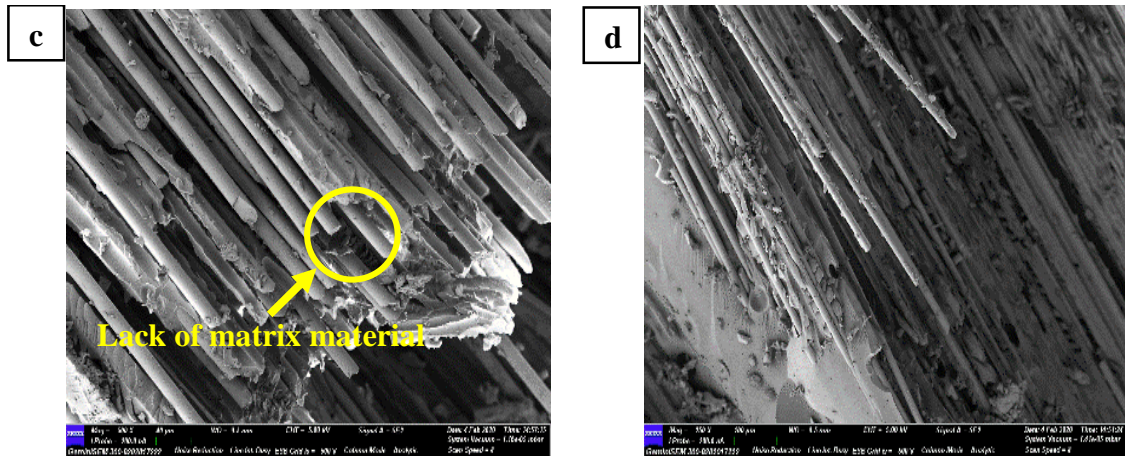
Figure 4.25B. (c) and (d) TWWO tensile sample

The fractography study of failed tensile tested samples is carried out with the help of SEM images. Figure 4.25A (a) and (b) which are exhibiting different modes of failure such as adhesive fracture, cohesive fracture, presence of voids, improper bonding among matrix material and fiber. The river flow pattern in Figure 4.25A (a) is an indication of resistance

offered by the matrix against deformation under the application of tensile load. The fibers have failed due to shearing action, which can be observed in SEM images.
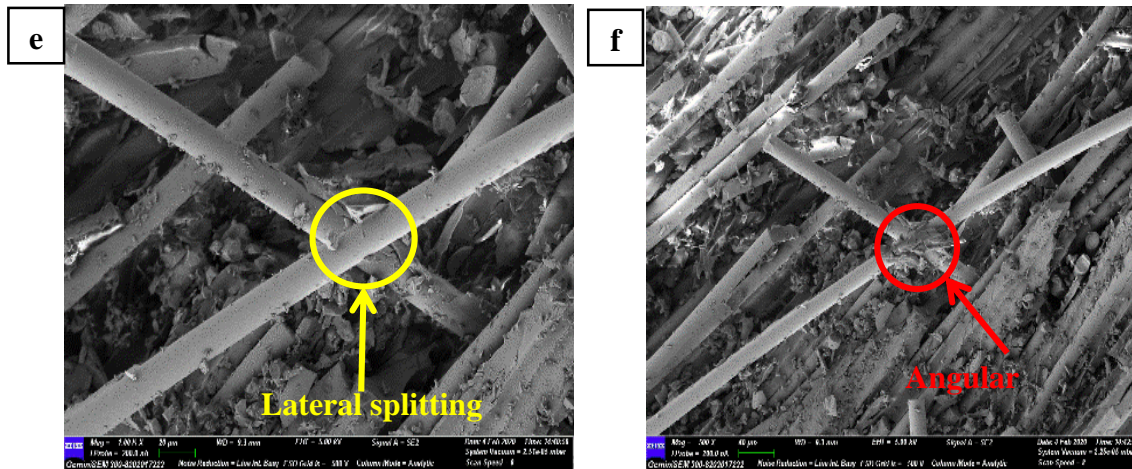
Figure 4.25C. (e) and (f) TW compression sample

The fractography study of failed Tap water with oil tensile tested samples is carried out with the help of SEM images. Figure 4.25B (c) and (d) which is also exhibiting different modes of failure such as adhesive fracture, cohesive fracture, presence of voids, improper bonding among matrix material and fiber.
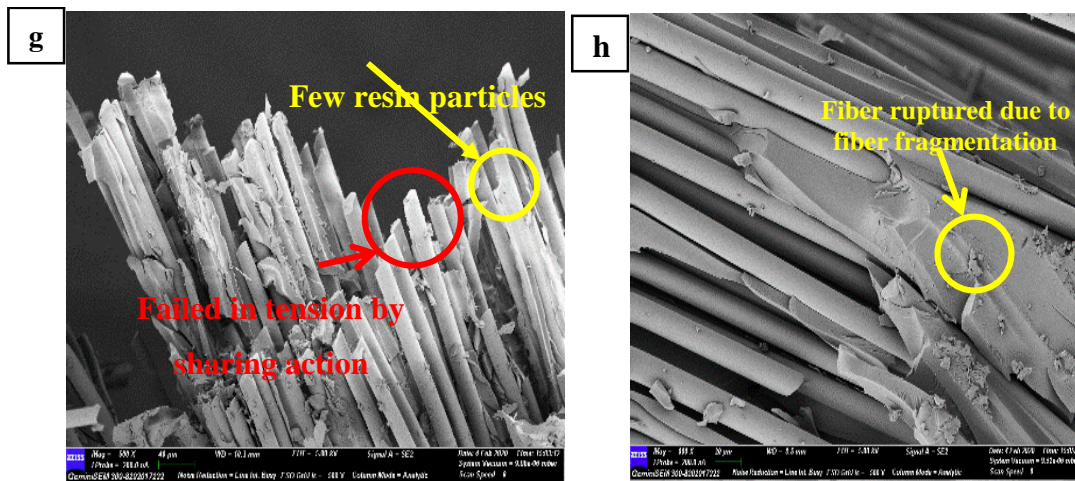
Figure 4.25D (g) and (h) TW bending sample

But TWWO aged samples can be seen without matrix particles, and hence there is poor tensile strength as bonding between fiber and matrix has reduced. The fibers have failed

due to shearing action, which can be observed in SEM images. Figure 4.25C (e) is clearing showing different modes of failure due to compressive load on filament-wound GFRP sample. Figure 4.25C (e) is highlighting the lateral splitting of fiber due to the high length to diameter ratio, poor interfacial bonding between fiber and matrix, and the presence of voids. The presence of void and lack of matrix due to TW ageing leads to fiber buckling as the gap between fiber and matrix is high, which is clearly visible in Figure 4.25C (f). The angular splitting of fibers in Figure 4.25C (f) is a clear indication of the shear mode of failure. The TW bending tested sample is shown in the above Figure 4.25D (g) and Figure 4.25D (h). The fibers in this flexural test have failed in different modes, such as the fibers which are at the bottom half of the test sample in a 3-point bend test have failed in tension by shearing action, a sample of such fiber failure is highlighted in above Figure 4.25D (g). At the same time, fibers at the uppers half have failed due to compression. Figure 4.25 (g) showing the end portion in the fiber due to applied load; this cut is due to a break in the crack generation at the bottom fiber. A rare resin particle sticking on fibers can be observed in the form of white spots in Figure 4.25D (g). Since the resin distribution is least and not uniform due to TW ageing and as we know that resin or matrix plays a very important role in the transfer of load from one fiber to another, pre-peak load failure is one of the modes of failure that can be anticipated because of poor distribution of resin. Hence overall flexural strength of the material also gets reduced.

4.7 Comparison of FE analysis of pressure vessel cylinder for varied composite materials

FE Simulation Results Comparison

The various FE results are tabulated in Table 4.15, Table 4.16, Table 4.17, Table 4.18, and Table 4.19. The FE analysis results of GFRP, CFRP, and AFRP pressure vessel cylinders are plotted in Figure 4.26A (a) to Figure 4.26C (e). Similarly, metallic pressure vessels LCS and Al 6061 T6 are also analyzed.

Table 4.15. FE analysis results for varied winding angle

S. No.	Winding angle, Ø	Maximum Von mises stress in [MPa]		
		GFRP pressure vessel	CFRP pressure vessel	AFRP pressure vessel
1	±45°	72.35	93.33	83.62
2	±55°	83.78	94.41	111.75
3	±65°	90.29	116.7	118.13

Table 4.16. FE analysis results for varied fiber volume fraction

S. No.	Fiber Volume fraction	Maximum Von mises stress in [MPa]		
		GFRP vessel	CFRP vessel	AFRP vessel
1	0.45	83.09	109.33	109.11
2	0.55	86.88	113.06	112.92
3	0.65	90.29	116.7	118.13

Table 4.15-Table 4.19 illustrates various outcomes of FE analysis of composite and metallic pressure vessels. From the observation of various stress values, in case of FRP composite vessels, it is clearly showing that winding angles of ±55° and ±65° have higher stress values compared to other winding angles. Similarly, for fiber volume fraction, V_f of 0.55 and 0.65 have a high-stress value when compared with 0.45.

Table 4.17. FE analysis results for varied Stacking Sequence

S. No.	Stacking Sequence	Maximum Von mises stress in [MPa]		
		GFRP vessel	CFRP vessel	AFRP vessel
1	P1(90°$_2$/Ø°$_2$/90°$_2$/-Ø°$_2$/90°$_2$)	90.29	116.7	118.13
2	P2(±Ø°$_2$/90°$_2$/(±Ø°$_2$))	73.05	98.1	88.88
3	P3(Ø°$_2$/90°/(-Ø°$_4$)/90°/Ø°$_2$)	73.08	96.52	85.72

Table 4.18. FE analysis results from comparison between metallic and composite pressure vessels

S. No.	Material for pressure vessels	Maximum Von mises stress in [MPa]	Maximum hoop stress in [MPa]
1	LCS	55.66	64.44
2	Al 6061 T6	44.22	50.8
3	GFRP	90.29	95.84
4	CFRP	116.7	116.14
5	AFRP	118.13	97.3

Table 4.19. Comparison of MSS of both metallic and composites pressure vessels based on FE analysis results

S. No.	Material for pressure vessels	Weight of pressure vessel in [kg]	MSS=Von mises stress/wt. of vessel	MSS=Hoop stress/wt. of vessel
1	LCS	5.75	9.68	11.20
2	Al 6061 T6	2.03	21.78	25.02
3	GFRP	1.49	60.59	64.32
4	CFRP	1.17	99.74	99.26
5	AFRP	0.98	120.54	99.28

The various graphs plotted are as shown in Figure 4.26A (a) to Figure 4.26C (e).
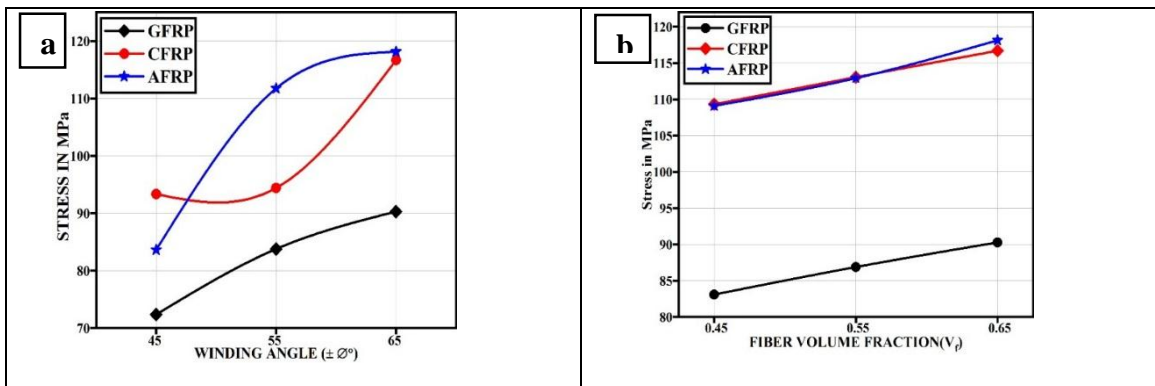
Figure 4.26A. FE analysis results based on the different comparative study: (a) Winding angle vs**.** Stress, (b) Volume Fraction vs**.** Stress
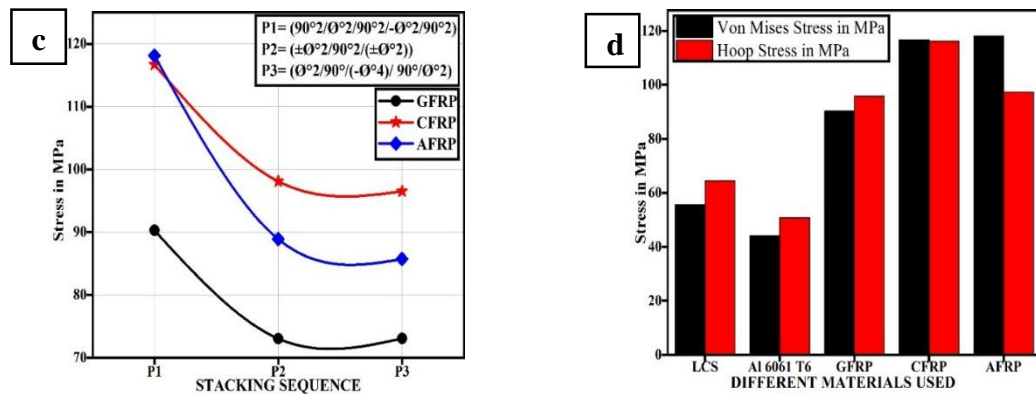
Figure 4.26B. FE analysis results based on the different comparative study: (c) Stacking Sequence vs**.** Stress, (d) Material vs**.** Stress

111
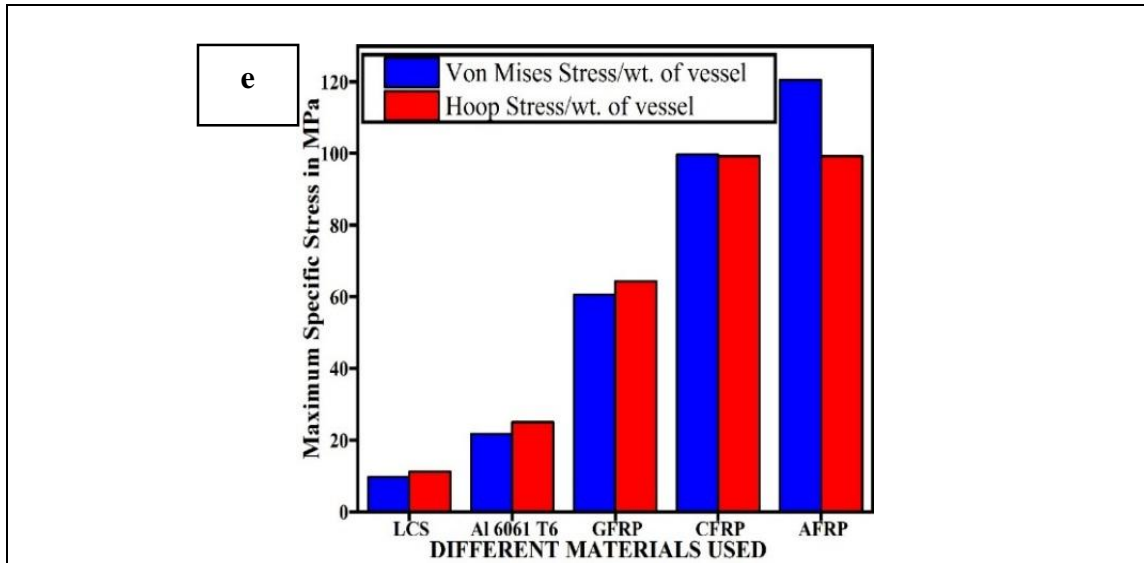
Figure 4.26C. FE analysis results based on the different comparative study: (e) Material vs. MSS

Among the composites, Aramid Fiber Reinforced Plastic (AFRP) composite pressure vessels come out as one of the best materials for pressure vessels when compared with other composite pressure vessels and Al 6061 T6 as best metallic pressure vessels from a maximum specific stress point of view.

From Figure 4.26A (a) and Figure 4.26A (b), it is clearly observed that with the increase in winding angle and fiber volume fraction, the stresses in vessels increases. For varied winding angle stresses are increased non-uniformly for CFRP and AFRP vessels when compared with GFRP pressure vessels. Whereas in the case of varied fiber volume fraction, the linear change in stress profile is observed. In Figure 4.26B (c) higher stress value is observed for stacking sequence 1 when compared to other stacking sequences. This behaviour is due to the presence of more hoop stacking sequence which does not resist stresses generated in other directions of the pressure vessel. From Figure 4.26B (d) by comparing the composite pressure vessels keeping stress as criteria, it was found that variations in stresses of AFRP and CFRP are almost negligible. Figure 4.26C (e) indicates when composite pressure vessels are compared with metallic pressure vessels with maximum specific stress (MSS) as comparison criteria, it was found that MSS is highest in the case of AFRP followed by CFRP, GFRP, Al 6061 T6, and LCS.

Below are few outcomes from a comparative study of five different materials used in FE analysis of pressure vessel cylinder

The FE analysis of AFRP, CFRP, GFRP composites along with LCS and Al 6061 T6 metallic pressure vessels are carried out in the present study. Based on the outcomes of the present study following conclusions are drawn: -

➢With the increase in winding angle from $\pm 45^{O}$ to $\pm 65^{O}$, the stress value is found to increase. The same is also observed with fiber volume fractions for 0.45 to 0.65.

➢The stacking Sequence P1 $((90°_2/\emptyset°_2/90°_2/-\emptyset°_2/90°_2))$ is having maximum von mises stress compared to the other two stacking Sequence.

➢Even though AFRP is having the highest MSS value followed by CFRP and GFRP, we can consider GFRP over CFRP and AFRP based on lower stress value, lower cost, availability, and application factors.

4.8 Summary

Results of FE simulation for applied internal pressure are listed and are compared among each other based on various factors (such as material selection, fiber volume fraction, winding angle, stacking sequence). VIKOR method has helped in selecting the best attributes (top 6) for experimental studies. The physical, tribological, and mechanical characterization has given various material properties (% void content, water absorption capacity, UTS, UCS, and UFS) of GFRP material used in the present study. The hygrothermal ageing of filament wound GFRP test coupons has clearly shown that the samples have a moderate influence of seawater and tap water oil ageing on HTS. The fractography study of different failed test coupons has helped in the clear understanding of the actual cause of failures in different mechanical testing's. Overall, the FE analysis and experimental results have clearly pointed out many highlighted learnings. The important inferences from this present research work are discussed in brief in the conclusion chapter.

CHAPTER 5

CONCLUSIONS

In the present work, three different levels of investigation are carried out. At the First level, FE analysis of pressure vessels with varied constitutive materials (LCS, Al 6061 T6, and GFRP) is carried out, and the best material is decided based on maximum specific strength. At the Second level, FE analysis of GFRP pressure vessel for varied fabrication parameters such as fiber volume fraction, winding angle, and stacking sequence. The third and final level involves the fabrication of pressure vessels and testing them for various physical, tribological, and mechanical properties. Another aspect of current work is the hygrothermal ageing study of filament wound GFRP test coupons for 45 days period at a constant temperature of 80°C. Few important conclusions made from the current investigation are as follows:

➢ FE analysis of pressure vessel which is carried out on two different metallic materials (LCS, Al6061 T6) and the results obtained are compared with results of FE analysis of GFRP material. This comparison has led to conclusion that GFRP found to be the best alternative to replace existing metallic material. The figure 4.1 in section 4.2.1 has given the clear picture of the above statement. Further, results obtained from FE analysis of GFRP pressure vessel are compared with CFRP and AFRP. This comparative study among GFRP, CFRP and AFRP has led to conclusion that AFRP is more superior material than CFRP and GFRP. Hence AFRP is most suitable material if only maximum specific strength as the material selection criteria for pressure vessels. The figure 4.26C from section 4.7 clearly showing why AFRP is best suited along with explanation. But from the domestic application point view (LPG storage, CNG storage, oxygen cylinders for mountain travellers and so on), from the basic need of product (necessary requirements such as light weight, long reliability, ease of handling, ease of availability) and cost of materials point of view, the GFRP material is having considerable advantage over AFRP and CFRP.

    ➢ The FE analysis of GFRP pressure vessel is carried out by varying fiber volume

fraction (0.45, 0.55, 0.65, 0.75), winding angle (±45°, ±50°, ±55°, ±60°, ±65°, ±70°, ±75°), and stacking sequence (SS1, SS2, SS3, SS4, SS5, SS6). As per the above combinations of variables, we got 168 FE simulations which were carried out separately with and without liner (168 with liner and 168 without liner). A total of 336 FE simulations have been completed. Here $V_f = 0.55$, WA = ±55°, SS = SS3 came out as the best specification for fabricating filament wound pressure vessel cylinder.

➢ The optimization MCDM tool VIKOR method is applied on 168 FE simulation alternatives (with liner) in order to obtain the best suitable winding specifications to fabricate and test for various physical, tribological, and mechanical properties.

➢ Top 6 ranked specifications are fabricated and are cut into test coupons for tensile, compression, bending, and hoop tensile property.

➢ Half of the test coupons are subjected to hydrothermal ageing before any mechanical tests for a period of 45-days at a constant temperature of 80°C in three different hot baths or a container.

➢ The unaged and aged samples reveal that tensile, compression and bending properties are almost nearly the same even after 45 days of ageing with few unaccountable differences in few products.

➢ The most observable outcome of the ageing study is hoop tensile strength which is reduced almost half in some of the products due to seawater and tap water with oil ageing. The product P1 has retained the highest percentage of HTS, which is 97% for seawater samples and 71% for tap water with oil samples. Overall, the products P1(HTS property only), P3(tensile, compression, and bending property only), P5, and P6 offer better resistance against the high temperature and varied working environment compared to other products to retain their mechanical property.

➢ The effect of void content on fabricated GFRP vessels is in the considerable zone since we all know that the filament winding process is highly prone to situations where voids are bound to come in the fabricated vessels, and hence as per individual application requirements, there exists a maximum permissible limit for the void. In

115

the present research work, average void content of 5.74% is recorded.

➢ In the present research work, an additional work of FE analysis of pressure vessel cylinder was carried out for 5 different materials (LCS, Al 6061 T6, GFRP, AFRP, and CFRP). The best material is chosen based on MSS value. Even though AFRP is having the highest MSS value followed by CFRP and GFRP, we can consider GFRP over other materials based on lower stress value, lower cost, availability, and application factors.

PUBLICATIONS

International Journals

1. Biradar, S., Joladarashi, S., & Kulkarni, S. M. (2019). Tribo-mechanical and physical characterization of filament wound glass/epoxy composites. Materials Research Express, 6(10), 105312. https://doi.org/10.1088/2053-1591/ab3685.

2. Srikumar Biradar, Sharnappa Joladarashi, S M Kulkarni "FE Analysis of FRP Pressure Vessel" Key Engineering Materials Vol. 801, pp 77-82 https://doi:10.4028/www.scientific.net/KEM.801.77 Trans Tech publishing. (Scopus indexed)

3. Srikumar Biradar, Joladarashi, S., & Kulkarni, S. M., " Effect of Hygrothermal Ageing on Hoop Tensile Strength of Filament Wound GFRP Composites," (under review-Arabian Journal for Science and Engineering, SPRINGER).

Conference Publications

1. Srikumar Biradar, Sharnappa Joladarashi, S M Kulkarni "Investigation on mechanical behaviour of filament wound glass/epoxy composites subjected to water absorption and also tribological studies using Taguchi Method," Material Today Proceedings, Vol. 10, page 2214-7853. https://doi.org/10.1016/j.matpr.2020.02.834

2. Srikumar Biradar, Sharnappa Joladarashi, Sangamesh Rajole, Shivashankar Hiremath, and S. M. Kulkarni "Comparative study on filament wounded and laminated GFRP composites for tensile characterization" AIP Conference Proceedings 2057, 020057 (2019); https://doi.org/10.1063/1.5085628. AIP Publishing. (Scopus indexed)

3. Srikumar Biradar, Sharnappa Joladarashi, S M Kulkarni "Analytical and FE analysis of Al 6061 T6 and laminated composite LPG cylinder" Young Journal, Vol 7850, Issue 2770, Page 1590, 2017. (Scopus indexed)

REFERENCES

Akderya, T. (2018). "Investigation of thermal-oil environmental ageing effect on mechanical and thermal behaviours of E-glass fibre / epoxy composites."

Aksoley, M. E., Ozcelik, B., and Bican, I. (2008). "Comparison of bursting pressure results of LPG tank using experimental and finite element method." *J. Hazard. Mater.*, 151(2–3), 699–709.

Ashby, M. F., and Ashby, M. F. (2011). "Chapter 1 – Introduction." *Mater. Sel. Mech. Des.*, 624.

ASTM. (2014). "ASTM D3039/D3039M." *Annu. B. ASTM Stand.*, 1–13.

ASTM D570. (2014). "Standard Test Method for Water Absorption of Plastics." *ASTM Stand.*, 98(Reapproved 2010), 25–28.

ASTM International. (2007). "ASTM D7264 Flexural Properties of Polymer Matrix Composite Materials." *Annu. B. ASTM Stand.*, i(C), 1–11.

Bae, J. H., and Kim, C. (2013). Optimal design for compressed natural gas composite vessel by using coupled model with liner and composite layer. *Int. J. Precis. Eng. Manuf.*

Bal, S., and Saha, S. (2015). "Effect of sea and distilled water conditioning on the overall mechanical properties of carbon nanotube / epoxy composites." *Int. J. Damage Mech.*, 0(0), 1–13.

Barboza Neto, E. S., Chludzinski, M., Roese, P. B., Fonseca, J. S. O., Amico, S. C., and Ferreira, C. A. (2011). "Experimental and numerical analysis of a LLDPE/HDPE liner for a composite pressure vessel." *Polym. Test.*, 30(6), 693–700.

Batra, R. C., and Hassan, N. M. (2007). "Response of fiber reinforced composites to underwater explosive loads." *Compos. Part B Eng.*, 38(4), 448–468.

Benyahia, H., Tarfaoui, M., Moumen, A. El, Ouinas, D., and Hassoon, O. H. (2018). "Mechanical properties of offshoring polymer composite pipes at various temperatures." *Compos. Part B Eng.*, 152(May), 231–240.

Canale, G. (2018). "Effects of hygrothermal history on the structural performance of aerospace composite materials : preliminary experiments and effects of hygrothermal history on the structural performance of aerospace composite materials : preliminary

experiments and mass ." (July).

Ch, A., Barbezat, M., Piskoty, G., Neuner, O., and Terrasi, G. (2018). "Failure of a sag water pipe triggered by aging of the GFRP composite relining." 84(September 2017), 358–370.

Charan, V. S. S., Vardhan, A. V., Raj, S., Rao, G. R., Rao, G. V., and Hussaini, S. M. (2019). "Experimental characterization of CFRP by NOL ring test." *Mater. Today Proc.*, 18, 2868–2874.

Choi, J. C., Kim, C., and Jung, S. Y. (2004). "Development of an automated design system of a CNG composite vessel using a steel liner manufactured using the DDI process." *Int. J. Adv. Manuf. Technol.*, 24(11–12), 781–788.

Chou, H. Y., Bunsell, A. R., Mair, G., and Thionnet, A. (2013). "Effect of the loading rate on ultimate strength of composites. Application: Pressure vessel slow burst test." *Compos. Struct.*, 104, 144–153.

Cohen, D. (1997). "Influence of filament winding parameters on composite vessel quality and strength." *Compos. Part A Appl. Sci. Manuf.*, 28(12), 1035–1047.

Cohen, D., Mantell, S. C., and Zhao, L. (2001). "The effect of fiber volume fraction on filament wound composite pressure vessel strength." *Compos. Part BEngineering*, 32(5), 413–429.

Dhanunjayaraju, M., and Babu, T. L. R. (2015). "Stress analysis of LPG cylinder with composites." 1, 1042–1045.

Dogan, A., and Atas, C. (2015). "Variation of the mechanical properties of E-glass / epoxy composites subjected to hygrothermal aging."

Dong, Q., and Gu, Y. (2014). "Experimental study on composite containment vessels." *Am. Soc. Mech. Eng. Press. Vessel. Pip. Div. PVP*, 1–5.

Ellul, B., and Camilleri, D. (2015). "The influence of manufacturing variances on the progressive failure of filament wound cylindrical pressure vessels." *Compos. Struct.*

Etemad, M. R., Pask, E., and Besant, C. B. (1992). "Hoop strength characterization of high strength carbon fibre composites." *Composites*, 23(4), 253–259.

Fitriah, S. N., Abdul Majid, M. S., Ridzuan, M. J. M., Daud, R., Gibson, A. G., and Assaleh,

T. A. (2017). "Influence of hydrothermal ageing on the compressive behaviour of glass fibre/epoxy composite pipes." *Compos. Struct.*, 159, 350–360.

Gascons, M., Blanco, N., and Matthys, K. (2012). "Evolution of manufacturing processes for fiber-reinforced thermoset tanks, vessels, and silos: A review." *IIE Trans. (Institute Ind. Eng.*, 44(6), 476–489.

Gemi, L., Kayrıcı, M., Uludağ, M., Gemi, D. S., and Şahin, Ö. S. (2018). "Experimental study on compressive behavior and failure analysis of composite concrete confined by glass/epoxy±55° filament wound pipes." *Compos. Part B*.

Gentilleau, B., Bertin, M., Touchard, F., and Grandidier, J. C. (2011). "Stress analysis in specimens made of multi-layer polymer/composite used for hydrogen storage application: Comparison with experimental results." *Compos. Struct.*, 93(11), 2760–2767.

Hamed, A. F., Khalid, Y. A., Sapuan, S. M., Hamdan, M. M., Younis, T. S., and Sahari, B. B. (2007). "Effects of Winding Angles on the Strength of Filament Wound Composite Tubes Subjected to Different Loading Modes." 15(3), 199–206.

Hawa, A., Abdul Majid, M. S., Afendi, M., Marzuki, H. F. A., Amin, N. A. M., Mat, F., and Gibson, A. G. (2016). "Burst strength and impact behaviour of hydrothermally aged glass fibre/epoxy composite pipes." *Mater. Des.*, 89, 455–464.

Hemmatnezhad, M., and Ansari, R. (2010). "Prediction of Vibrational Behavior of Composite Cylindrical Shells under Various Boundary Conditions." 225–241.

Hemmatnezhad, M., Rahimi, G. H., Tajik, M., and Pellicano, F. (2015). "Experimental, numerical and analytical investigation of free vibrational behavior of GFRP-stiffened composite cylindrical shells." *Compos. Struct.*, 120, 509–518.

Hocine, A., Chapelle, D., Boubakar, M. L., Benamar, A., and Bezazi, A. (2009). "Experimental and analytical investigation of the cylindrical part of a metallic vessel reinforced by filament winding while submitted to internal pressure." *Int. J. Press. Vessel. Pip.*, 86(10), 649–655.

Hu, H., Li, S., Wang, J., and Zu, L. (2015). "Structural design and experimental investigation on filament wound toroidal pressure vessels." *Compos. Struct.*, 121, 114–120.

Islam, M., Aravinthan, T., Manalo, A., and Lau, K. (2013). "Effectiveness of using fibre-reinforced polymer composites for underwater steel pipeline repairs." *Compos. Struct.*, 100, 40–54.

Joselin, R., and Chelladurai, T. (2011). "Burst pressure prediction of composite pressure chambers using acoustic emission technique: A review." *J. Fail. Anal. Prev.*, 11(4), 344–356.

K.S.S., R. Y., Mohan, R. K., and Kiran, B. V. (2012). "Composite Pressure Vessels." *IJRET Int. J. Res. Eng. Technol.*, 01(04), 597–618.

Kaelble, D. H. (1974). *Detection of Hydrothermal Aging in Composite Materials*.

Kamal, A. M., El-Sayed, T. A., El-Butch, A. M. A., and Farghaly, S. H. (2016). "Analytical and finite element modeling of pressure vessels for seawater reverse osmosis desalination plants." *Desalination*, 397, 126–139.

Kandasamy, J., Madhavi, M., and Haritha, N. (2016). "Free vibration analysis of thin cylindrical shells subjected to internal pressure and finite element analysis." 40–48.

Kaw, A. K., and Group, F. (2006). *Mechanics of Composite Materials*.

Kaynak, C., Erdiller, E. S., Parnas, L., and Senel, F. (2005). "Use of split-disk tests for the process parameters of filament wound epoxy composite tubes." *Polym. Test.*, 24(5), 648–655.

Keller, M. W., Jellison, B. D., and Ellison, T. (2013). "Moisture effects on the thermal and creep performance of carbon fiber/epoxy composites for structural pipeline repair." *Compos. Part B Eng.*, 45(1), 1173–1180.

Khalili, S. M. R., Soroush, M., Davar, A., and Rahmani, O. (2011). "Finite element modeling of low-velocity impact on laminated composite plates and cylindrical shells." *Compos. Struct.*, 93(5), 1363–1375.

Kotani, M., Yamamoto, Y., Shibata, Y., and Kawada, H. (2011). "Strength prediction method for unidirectional GFRP after hydrothermal aging." *Adv. Compos. Mater.*, 20(6), 519–535.

Krishan K, C. (2013). *Composite materials. Springer Sci. + BusinessMedia New York 2012*.

Krishnan, P., Abdul Majid, M. S., Afendi, M., Yaacob, S., and Gibson, A. G. (2016). "Effects of hydrothermal ageing on the behaviour of composite tubes under multiaxial stress ratios." *Compos. Struct.*, 148, 1–11.

Liao, M., Yang, Y., Yu, Y., and Hamada, H. (2012). *Hydrothermal ageing mechanism of natural fiber reinforced composite in hot water*. *ASME Int. Mech. Eng. Congr. Expo. Proc.*

Liu, P. F., Chu, J. K., Hou, S. J., Xu, P., and Zheng, J. Y. (2012). "Numerical simulation and optimal design for composite high-pressure hydrogen storage vessel: A review." *Renew. Sustain. Energy Rev.*

Liu, P. F., Xing, L. J., and Zheng, J. Y. (2014a). "Composites : Part B Failure analysis of carbon fiber / epoxy composite cylindrical laminates using explicit finite element method." *Compos. Part B*, 56, 54–61.

Liu, P. F., Xing, L. J., and Zheng, J. Y. (2014b). "Failure analysis of carbon fiber/epoxy composite cylindrical laminates using explicit finite element method." *Compos. Part B Eng.*

LUCIEN DUCKSTEIN, S. O. (1980). "Multiobjective Optimization in River Basin Development." 16, 14–20.

M. Kuhn, N. Himmel, M. M. (2000). "Design and analysis of full composite pressure vessels." *Adv. Compos. Mater. Struct.*

Ma, Y., Jin, S., Ueda, M., Yokozeki, T., Yang, Y., Kobayashi, F., Kobayashi, H., Sugahara, T., and Hamada, H. (2018). "Higher performance carbon fi ber reinforced thermoplastic composites from thermoplastic prepreg technique : Heat and moisture e ff ect." 154(April), 90–98.

Madhavi, M., Rao, K. V. J., Rao, K. N., and College, M. V. S. R. E. (2009a). "<Design and Analysis of Filament Wound Composite Pressure Vessel with Integrated-end Domes.pdf>." 59(1), 73–81.

Madhavi, M., Rao, K. V. J., Rao, K. N., and College, M. V. S. R. E. (2009b). "<Design and Analysis of Filament Wound Composite Pressure Vessel with Integrated-end Domes.pdf>." *Def. Sci. J.*, 59(1), 73–81.

Mehar, A., Ahmed, G. M. S., Kumar, G. P., Rahman, M. A., and Qayum, M. A. (2015).

"Experimental Investigation and FE Analysis of CFRP Composites." *Mater. Today Proc.*, 2(4–5), 2831–2839.

Method, T. (2017). "D3410 Standard Test Method for Compressive Properties of Polymer Matrix Composite Materials with Unsupported Gage Section by Shear." 08(2008), 1–16.

Mian, H. H., Wang, G., Dar, U. A., and Zhang, W. (2013). "Optimization of composite material system and lay-up to achieve minimum weight pressure vessel." *Appl. Compos. Mater.*, 20(5), 873–889.

Moketla, M. B., and Shukla, M. (2012). "Design and Finite Element Analysis of Frp Lpg Cylinder." *Int. J. Instrumentation, Control Autom.*, 1(3), 121–124.

Moon, C. J., Kim, I. H., Choi, B. H., Kweon, J. H., and Choi, J. H. (2010). "Buckling of filament-wound composite cylinders subjected to hydrostatic pressure for underwater vehicle applications." *Compos. Struct.*, 92(9), 2241–2251.

Moskvichev, E. (2016). "Numerical modeling of stress-strain behavior of composite overwrapped pressure vessel." *Procedia Struct. Integr.*, 2, 2512–2518.

Naser S. A-Huniti, O. M. A.-H. (2014). "Composite LPG Cylinders as an Alternative to Steel Cylinders : Finite Element Approach." c(January 2006), 363–368.

Naseva, S., Srebrenkoska, V., Risteska, S., Stefanovska, M., and Srebrenkoska, S. (2015). "Mechanical Properties of Filament Wound Pipes: Effects of Winding Angles." *Qual. Life (Banja Luka) - APEIRON*, 11(1–2), 10–15.

"Opricovic, S." (1990). .

Opricovic, S. (2004). "Compromise solution by MCDM methods : A comparative analysis of VIKOR and TOPSIS." 156, 445–455.

Opricovic, S. (2007). "Extended VIKOR method in comparison with outranking methods." 178, 514–529.

P. Sampath Rao, M. Manzoor Husain, D. V. R. S. (2012). "Hygrothermal characterization of gfrp laminates subjected to different water conditions." *IOSR J. Mech. Civ. Eng.*, 1(1), 12–25.

Perillo, G., Grytten, F., Sørbø, S., and Delhaye, V. (2015). "Numerical/experimental impact events on filament wound composite pressure vessel." *Compos. Part B Eng.*, 69,

406–417.

Perillo, G., Vacher, R., Grytten, F., Sørbø, S., and Delhaye, V. (2014). "Material characterisation and failure envelope evaluation of filament wound GFRP and CFRP composite tubes." *Polym. Test.*, 40, 54–62.

Quanjin, M., Rejab, M. R. M., Kaige, J., Idris, M. S., and Harith, M. N. (2018). "Filament winding technique, experiment and simulation analysis on tubular structure." *IOP Conf. Ser. Mater. Sci. Eng.*, 342(1).

Rafiee, R. (2013). "Apparent hoop tensile strength prediction of glass fiber-reinforced polyester pipes." *J. Compos. Mater.*, 47(11), 1377–1386.

Rafiee, R. (2016). "On the mechanical performance of glass-fibre-reinforced thermosetting-resin pipes : A review." *Compos. Struct.*, 143, 151–164.

Rajendra Prasad, K., and Syamsundar, C. (2019). "Theoretical and FE analysis of epoxy composite pressure cylinder used for aerospace applications." *Mater. Today Proc.*, 19(xxxx), A1–A9.

Raju, K. S., and Rao, S. S. (2015). "Design Optimisation of a Composite Cylindrical Pressure Vessel Using Fea." *Int. J. Sci. Res. Publ.*, 5(12), 522.

Ramesh, G., Gettu, R., and Bharatkumar, B. H. (2017). "Modified split disk test for characterization of frp composites." 43(5), 477–487.

Rao, P. S. (2013). "Effect of Hydrothermal Ageing on Glass Fibre Reinforced Plastic (GFRP) Composite Laminates exposed to Water and Salt Water." *Int. J. Curr. Eng. Technol.*, 2(2), 47–53.

Rao, S., and Hussain, M. (2013). *Hydrothermal ageing effects on flexural properties of GFRP composite laminates*. *Indian J. Eng. Mater. Sci.*

Reddy, S. S., Yuvraj, C., and Rao, K. P. (2015). "Design, Analysis, Fabrication and Testing of CFRP with CNF Composite Cylinder for Space Applications." *Int. J. Compos. Mater.*, 5(5), 102–128.

Ren, M. F., Chang, X., Xu, H. Y., and Li, T. (2017). "Trans-scale analysis of composite overwrapped pressure vessel at cryogenic temperature." *Compos. Struct.*, 160, 1339–1347.

Ren, Z. H., Zheng, Y. G., Jiang, C. H., Cao, X. M., Jin, P., and Zhang, J. S. (2018).

"Mechanical properties and slurry erosion resistance of a hybrid composite SiC foam/SiC particles/EP." *Polym. Compos.*, 39(7), 2277–2286.

Ronagh, H., and Saeed, N. (2016). "Changes in mechanical properties of GFRP composite after exposure to warm seawater." *2 J. Compos. Mater.*, 0(0).

S. Larbi, R. Bensaada, A. B. and S. D. (2015). "Hygrothermal ageing effect on mechanical properties of FRP laminates Hygrothermal Ageing Effect on Mechanical Properties of FRP laminates." *AIP Conf. Proc.*, 020066(April).

Sangamesh, Ravishankar, K. S., and Kulkarni, S. M. (2017). "Synthesis and comparison of mechanical behavior of fly ash-epoxy and silica fumes-epoxy composite." *IOP Conf. Ser. Mater. Sci. Eng.*, 225(1).

Sanjay K. Mazumdar. (2001). *Composites Manufacturing, materials, Product, and Process Engineering. Science (80-.).*

Santhosh, K., Muniraju, M., and Raguraman, M. (2012). "Hygrothermal durability and failure modes of FRP for marine applications." *J. Compos. Mater.*, (November 2011).

Sasanka, C. T., and Ravindra, K. (2015). "Implementation of VIKOR Method for Selection of Magnesium Alloy to Suit Automotive Applications." 83, 49–58.

Sayadi, M. K., Heydari, M., and Shahanaghi, K. (2009). "Extension of VIKOR method for decision making problem with interval numbers." *Appl. Math. Model.*, 33(5), 2257–2262.

Search, H., Journals, C., Contact, A., Iopscience, M., and Address, I. P. (n.d.). "The modelling of hydrothermal aging in glass fibre reinforced epoxy composites." 2079.

Shao, Y., Betti, A., Carvelli, V., Fujii, T., Okubo, K., Shibata, O., and Fujita, Y. (2016). "High pressure strength of carbon fibre reinforced vinylester and epoxy vessels." *Compos. Struct.*, 140, 147–156.

Sheet, T. D., and Business, P. (2017). "LAPOX ® L-12 | K-5." (August), 2–5.

Shettar, M., Chaudhary, A., Hussain, Z., and Kini, U. A. (2018). "Hygrothermal Studies on GFRP Composites : A Review." 02026, 1–9.

Silva, N. S., Netto, T. A., Bastian, F. L., and Silva, R. A. F. (2020). "On the effect of the ply stacking sequence on the failure of composite pipes under external pressure." *Mar. Struct.*, 70(April 2019), 102658.

Toh, W., Tan, L. Bin, Tse, K. M., Giam, A., Raju, K., Lee, H. P., and Tan, V. B. C. (2018). "Material characterization of filament-wound composite pipes." *Compos. Struct.*, 206(July), 474–483.

Trabia, M. B., O'Toole, B. J., Thota, J., and Matta, K. K. (2008). "Finite Element Modeling of a Lightweight Composite Blast Containment Vessel." *J. Press. Vessel Technol.*, 130(1), 011205 1–7.

Vasiliev, V. V., Krikanov, A. A., and Razin, A. F. (2003). "New generation of filament-wound composite pressure vessels for commercial applications." *Compos. Struct.*, 62(3–4), 449–459.

Wang, L., Zheng, C., Luo, H., Wei, S., and Wei, Z. (2015). "Continuum damage modeling and progressive failure analysis of carbon fiber/epoxy composite pressure vessel." *Compos. Struct.*, 134, 475–482.

Wang, L., Zheng, C., Wei, S., and Wei, Z. (2016). "Micromechanics-based progressive failure analysis of carbon fiber/epoxy composite vessel under combined internal pressure and thermomechanical loading." *Compos. Part B Eng.*, 89, 77–84.

Weisberg, A. H., Aceves, S. M., Espinosa-Loza, F., Ledesma-Orozco, E., Myers, B., and Spencer, B. (2013). "Cold hydrogen delivery in glass fiber composite pressure vessels: Analysis, manufacture and testing." *Int. J. Hydrogen Energy*, 38(22), 9271–9284.

Xu, P., Zheng, J. Y., and Liu, P. F. (2009). "Finite element analysis of burst pressure of composite hydrogen storage vessels." *Mater. Des.*, 30(7), 2295–2301.

Yu, P. L. (1973). "A Class of Solutions for Group Decision Problems." (August 2015).

ZELENY, M. (1974). "A Concept of Compromise Solutions and the Method of the Displaced Ideal." I, 479–496.

Zhao, D., Dong, Y., Xu, J., Yang, Y., Fujiwara, K., Suzuki, E., Furukawa, T., Takai, Y., and Hamada, H. (2016). "Flexural and hydrothermal aging behavior of silk fabric/glass mat reinforced hybrid composites." *Fibers Polym.*, 17(12), 2131–2142.

Zu, L., Zhu, W., Dong, H., and Ke, Y. (2017). "Application of variable slippage coefficients to the design of filament wound toroidal pressure vessels." *Compos. Struct.*, 172, 339–344.

ASTM Standard. (2016). "ASTM 2290-12 Standard Test Method for Apparent Hoop Tensile Strength of Plastic or Reinforced." *ASTM B. Stand.*, 1–8.

Siddiqui, N. A., Ramakrishna, A., & Lal, P. S. (2013). Review on Liquefied Petroleum Gas Cylinder Design and Manufacturing Process as per Indian Standard, IS 3196 (Part 1): 2006. Int. J. Adv. Eng. Technol, 4(2), 124-127.

Ashok, T., & Harikrishna, A. (2013). Analysis Of LPG Cylinder Using Composite Materials. IOSR Journal of Mechanical and Civil Engineering, 9(2), 33-42.

List of Publications based on PhD Research Work

[to be filled-in by the Research Scholar and to be enclosed with Synopsis Submission Form]

Details of Publication:

International/National Journals

Sl. No.	Title of Paper	Authors (in the same order as in the paper. Underline the Research Scholar's name)	Name of the Journal/ Conference/ Symposium, Vol., No., Pages	Month & Year of Publication	Category *
1	Tribo-mechanical and physical characterization of filament wound glass/epoxy composites	Biradar S., Joladarashi S., & Kulkarni S. M.	Materials Research Express, 6(10), 105312.	JULY 2019	1
2	FE Analysis of FRP Pressure Vessel	Srikumar Biradar, Sharnappa Joladarashi, S M Kulkarni	Trans Tech Publishing, Vol. 801, pp 77-82.	MAY 2019	1
3	Investigation on mechanical behaviour of filament wound glass/epoxy composites subjected to water absorption and also tribological studies using Taguchi Method	Srikumar Biradar, Sharnappa Joladarashi, S M Kulkarni	Material Today Proceedings, Vol. 33, page 5007-5013	JAN 2020	3
4	Comparative study on filament wounded and laminated GFRP composites for tensile characterization	Srikumar Biradar, Sharnappa Joladarashi, Sangamesh Rajole, Shivashankar Hiremath, and S. M. Kulkarni	AIP Conference Proceedings, 2057, 1, 020057	JAN 2019	3

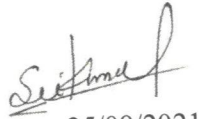| Sl. No.	Title of Paper	Authors (in the same order as in the paper. Underline the Research Scholar's name)	Name of the Journal/ Conference/ Symposium, Vol., No., Pages	Month & Year of Publication	Category *
5	Analytical and FE analysis of Al 6061 T6 and laminated composite LPG cylinder	Srikumar Biradar, Sharnappa Joladarashi, S M Kulkarni	Young, vol. 7850, issue 2770,page 1590	2018	4

International/National Conferences

Sl. No.	Title of Paper	Name of Authors	Name of the Conference, Year, Place, Date	Published in Journal (Yes/No)
1	Investigation on mechanical behaviour of filament wound glass/epoxy composites subjected to water absorption and also tribological studies using Taguchi Method	Srikumar Biradar, Sharnappa Joladarashi, S M Kulkarni	ICPCM 2019, NIT Rourkela, 14-16 DEC2019	YES
2	FE Analysis of FRP Pressure Vessel	Srikumar Biradar, Sharnappa Joladarashi, S M Kulkarni	ICCMME 2019, TOKYO, 19-22,2019	YES
3	Comparative study on filament wounded and laminated GFRP composites for tensile characterization	Srikumar Biradar, Sharnappa Joladarashi, Sangamesh Rajole, Shivashankar Hiremath, and S. M. Kulkarni	ICPC 2018, NITK SURATHKAL, 15-16, 2018	YES

Sl. No.	Title of Paper	Name of Authors	Name of the Conference, Year, Place, Date	Published in Journal (Yes/No)
4	Analytical and FE analysis of Al 6061 T6 and laminated composite LPG cylinder	Srikumar Biradar, Sharnappa Joladarashi, S M Kulkarni	ICMTS 2017, IIT MADRAS, 7-8 JULY 2017	YES

* Category: 1 : Journal paper, full paper reviewed

2 : Journal paper, Abstract reviewed

3 : Conference/Symposium paper, full paper reviewed

4 : Conference/Symposium paper,

abstract reviewed 5 : others (including papers in Workshops, NITK Research Bulletins, Short notes etc.)

(If the paper has been accepted for publication but yet to be published, the supporting documents must be attached.)

Research Scholar   25/09/2021

Name & Signature, with Date   (SRIKUMAR BIRADAR)

(Sharnppa-ū) **Research Guide**   27/09/2021 (S. M. kulkarni)

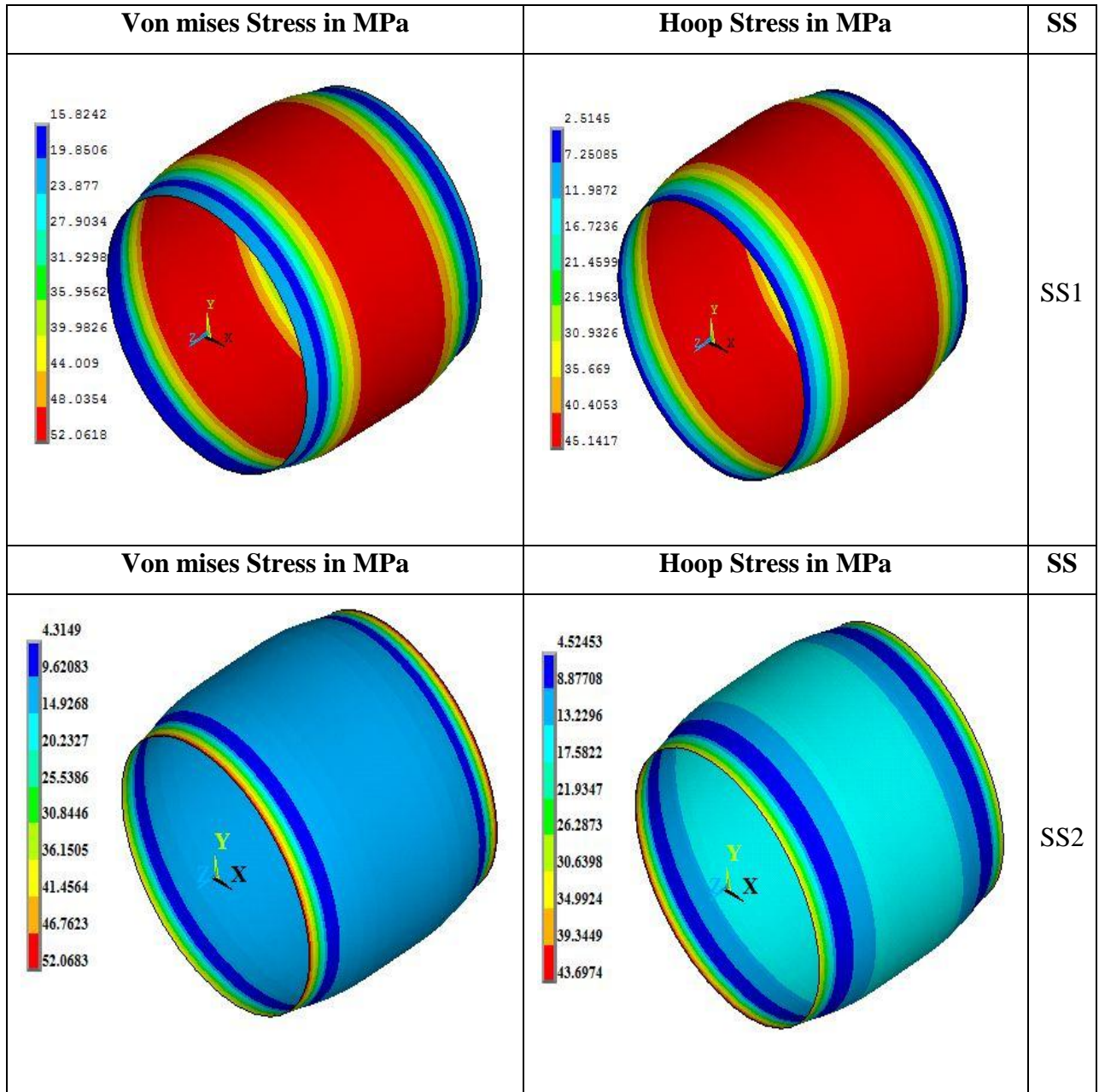2 SEP 2021

Name & Signature, with Date

APPENDIX-A

The Table below is highlighting various stresses outcome of the FE simulation of pressure vessel cylinder with PVC liner. In this Table A1, out of a total of 168 results, only the first 42 results, i.e., for the volume fraction of $V_f = 0.45$, are shown. Similarly, other remaining 126 FE simulation results are also obtained.

Table A1: FE simulations results for the volume fraction of 0.45, winding angles (all 7 as mentioned earlier), and stacking sequence (all six as mentioned as earlier)
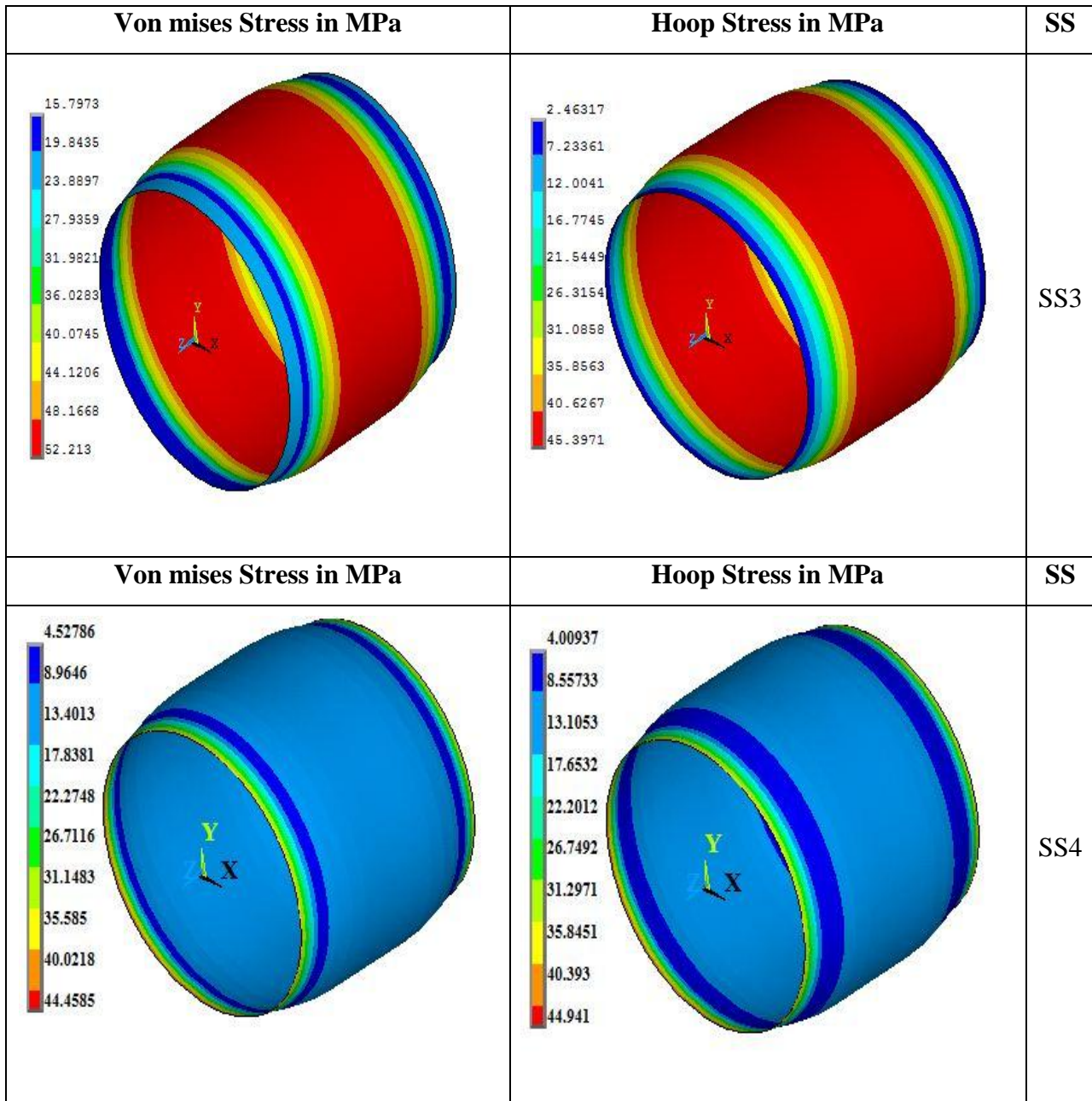
S.no	Volume fraction, V_f	Winding angle, φ	Stacking Sequence (SS)	Von Mises, MPa	Hoop Stress, MPa
1.	0.45	45	SS1	41.35	40.72
2.	0.45	45	SS2	39.32	40.20
3.	0.45	45	SS3	42.95	42.01
4.	0.45	45	SS4	42.72	42.24
5.	0.45	45	SS5	42.92	42.72
6.	0.45	45	SS6	43.14	42.18
7.	0.45	50	SS1	40.50	40.59
8.	0.45	50	SS2	38.92	40.16
9.	0.45	50	SS3	42.03	41.74
10.	0.45	50	SS4	41.79	41.98
11.	0.45	50	SS5	42.31	42.66
12.	0.45	50	SS6	42.04	41.78
13.	0.45	55	SS1	39.88	40.38
14.	0.45	55	SS2	38.34	40.01
15.	0.45	55	SS3	40.81	41.39
16.	0.45	55	SS4	41.07	41.62
17.	0.45	55	SS5	41.70	42.44
18.	0.45	55	SS6	40.61	41.32
19.	0.45	60	SS1	39.11	40.08
20.	0.45	60	SS2	37.55	39.71
21.	0.45	60	SS3	39.92	40.92
22.	0.45	60	SS4	40.10	41.12

23.	0.45	60	SS5	40.80	42.02
24.	0.45	60	SS6	39.59	40.76
25.	0.45	65	SS1	38.05	39.62
26.	0.45	65	SS2	36.53	39.24
27.	0.45	65	SS3	38.72	40.29
28.	0.45	65	SS4	38.85	40.46
29.	0.45	65	SS5	39.57	41.39
30.	0.45	65	SS6	38.36	40.07
31.	0.45	70	SS1	36.68	38.98
32.	0.45	70	SS2	35.34	38.59
33.	0.45	70	SS3	37.19	39.46
34.	0.45	70	SS4	37.31	39.61
35.	0.45	70	SS5	38.01	40.51
36.	0.45	70	SS6	36.84	39.23
37.	0.45	75	SS1	35.06	38.14
38.	0.45	75	SS2	34.09	37.83
39.	0.45	75	SS3	35.39	38.45
40.	0.45	75	SS4	35.54	38.58
41.	0.45	75	SS5	36.19	39.38
42.	0.45	75	SS6	35.12	38.23

Some of FE analysis results highlighting about variation in stresses for varied stacking sequences

Von mises Stress in MPa	Hoop Stress in MPa	SS
		SS1

Von mises Stress in MPa	Hoop Stress in MPa	SS
		SS2

FigureA1.1 The FE analysis results as per stacking sequences (SS1 and SS2)

Von mises Stress in MPa	Hoop Stress in MPa	SS
		SS3
Von mises Stress in MPa	Hoop Stress in MPa	SS
		SS4

FigureA1.2 The FE analysis results as per stacking sequences (SS3 and SS4)

Von mises Stress in MPa	Hoop Stress in MPa	SS
		SS5
Von mises Stress in MPa	Hoop Stress in MPa	SS
		SS6
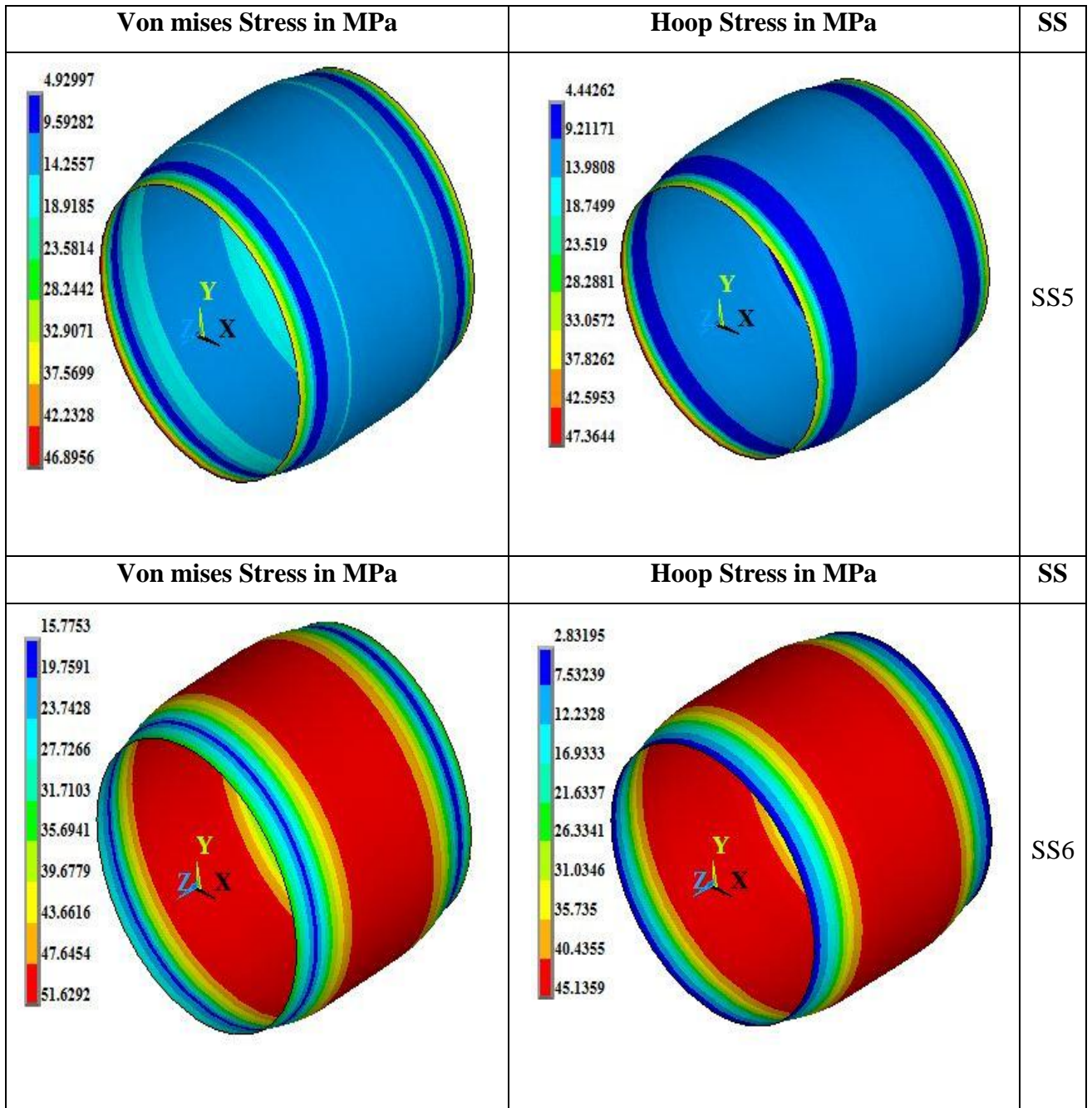
FigureA1.3 The FE analysis results as per stacking sequences (SS5 and SS6)

APPENDIX-B

Thickness Calculation for LCS Cylinder:

Thickness requirement considering internal pressure (as per IS3196): (Siddiqui, N. A. et al.)

The thickness equation considering internal pressure is given as

$$t = \frac{P_h D_i}{((200 \times 0.8 \times J \times R_e) - P_h)} \qquad \text{-----------------(EQ-B1)}$$

Where,

P_h = Test pressure = 25 kgf/mm²

D_i = Internal diameter of the cylinder = 206 mm

J = Weld joint factor = 0.9 (for non-radiographed welded joint)

R_e = Yield strength = 250 MPa = 25.48kgf/mm²

E = Young's Modulus =207 X 10³ MPa

Poisson's Ratio, μ = 0.3,   ∴t = **1.4 mm**

Total thickness requirement,

t =1.4 + Corrosion Allowance+ Transportation Allowance=1.4+0.6+2= 4.0 mm

Same thickness value is used in all other material cases (Al 6061 T6, GFRP, AFRP, CFRP) in FE analysis studies.

FE analysis of full cylindrical pressure vessels with hemispherical end domes
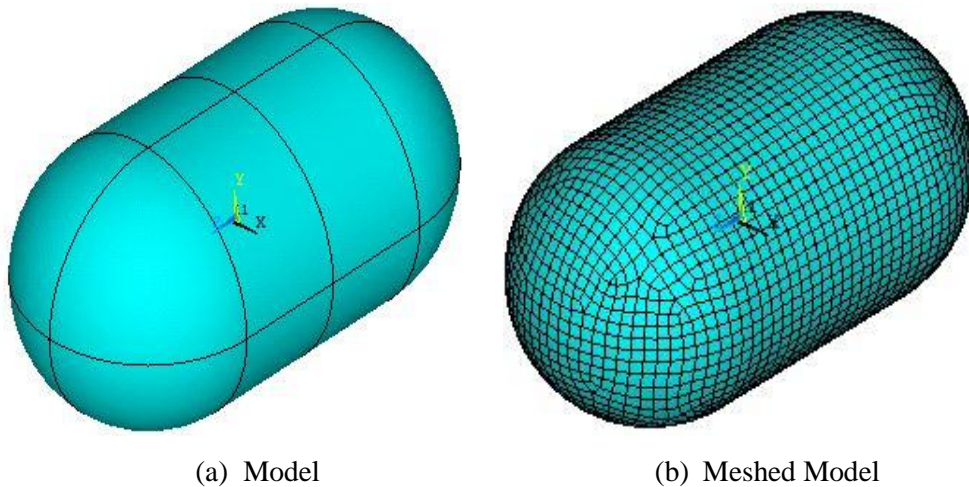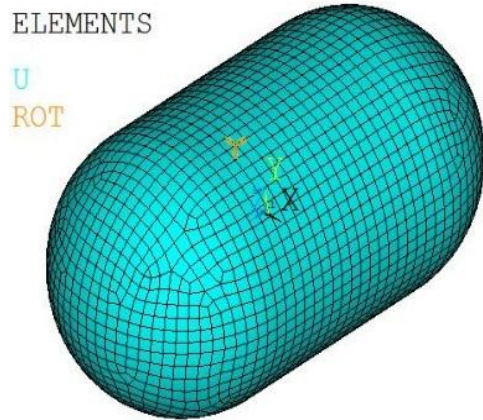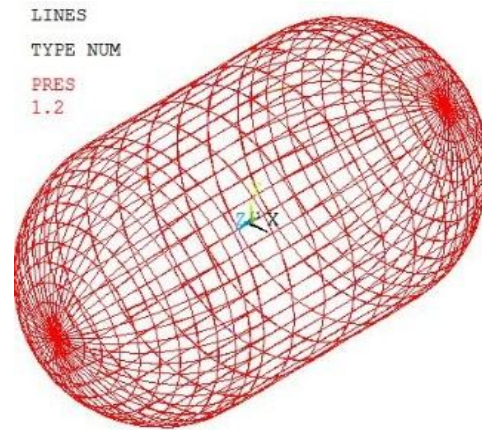

(a) Model   (b) Meshed Model

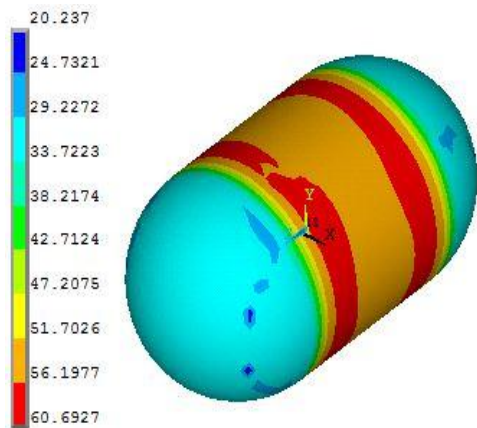Figure:B1.1 (a) Shell Model, (b) Meshed Model
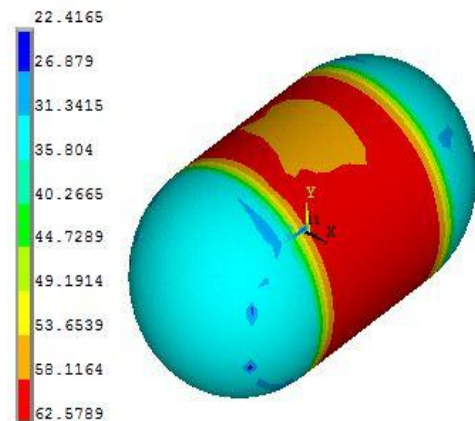
(c) Applying boundary conditions   (d) Pressure load is applied

Figure:B1.2 (c) Applying boundary conditions, (d) Applying pressure load

FE analysis results of FRP pressure vessel Figure. are shown in figure below. Similarly, metallic pressure vessels LCS and Al 6061 T6 are also analysed.

(a) Von mises stress   (b) Hoop stress

Figure:B1.3 Stresses distribution in pressure vessel

Mechanical properties tested samples images

Figure:B1.4 Samples tested for hoop tensile strength (d-unaged tested sample, e-sea water aged tested sample, f-tap water with oil aged tested sample)

Figure:B1.5 Tensile tested samples

Figure:B1.6 Bending tested samples

Figure:B1.7 Compression tested samples

BIO-DATA

MR. SRIKUMAR BIRADAR

Contact Details:

#870/D, 17TH A MAIN 4TH STAGE, 2ND BLOCK,

BTM LAYOUT, DEVERACHIKKANAHALLI,

Bangaluru-560076.

Email-ID: srikumar.biradar@gmail.com,
Phone Number: 9964824617

Academic Qualifications:	Bachelor of Engineering in Mechanical Engineering (2007), from Poojya Doddappa Appa College of Engineering (College under Visvesvaraya Technological University, Belgaum), Kalaburgi, Karnataka, India.
	Master of Technology in Industrial Process Equipment Design (2011), from Department of Mechanical Engineering, Sardar Vallabhbhai National Institute of Technology (Deemed University), Surat, Gujarat, India.
Research publications:	Articles in International Journals: 05 Articles in Conference Proceedings: 04
Professional experience	Worked as Assistant Professor in K.S. Institute of Technology, Bengaluru (July-2015 to Dec 2015).
	Worked as Assistant Professor in Vijaya Vittala Institute of Technology, Bengaluru (August-2012 to June 2015).
	Worked as Design Engineer at Bran Engineering Pvt. Ltd, Pune. India